Artiodactyl brain-size evolution

A phylogenetic comparative study of brain-size adaptation

Bjørn Tore Kopperud

Oppgave for graden
Master i Biologi
(Økologi og evolusjon)
60 studiepoeng

Centre for ecological and evolutionary synthesis
Institutt for biovitenskap
Det matematisk-naturvitenskapelige fakultet

UNIVERSITETET I OSLO

Høsten 2017

Artiodactyl brain-size evolution

A phylogenetic comparative study of brain-size adaptation

Bjørn Tore Kopperud

Artiodactyl brain-size evolution

http://www.duo.uio.no/

Trykk: Reprosentralen

Abstract

The evolutionary scaling of brain size on body size among species is strikingly constant across vertebrates, suggesting that the brain size is constrained by body size. Body size is a strong predictor of brain size, but the size variation in brain size independent of body size remains to be explained. Several hypotheses have been proposed, including the social-brain hypothesis which states that a large brain is an adaptation to living in a group with numerous and complex social interactions. In this thesis I investigate the allometric scaling of brain size and neocortex size and test several adaptive hypotheses in Artiodactyla (even-toed ungulates), using a phylogenetic comparative method where the trait is modeled as an Ornstein-Uhlenbeck process. I fit models of brain size and neocortex size, absolute and relative, in response to diet, habitat, gregariousness, gestation length, breeding group size, sexual dimorphism, and metabolic rate. Most of the investigated variables have no effect on the relative size of brain and neocortex, but the optimal relative size of the brain and neocortex is 20% and 30% larger, respectively, in gregarious species than in solitary species. Once allometric scaling and adaptation is taken into account, the phylogenetic half-lives of brain size and neocortex size are small on evolutionary timescales. In other words, there seems to be not much, if any phylogenetic inertia constraining the evolution of brain size and neocortex size. In the first appendix, I present the summary of revisions for a new and improved version of the software SLOUCH (Stochastic Linear Ornstein-Uhlenbeck Comparative Hypotheses) that was used to fit the phylogenetic comparative models.

Acknowledgements

I am very grateful to my supervisors Thomas F. Hansen, Olja Toljagić and Kjetil Lysne Voje, thank you for the ever excellent guidance and criticism, and for the opportunity you have given me to experience and be a small part of the scientific community. Furthermore, I want to thank several people:

Francisco Javier Pérez-Barbería and collaborators for their willingness to share a dataset of ungulate brain size and body size (Pérez-Barbería & Gordon, 2005). Without this contribution my analyses would have been less accurate, and accounting for observational error would have been far more difficult.

Masahito Tsuboi for allowing me to assist with his antler project, his thoughts on brain evolution, and for discussing all the silly ideas I had while we were visiting museums. Seeing the giant deer (*Megaloceros giganteus*) was fun!

My friends at the student's office from the bryozoan lab, the pollination project and other students, and the numerous roommates I've been living with these past two years (you know who you are!). Thank you for all the fun times and pleasant conversations that have kept me sane.

My parents Astrid and Øystein for providing the genes without which this thesis would not have been possible, and together with my brother Trond for always being encouraging and supportive of everything I do.

Contents

1 Introduction

1.1 Comparative study of brain size

The study of brain size as a topic of scientific interest is perhaps grounded in the fact that humans have a large brain compared to other animals (Striedter, 2005). Since there is a distinct disparity of brain size, shape and form in various mammals, this begs the questions on how and why this has evolved.

The term allometry was coined by Huxley & Teissier (1936) for describing the scaling relationship between the changes in shape and overall size, using the power function $y = a \cdot x^b$. Already before the turn of the 19th century this equation was used to explain how brain size scales with body size, where y is the brain mass and x is the body mass (Snell, 1892). Some later studies assembled large collections of brain size data (Weber, 1896) in order to estimate the allometric exponents in mammals. If brain size scales isometrically, or in other words proportionally to body size, the exponent would be unity. Dubois (1898) found that the interspecific relationship was approximately $b = 0.55$ in mammals, while Lapicque (1898) found that the intraspecific relationship in dogs (*Canis lupus familiaris*) was much lower, approximately $b = 0.25$. These were estimated using pairwise comparisons of similar species or similar individuals, not linear regression.

While the primates have been a clade of interest for studying brain-size evolution (Gould, 1975; Harvey *et al.*, 1980), I have focused on the even-toed ungulates (Artiodactyla) to see what kinds of adaptive hypotheses hold for these predominantly herbivorous mammals. The artiodactyls are a diverse group dating back as far as 50 myr (million years) ago (Hernández Fernández & Vrba, 2005), and they exhibit remarkable variation in body size, ranging from the southern pudú (*Pudu puda*) weighing 5-6 kg (Wilson & Mittermeier, 2011) to the massive hippopotamus (*Hippopotamus amphibius*) at 1100-2600 kg (Grubb, 1993). One big surprise came with the advances in molecular DNA sequencing and the volumes of genomic data that became available in the 90s and 2000s. It was discovered that cetaceans (whales and dolphins) are a sister-clade to the hippopotamus, rendering Artiodactyla a paraphyletic group (Price *et al.*, 2005). For the purposes of this project the whales and dolphins are not included, given their dissimilar mode of evolution and ecology in comparison with ungulates.

In the case of ungulate brain-body allometric scaling there have been quite a few studies, and perhaps the largest single contributor is Henriette Oboussier. In the 1960s and 1970s she published many papers on the brain-body scaling in bovids, after several expeditions to the african continent (Oboussier & Schliemann, 1966; Oboussier, 1979). She and her collaborators also examined the neocortex extensively, in at least 54 species of bovids (Ronnefeld, 1970; Haarmann & Oboussier, 1972; Oboussier, 1972). While their original aim was to reconstruct phylogenetic relationships based on comparative brain morphology and size, we can also use these data to make inferences about the mode of evolution.

Later, arguments were made that standard statistical methods like regression were not well suited for analyzing among-species comparative datasets (Clutton-Brock & Harvey, 1977). Since

a pair of related species share a history of diversification, their traits can be expected to be more similar than by chance. If the traits of each species can not be considered to be independently "sampled", then one of the assumptions of standard linear regression is violated. Felsenstein (1985) noted that since phylogenetic trees are essentially diagrams of non-independence, it is possible to model the evolution of the traits on the tree, incorporating divergence times and branch lengths. For this to be feasible, the phylogenetic tree has to be estimated independently of the modelled trait. In Felsenstein's method, the independent contrasts, his model of choice was the Brownian motion or Wiener process, in which the the change in the trait evolves as an independently normally distributed variable with a mean of zero and a variance proportional to time. If there has been no directional or stabilizing trend in the evolutionary history of the trait, e.g. due to neutral genetic drift or fluctuating directional selection, this could be an appropriate model of evolution.

More recent studies of ungulate brain size are usually model based, and include some estimate of whether there is any evident historical constraint on the evolution of the brain size; whether there exists a phylogenetic *signal*, or *inertia*. Pérez-Barbería & Gordon (2005) estimated the brain size by measuring endocranial volumes, and found that *gregarious* species had larger relative brain size than *nongregarious* species, and that relative brain size correlates positively with gestation length. Other studies have found that social species have larger relative brain size than non-social species (Shultz & Dunbar, 2006), and that species with monogamous or harem/seasonal social system have larger brains than species living in large mixed groups. The ungulates have also been part of recent studies including other mammalian groups (Pérez-Barbería *et al.*, 2007; Shultz & Dunbar, 2010). To my knowledge, all of the recent model-based comparative brain studies in ungulates are based on the Brownian-motion model, if not as originally implemented in the independent contrasts, then using a more modern framework such as the phylogenetic generalized least squares (PGLS), first described in Grafen (1989). For this thesis I will explore a variety of adaptive hypotheses and employ a more extensive model of trait evolution, the Ornstein-Uhlenbeck process, in which the modelled trait is allowed to evolve towards an optimal state (Hansen, 1997). Not only is this a better conceptual model of adaptation, but also a framework in which we will estimate concepts such as a phylogenetic signal in a more mathematically and statistically rigorous way in comparison with previous phylogenetic comparative studies.

1.2 Hypotheses & predictions

Aside from the allometric scaling with body size, one may ask what the chief drivers of brain-size evolution are. I present several broad-context hypotheses, and later examine the relationship with both brain size and neocortex size.

1. The social-brain hypothesis
The social-brain hypothesis (Dunbar, 1998) states that increased brain size is an adaptation to living in a social environment. If a species tends to aggregate in large groups where each individual interacts with many others, there needs to be enough brain matter to match the cognitive demands. However, using the reported group size of a species as a measure of social complexity is problematic, as it may be confounded by other ecological factors, for example anti-predator strategies. If a particular species has a harem or a polygynous mating system, then the group size in the breeding season may also be a proxy for the degree of sexual selection. Also, if the viable foraging sites in a particular habitat are distributed unevenly or in patches, some species may exhibit a large group size without necessarily having any more social cohesion because of it.

2. Browsers have larger brains than grazers
Mink *et al.* (1981) showed in that, in a predominantly mammalian dataset, the evolutionary allometry of the central nervous system (CNS) metabolism on total body metabolism is much steeper ($b = 0.91$) than the evolutionary brain-body allometry in mammals ($b = 0.75$, Harvey & Pagel, 1988). If brain tissue is more metabolically expensive than other organs, evolutionary increase in brain size could be constrained by energetic intake. Brain size is negatively correlated with gut size in guppies (selection experiment, Kotrschal *et al.*, 2013). If this is the case, one can expect there to be different brain-sizes for species with different foraging modes and diet, e.g that browsers with a high-nutrient diet have larger a brain size than grazers.

3. Species living in open habitats have larger brain size Species that live in open habitats such as grasslands or a savannah must process more visual information in order to detect potential predators. If this task is cognitively demanding, it is possible that brain size is larger in species that live in open habitats.

4. Brain size is a sexually-selected trait
Mate preference is an important mechanism of sexual selection. If being more intelligent can aid in acquiring features that are attractive to the opposite sex, such as having a larger territory or outcompeting members of the same sex, it is possible that brain size correlates with other traits that are markers of sexual selection. Many artiodactyls are sexually dimorphic, and most often the males are larger than the females (Pérez-Barbería *et al.*, 2002). In this thesis I test whether brain size correlates with sexual dimorphism in body mass.

5. Species with longer gestation times have larger brain size
The ontogenetic allometry of brain size in primates shows that the brain grows mostly during

prenatal development, with relatively little growth after birth. In non-primate mammals this pattern is not as pronounced, but still brain size grows faster prepartum (Halley, 2016), and the nutrients received during gestation might in large part determine the brain size in the offspring. Thus, if the gestation time is long, or the newborns are larger than usual, one can expect the brain to be larger.

6. Increased brain size is predicted by increased metabolic rate

Mink *et al.* (1981) studied energy expenditure in a sample mostly comprised of mammals, and found that the average species spends 5.3% of basal metabolic rate (BMR) on their central nervous system (CNS). Sheep, pigs, camels and cattle spend 3.16, 1.99, 2.72 and 1.74%, respectively - much less than the mammalian average. While this could be due to smaller brains, larger intestines or larger body size in artiodactyls, another reason could be that the BMR is inflated. If the BMR is defined as energy expenditure when an individual is inactive, adult, nonreproductive and is not actively digesting food (McNab, 1997), the artiodactyls do not really fit the measurement criteria. As herbivorous mammals they consume large amounts of low-nutritional food compared to frugivorous or carnivorous animals. As such, perhaps especially in the case of ruminants, they will inevitably be digesting food all the time, and there is no true period of the day at which artiodactyls are metabolically *at rest*. Despite this caveat, it is possible to test whether brain size is correlated with higher metabolic rates.

2 Materials & methods

2.1 Comparative method

One of the most important assumptions when using conventional statistical methods is that the data have to come from independent observations. When comparing species data, we know that they are not necessarily independent observations; closely related species have a shared history and we can expect them to be more similar than by chance. Depending on how brain size has evolved, ignoring this violation may result in misleading inferences (Felsenstein, 1985). In the interest of testing adaptive hypotheses on an among-species dataset, I assume that the trait of interest evolves according to an Ornstein-Uhlenbeck process (Hansen, 1997; Butler & King, 2004) in every lineage of the phylogenetic tree,

$$dy = -\alpha(y - \theta)dt + \sigma_y dB_y \tag{1}$$

$$dB_y \sim N(0, dt) \tag{2}$$

with y being the trait, θ the primary optimum, and α the rate of adaptation towards the optimum. B_y is the Brownian motion whose increments are normally distributed with mean zero and variance proportional to time. The method assumes that, aside from the attraction towards the optimum, the trait evolution in any segment of a lineage is independent of the change in any other subsequent or preceding segment. If α is large and the phylogenetic half-life $t_{1/2} = \log(2)/\alpha$ is close to zero, then the trait adapts towards the optimum at a fast pace, independently of phylogenetic relatedness. Conversely, if α is small or zero, the evolution of the trait y approaches a Brownian-motion process, with considerable phylogenetic signal. I model the optimum θ either as a single parameter or as a function of several explanatory variables. Consider the scenario where the primary optimum of a species changes through the history of its lineage. For species i, suppose its history is divided in κ segments. The expected trait value is then

$$E[y_i|y_a] = e^{-\alpha t_{ai}} y_a + \sum_{\gamma=1}^{\kappa(i)} (e^{-\alpha t_e} - e^{-\alpha t_b})\beta_i^\gamma \tag{3}$$

where y_a is the ancestral state, t_{ai} is the time from the tip to the root, t_e is the time from the tip to the end of the γth segment, and t_b is the time from the tip to the beginning of the γth segment. Since I only work with extant species and an ultrametric phylogeny, I do not estimate y_a but map it to the primary optimum estimated by ancestral state reconstruction. Next, we sum the coefficients that belong to the same selective regime such that

$$E[y_i|y_a] = c_{i1}\theta_1 + c_{i2}\theta_2 + \cdots = \sum_k c_{ik}\theta_k$$

where c_{ik} is the sum of coefficients for the kth optimum, for lineage i. The coefficients and continuous explanatory variables enter in the model matrix $\mathbf{X}$ in a linear model $\mathbf{Y} = \mathbf{X}\theta + \mathbf{r}$, where $\mathbf{r} \sim N(\mathbf{0}, \mathbf{V})$. $\mathbf{V}$ is the matrix of phylogenetic variances and covariances for the residuals,

see equation (4). I assume that the continuous explanatory variables influence the response trait directly and immediately. In the case of brain-size scaling with e.g. body size, it is likely that the correlated response is instantaneous, as would be the case if the influence is due to constraints, developmental or otherwise. Then, the phylogenetic covariance between residuals r_i, r_j is

$$Cov[r_i, r_j] = \frac{\sigma_y^2}{2\alpha}(1 - e^{-2\alpha t_a})e^{-at_{ij}} \tag{4}$$

where t_a is the time from the the root node to the most recent common ancestor (MRCA) of species i, j, and t_{ij} is the time that separates the two species through their MRCA. Next, the optima are estimated using the generalized least squares estimator, $\hat{\theta} = (\mathbf{X}^T\mathbf{V}^{-1}\mathbf{X})^{-1}\mathbf{X}^T\mathbf{V}^{-1}\mathbf{y}$. Since the covariance structure is conditional on α, σ_y, the optima are as well. To find the maximum-likelihood estimates for α and σ_y, I perform a grid-search of likely parameter estimates, where the likelihood function is evaluated in each iteration. Next, I use the "Low-memory Broyden-Fletcher-Goldfarb-Shanno" algorithm with Bound constraints (L-BFGS-B) (Byrd *et al.*, 1995) implemented in R (R Core Team, 2017) to further optimize the parameters. I plot the likelihood surface from the grid search within two units of log-likelihood, and use it to report marginal support regions for $t_{1/2}$ and $\sigma_y^2/2\alpha$. Then, I use the Akaike information criterion with a small-sample correction (AICc) to select the best model (Hurvich & Tsai, 1989). All equations are based on Hansen (1997) and Butler & King (2004). Because observational error was incorporated in the model, the naive GLS-estimator is possibly biased, and I performed a bias correction on the regression coefficients, where $\widetilde{\theta} = \mathbf{K}\hat{\theta}$ (Hansen & Bartoszek, 2012, eq. A.5). In almost all cases this attenuation factor $\mathbf{K}$ was close to the identity matrix and hence it is not reported unless it deviated by a noticeable amount. The Ornstein-Uhlenbeck models were fitted using the software SLOUCH (Stochastic Linear Ornstein-Uhlenbeck Comparative Hypotheses), first presented in Hansen *et al.* (2008). As part of this thesis I have refactored and rewritten the majority of SLOUCH and assembled it into an R package with documentation. See appendix A for details on the changes, including a worked example with in-line R code where the general workflow is explained.

2.2 Data

Data on brain size, body size and neocortex size were taken from existing literature datasets, see appendix B for references. Since the individual observations of brain mass were measured by many different authors, there have been several methods employed. Techniques include weighing the fresh tissue (Oboussier & Schliemann, 1966), weighing a brain fixated in a solute (e.g. formaldehyde) (Ronnefeld, 1970), as well as measuring the endocranial volume and calculating a predicted brain mass (Pérez-Barbería & Gordon, 2005) using the specific gravity of brain tissue (1.036 g/cm^3) (Stephan, 1960; Ebinger, 1974). The measurement practice is often incompletely described, making it difficult to account for error caused by measurement technique. This is also a problem in comparative analyses in general (Smith & Jungers, 1997). Observations of brain mass and body mass for individuals whose sex was unknown was discarded.

Observations of domesticated lineages of animals were removed in order to avoid any negative bias in relative brain-size as is the trend with domesticated animals (Kruska, 1987). Individuals who were either not sexually mature or in senescence were also excluded.

The scaling relationship between shape and size is the study of allometric scaling, often described with a power function: $\text{brain} = a \cdot \text{body}^b$ (Huxley & Teissier, 1936). When log-transformed this is a linear equation: $\log(\text{brain}) = \log(a) + b \cdot \log(\text{body})$, allowing the convenience of using linear models when estimating parameters. For this reason, all measures of mass were transformed to units of grams, as well as natural log-transformed. In the phylogenetic analyses I used a phylogenetic tree of Artiodactyla estimated based on mitochondrial genomes, including reconstructed ancestral states of diet (grazers, browsers, mixed feeders) and habitat (open, closed, mixed) (Toljagić *et al.*, 2017). The brain data for which there were no corresponding species in the phylogenetic tree were not used in the comparative analyses, and the species for which there was no available brain data were pruned from the phylogenetic tree.

2.2.1 Observational uncertainty

Brain size for each species was estimated as $\bar{x} = \frac{1}{n}\sum_{i=1}^{n} x_i$, with x_i being the log brain mass (g) of individual i. Since the sample size of observations can both be quite low and vary considerably, I estimated the within-species variance of the mean brain size, $s_{\bar{x}}^2$ for use in the regression analyses. This includes both biological and measurement error. When the sample size is low and estimation of the mean brain mass is uncertain, using the unbiased variance estimator

$$s_x^2 = \frac{1}{n-1}\sum_{i=1}^{n}(x_i - \bar{x})^2 \tag{5}$$

is yet more uncertain. For this reason, the sample variance s_x^2 was only calculated for a subset of the dataset where species whose sample size was greater than or equal to five. Since the observations were first transformed to a proportional scale, the within-species sample variances are roughly on the same scale when compared among species. Next, I calculated a weighted average of the species sample variances,

$$\hat{s}_x^2 = \frac{\sum_j s_{xj}^2(n_j - 1)}{\sum_j (n_j - 1)} \tag{6}$$

where n_j is the sample size for species j (Labra *et al.*, 2009; see also Grabowski *et al.*, 2016). The variances of the mean log brain mass are then $\text{Var}[\bar{x}_j] = \hat{s}_x^2/n_j$ for each species. These estimation variances were incorporated in the comparative analyses in order to correct for possible bias. The same calculations were done for log body mass (g).

2.2.2 Neocortex

Observations of neocortex were taken from publications with comparable measurement technique (Ronnefeld, 1970; Haarmann & Oboussier, 1972; Oboussier, 1972, 1978). Since this dataset was small to begin with, observations of individuals whose sex was unknown were kept, and no attempt was made to correct for influence of sex. The neocortex is measured in surface

area (mm^2) for the left, right or both hemispheres. After log transformation, the neocortex was estimated for each species as $\bar{x} = \frac{1}{n}\sum_{i=1}^{n} x_i$, x_i being the neocortex of a single hemisphere i. The within-species variances of the mean neocortex sizes were estimated as with brain size, however with s_x^2 estimated for species where $n \geq 2$, see equations (5,6).

2.2.3 Social behaviour

The social brain hypothesis states that species that are more social can be expected to have a larger brain than species that are less social. When comparing social behaviour in a large clade such as Artiodactyla, it is not entirely obvious how to describe each species "degree of sociality" in a single measurement. I used three separate measures of the degree of social cognition. Pérez-Barbería & Gordon (2005) used a binary classification, where a species is considered *gregarious* if, all year-round, the group size is at least 6 or more individuals, including offspring, and *solitary* if not. I also used an alternative categorical measure of social complexity from Caro *et al.* (2004). In this system, *solitary* species are found primarily alone or in pairs, while *intermediate*-sized groups are aggregations of 3-50 individuals, and *large* include species with a group size larger than fifty. These categories are not mutually exclusive, and species that exhibit considerable variation in group size are classified as a combination of the three. In order to fit these categories as optima, I reconstructed the sociality measures for each node in the phylogenetic tree using two Markov-chain models with equal rates for all transitions (Pagel, 1994), implemented in R-package "ape" (Paradis *et al.*, 2004). Any alternative models with additional free parameters were not favoured by AIC. I used the posterior probabilities at each internal node to paint the most probable regimes on the trees (Figures S1 and S2). The reconstructions were estimated with error, but these errors were not accounted for in the comparative analyses. For the neocortex models, I used the same ancestral-trait reconstructions, and pruned the species lacking neocortex data last, see Figures S7 and S8. For the third measure of sociality, I used the mean group size in the breeding season, and the observations (n = 42) were taken from literature datasets (Bro-Jørgensen, 2007; Bercovitch & Berry, 2010; Wilson & Mittermeier, 2011; Myers *et al.*, 2017). Since many of these species have a polygynous mating system, this measure can also be a measure of sexual selection by proxy.

2.2.4 Diet and habitat

Information about diet and habitat, including ancestral state reconstructions, was taken from Toljagić *et al.* (2017). The diet categories were defined based on percentage of grass intake as part of the diet (>75% for grazers, 25-75% for mixed feeders and <25% for browsers) (Mendoza *et al.*, 2002; Mendoza & Palmqvist, 2008). Habitat types were divided in open habitat, mixed habitats and closed habitats (Mendoza *et al.*, 2005; Mendoza & Palmqvist, 2008).

2.2.5 Sexual dimorphism

As a proxy for sexual selection, the degree of sexual dimorphism in body mass was used, $z = \bar{m} - \bar{f}$, z being the within-species dimorphism, m and f being log-transformed male and female body

mass, respectively. Subsequently, I calculated the estimation variances: $\mathrm{Var}[z] = \hat{s}_m^2/n_m + \hat{s}_f^2/n_f$, with $\hat{s}_m^2$ and $\hat{s}_f^2$ estimated as with body size with a weighted average of a data subset where $n \geq 5$, see equations (5,6). In order to estimate sexual dimorphism, I supplemented my records of body mass with additional data (Silva & Downing, 1995; Nchanji & Amubode, 2002; Wilson & Mittermeier, 2011), including observations of individuals where brain mass was not measured.

2.2.6 Gestation length

Information about gestation length were obtained from literature datasets (Pérez-Barbería & Gordon, 2005), descriptions of species ecology (Wilson & Mittermeier, 2011), and web articles for *Tragelaphus imberbis* (*Tragelaphus imberbis*, lesser kudu, n.d.), *Madoqua saltiana* (Estes *et al.*, 1998) and *Cephalophus natalensis* (Duiker, n.d.). The records for gestation length are not very precise, often a count of months with no reported sample size or standard error. When only a range was reported, I used the arithmetic mean of the lower and upper bounds as the mean gestation length. Due to lack of data, it was not feasible to account for observational error in gestation length in the comparative models.

2.2.7 Metabolic rate

Measurements of basal metabolic rate (BMR) were taken from Savage *et al.* (2004). Since there were few species with data for BMR ($n = 20$), I also included brain data from domesticated species (*Sus scrofa*, *Bos taurus*) and an outgroup species (*Pecari tajacu*) in these analyses. There were not enough data to fit models of neocortex on metabolic rate ($n = 8$).

2.3 Uneven sex-sampling

The proportion of sexes sampled can in some species vary a great deal. In order to assess whether this had any effect on model selection, and to test for the influence of sex on brain mass, a mixed-effect model was fitted on all of the individual observations. Species were modeled as a random effect,

$$\text{brain} = \beta_0 + \beta_1 \text{male} + \beta_2 \text{body} + u_0 \text{species} + r \tag{7}$$

where all species were assumed to have the same slope, and females were included in the intercept. While we can assume that the observations were independently sampled within each species, the same does not apply among species. While there is a method for phylogenetic generalized mixed-effect models (Hadfield, 2010), it assumes that the trait value has evolved according to a Brownian motion. As we will see, and estimate, this assumption might indeed be more unrealistic than the assumption of phylogenetically independent trait evolution. In lieu of other methods, the model was fitted using the R-package "lme4" (Bates *et al.*, 2015). Two alternative models were fitted; one with a separate slope for the sex term, as well as a model without the sex term. Since all models had the same random structure, but different fixed effects, the likelihoods and AICc were computed using maximum likelihood in order to be comparable (Zuur *et al.*, 2009, p. 122). The effect sizes of the fixed effects were computed from models fitted with

restricted maximum likelihood. To assess whether the impact of uneven sex sampling would bias model selection in the comparative analyses, I created a separate "female equivalent" brain mass variable. For all male individuals, their estimated effect on brain size was removed.

$$\text{brain}_{\text{female-equivalent}} = \text{brain}_{\text{male}} - \beta_1 \tag{8}$$

The within-species means and variances for this variable were recalculated as described above, see equations (5,6). The female equivalent brain size does not replace the original mean brain size. Instead, all comparative analyses of brain size were run on both datasets separately, to test whether model selection is robust to uneven sampling of sexes.

3 Results

3.1 Effects of sex on brain size

In order to assess the effects of sex on brain size, I fitted three mixed-effect models with species as a random effect. These models do not incorporate the phylogenetic topology or branch lengths. The body size was centered on its arithmetic mean prior to model fitting, meaning that the intercept is the expected brain size for an individual at about 57.5 kg. The reported R^2_{marginal} represents only the variance accounted for by the fixed effects (Nakagawa & Schielzeth, 2013).

Table 1: Mixed models of log brain (g) on log body (g) and sex. $n_{obs} = 357$, $n_{species} = 75$.[a]

Model	Intercept		log body (g)		$\sigma^2_{\text{species}}$	σ^2_r	R^2_{marginal} (%)	AICc
Allometry	5.00 ±0.04		0.46 ±0.02		0.089	0.017	76.03	-215.73
	Female	Male						
Sex+Body	5.03 ±0.03	4.99 ±0.02	0.49 ±0.02		0.073	0.018	81.02	-220.80
			Female : log body(g)	Male : log body (g)				
Sex*Body	5.03 ±0.03	4.98 ±0.02	0.51 ±0.02	0.49 ±0.01	0.069	0.018	82.30	**-221.38**

[a] Results include fixed effects ± standard error (SE), variance of the random effect ($\sigma^2_{\text{species}}$), the residual variance (σ^2_r), percent of the variance accounted for by the fixed effects (R^2_{marginal}), and the Akaike Information Criterion with small-sample bias correction (AICc).

These models show a clear pattern of males having a smaller relative brain size than females, but the effect size is not very large. If for instance a species doubles in body mass, the brain mass will increase by a factor of $e^{0.51 \cdot \log(2)}$ in females and $e^{0.49 \cdot \log(2)}$ in males (Table 1, model "Sex*Body"). In this example, the female brain mass would increase by $e^{\log(2) \cdot 0.02} = 1.4\%$ more than males. Since in some species the individuals are sampled unevenly with regards to sex, this gives an error which, if systematic, may bias the results in the comparative analysis. I tried to assess the potential impact of this error by running all the brain models twice, with a separate "female-equivalent" brain size variable. Although the "Sex*Body" model is the best fitting model, the next best model "Sex+Body" is also a good fit (ΔAICc = 0.58). Since not all individuals had an associated body mass estimate, I used the "Sex+Body" model estimates to add 0.04 units of log brain (g) to all male individuals prior to computing the species mean and the standard error of the mean (see Materials & Methods). Since the neocortex data did not include adequate information about sex for each individual, this assessment was only made for the brain models. The impact of this correction was in all cases miniscule in terms of estimates of $t_{1/2}$, $\sigma^2_y/2\alpha$, the regression coefficients and model fit statistics, and is hence not reported in detail. This could be due to the large among-species variation in body size in artiodactyls and that the relative error as such is minimal, or that there is no systematic error introduced by the variation in sampling of individuals with regards to sex.

3.2 Static allometries

I estimated the within-species scaling of log brain mass on log body mass for the twelve species that have the largest sample size ($n \geqslant 9$) using ordinary least squares regression (Figure 1). These static allometries (mean slope is $b = 0.16 \pm 0.04$ SE, $n = 12$) are much shallower than the evolutionary allometry ($b = 0.61 \pm 0.02$, Table 2, model "Allometry"). Figure 2 displays the equivalent in the within-species scaling of log neocortex area on log brain mass for the five species with the largest sample size ($n \geqslant 8$, mean slope is $b = 0.81 \pm 0.19$ SE, $n = 5$). With neocortex, the static allometries are much steeper, almost as steep as the evolutionary allometry ($b = 0.86 \pm 0.04$, Table 3, model "Allometry"). While most individuals in the neocortex sample had both of their hemispheres measured, for some individuals only the left or the right hemisphere were measured. The left hemisphere is on average slightly larger (mean($\text{neocortex}_{\text{left}} - \text{neocortex}_{\text{right}}$) $= 91 \pm 102$ SE (mm^2), $n_{\text{obs}} = 137, n_{\text{sp}} = 47$), but the deviation is only 0.5% of the mean left neocortex size. There is some variation between the left and right hemisphere, which could either be due to measurement error or a small tendency for fluctuating asymmetry (see Ronnefeld, 1970). Since the sample sizes are relatively small, sex was not accounted for, and this may possibly cause a small bias in terms of shallower static allometric slopes.

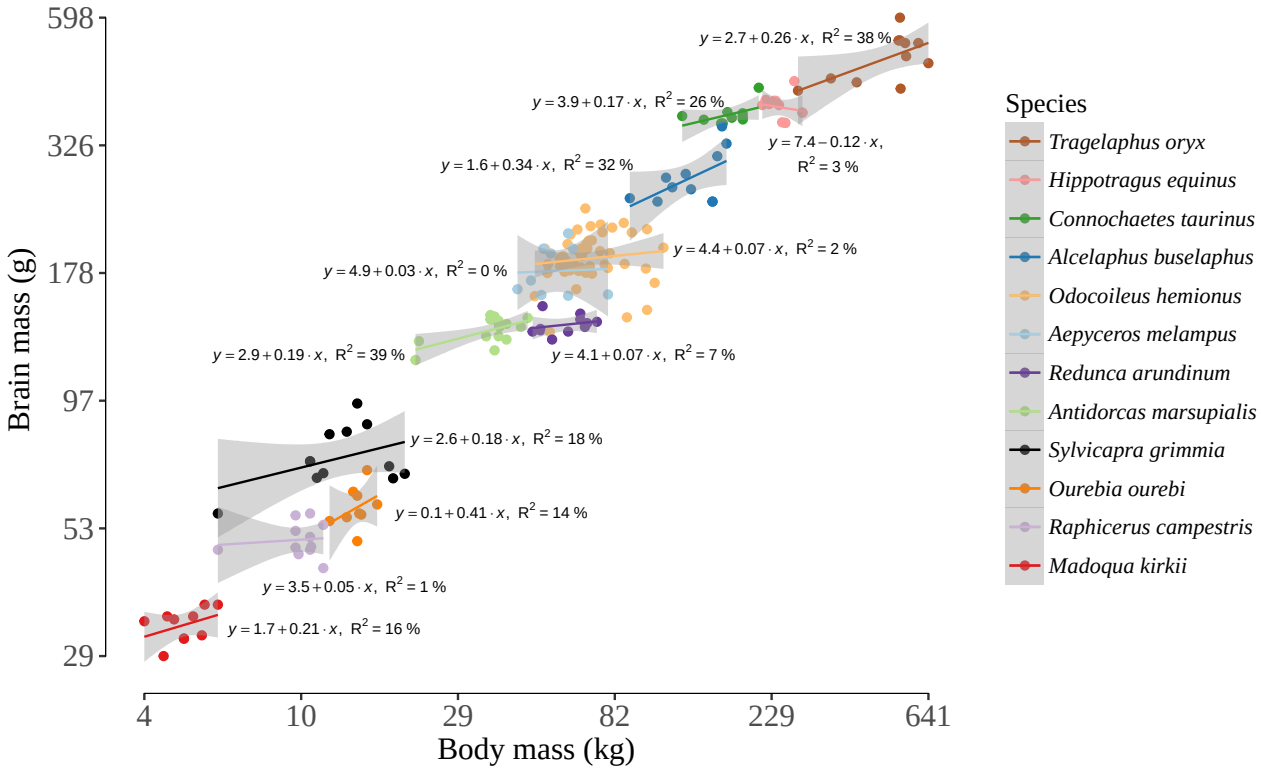

Figure 1: Static allometries of log brain mass on log body mass, where each point is an individual. The axis labels have been back-transformed to arithmetic units. The regression lines have been estimated using the ordinary least squares method, and the shaded areas represent 95% confidence intervals.

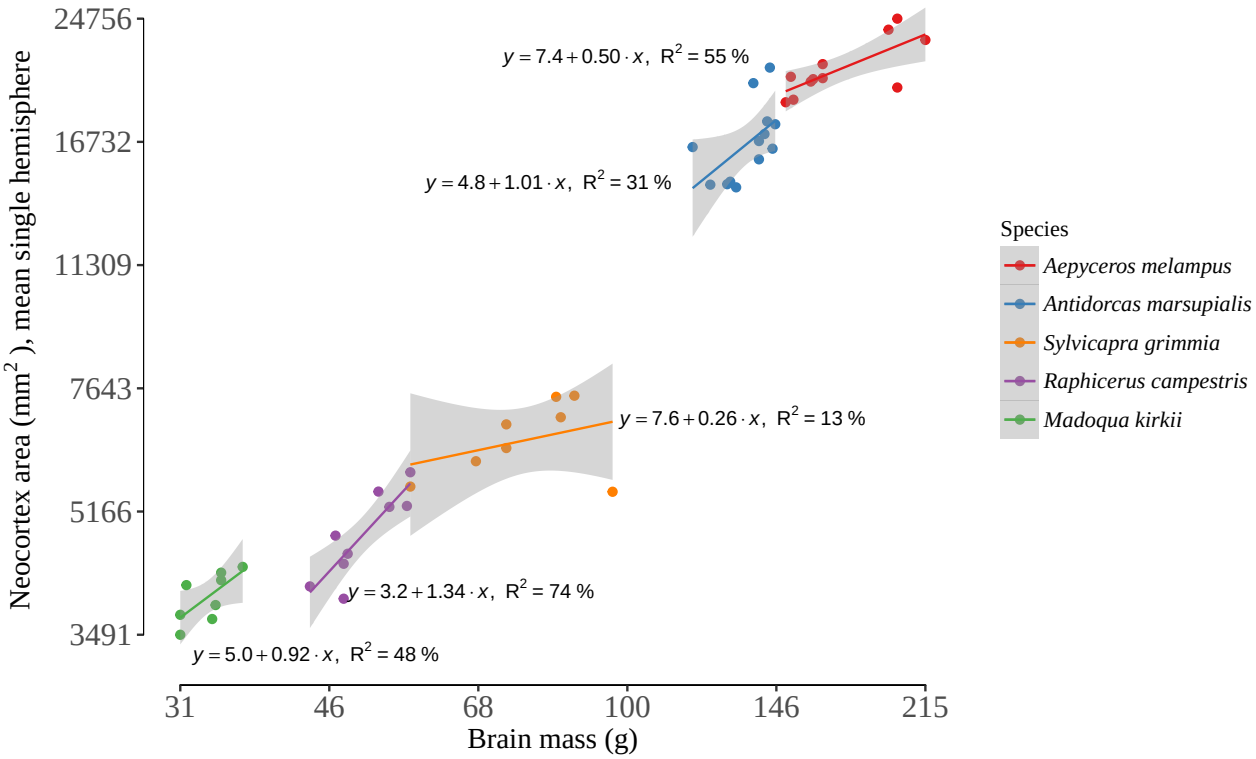

Figure 2: Static allometries of log neocortex area on log brain mass, where each point is an individual. The axis labels have been back-transformed to arithmetic units. The regression lines have been estimated using the ordinary least squares method, and the shaded areas represent 95% confidence intervals.

3.3 Evolutionary allometry

I fitted the evolution of brain size as an Ornstein-Uhlenbeck process with $n_{species} = 75$. The log body mass variable was centered on its arithmetic mean prior to fitting the models, so the intercepts represent brain size for a species at about 56.5 kg. Brain size seems to have a considerable phylogenetic effect, as the phylogenetic half-life ($t_{1/2}$) was near infinitely large (Table 2, model "Single optimum"). I also ran a single-optimum model with body size as the response variable, and it showed a strong phylogenetic effect, $t_{1/2} = \infty$ with the support region $(21, \infty)$. When the optimal brain size is modeled as a function of body size, however, there is only a small phylogenetic effect (Table 2, model "Allometry"). While $t_{1/2} = 5$ myr might seem like a long time, in the context of the whole phylogeny this is only about 11% of the total tree depth, which is 45 million years.

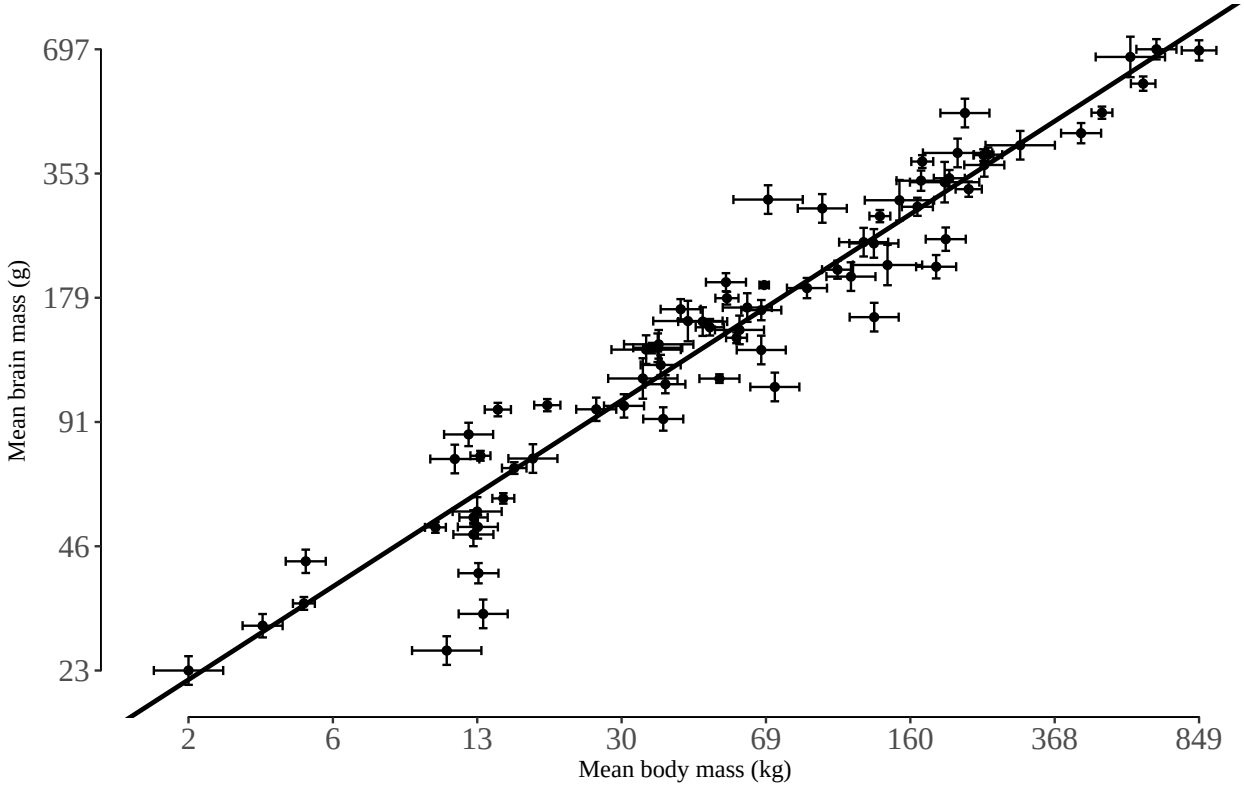

Figure 3: Evolutionary allometry of brain size on body size, where each point is a species. The regression line corresponds to the allometry model in Table 2, where $\theta = 5.01 + 0.61 \cdot \log$ body (g), but the axis labels have been back-transformed to arithmetic units. The error bars are standard errors. See Figure S1 for the tree used.

Table 2: Evolutionary allometry of log brain mass (g) on log body mass(g). $n_{species} = 75$. Root depth of the tree is 44.8 myr, see Figure S1.[a]

Model	$t_{1/2}$ (myr)		$\sigma^2_y/2\alpha$ ((log brain(g))^2)		Optima		R^2 (%)	logL	AICc
	(Support region)		(Support region)		Intercept	log body (g)			
Single optimum	∞	(23.8, ∞)	∞^b	(0.89, ∞)	4.46 ±0.75			-72.01	150.34
Allometry	4.99	(0, 30)	0.04	(0.03, 0.09)	5.01 ±0.03	0.61 ±0.02	91.72	7.47	-6.37

[a] Results include the phylogenetic half-life ($t_{1/2}$) and the equilibrium variance ($\sigma^2_y/2\alpha$). The marginal support regions include all values of $t_{1/2}$, $\sigma^2_y/2\alpha$ for which the log likelihood is within two units of the maximum likelihood. The optima with fixed effects ± standard error (SE) have been bias-corrected with an attenuation factor ($\mathbf{K}\hat{\theta}$), see methods. The reported model fit statistics include the amount of variance accounted for (R^2), the log likelihood (logL) and the Akaike Information Criterion with small-sample bias correction (AICc).

[b] $\sigma^2_y = 0.037$ for the "Single optimum" model, in units (log brain(g))^{2}myr^{-1}.

I also estimated the allometric model in bovids alone ($\log \text{brain(g)} = 5.06 \pm 0.04 + 0.59 \pm 0.02 \cdot \log \text{body(g)}$, where $t_{1/2} = 19.7$ $(1.88, \infty)$ myr, $R^2 = 96.41\%$, $n_{\text{species}} = 46$), in order to compare with previous studies.

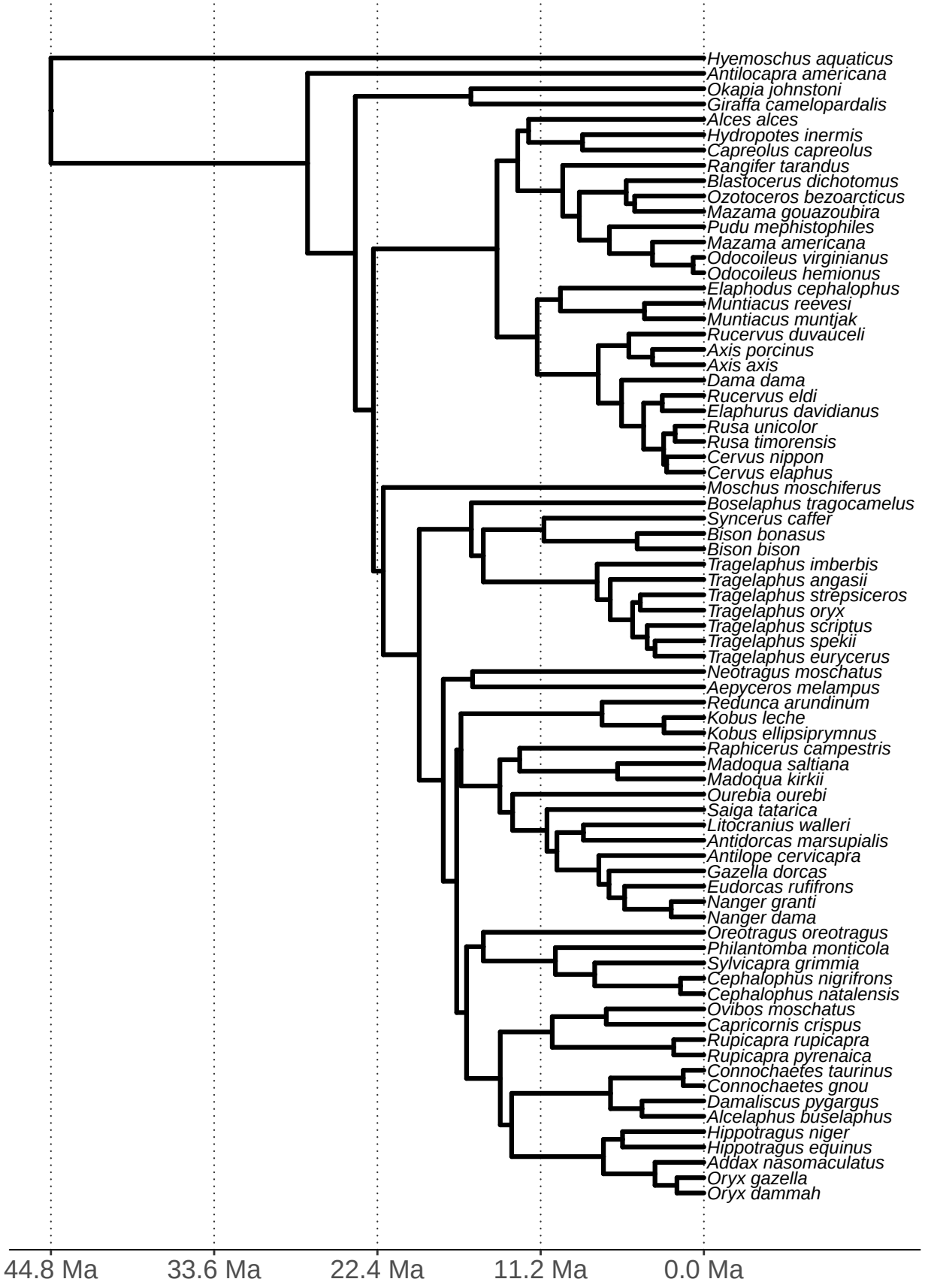

Figure 4: Phylogenetic tree of Artiodactyla. This tree corresponds to all models in Tables 1, 2, 4, 10, and 12, and is based on Toljagic *et al.* (2017).

As an alternative to relative brain size, I fitted several models with the relative neocortex area. I centered the explanatory variables on their respective arithmetic means before fitting the models, which means that the intercept is the optimal neocortex size for a species with 56.5 kg body mass and/or with a brain mass of 160 g. One caveat with all of the models with neocortex is that they have a smaller sample size, and thus the phylogenetic half-lives and stationary variances are estimated with less precision than with relative brain size. As expected, the size of the neocortex is predicted much better by brain size than by body size (Table 3). Also, there seems to be more phylogenetic inertia when the neocortex is modeled as a function of brain size rather than body size (Table 3). The species included in the neocortex analyses are almost exclusively bovids, with the exception of *Giraffa camelopardalis*, *Okapia johnstoni*, *Capreolus capreolus* and *Antilocapra americana*, meaning that cervids are underrepresented.

Table 3: Evolutionary allometry of log neocortex (mm^2), single hemisphere, on log brain mass (g) and log body mass (g). $n_{species} = 42$. Root depth of the tree is 27.19 myr, see Figure S7.[a]

Model	$t_{1/2}$ (myr)		$\sigma_y^2/2\alpha$ [b,c]		Optima			R^2 (%)	logL	AICc
	(Support region)		(Support region)		Intercept	log brain (g)	log body (g)			
Single optimum	∞	(16.9, ∞)	∞	(0.46, ∞)	9.76 ±0.37			-	-32.2	71.10
Brain	∞	(2.14, ∞)	∞	(0.02, ∞)	9.69 ±0.10	0.86 ±0.04		90.88	15.5	-21.97
Body	11.44	(0, ∞)	0.05	(0.02, ∞)	9.64 ±0.07		0.50 ±0.03	88.30	7.8	-6.52
Brain+Body	∞	(1.82, ∞)	∞	(0.02, ∞)	9.69 ±0.10	0.88 ±0.20	-0.011 ±0.12	90.89	15.5	-19.35

[a] See note in Table 2.

[b] The equilibrium variances are in units (log neocortex(mm^2))^2

[c] $\sigma_y^2 = 0.023$ for the "Single optimum" model, $\sigma_y^2 = 0.002$ for the "Brain" model, $\sigma_y^2 = 0.002$ for the "Brain+Body" model, in units (log neocortex(mm^2))$^2 myr^{-1}$.

Since the neocortex and brain mass are measured on different scales, this presents a small challenge when interpreting the allometric slopes. Mass is more comparable to volume than area, and if we assume that the shape of the neocortex neocortex is a approximately like that of a sphere, we can get the volume by scaling up the surface area, $mm^{2 \cdot (3/2)} = mm^3$. Since the data are log-transformed, this is equivalent to multiplying the slopes with 3/2, and we get a positive neocortex-brain allometry with a slope of $b = 0.86 \cdot (3/2) = 1.29$. This is steeper than the equivalent regression of neocortex volume on brain mass in primates (ordinary least-squares model, $\log \text{neocortex}(mm^3) = -1.58\ (\pm 0.11) + 1.10\ (\pm 0.01) \cdot \log \text{brain}(mg), R^2 = 99.6\%, n_{\text{species}} = 45$). This model includes *Homo sapiens*, but the allometric slope is not sensitive to the inclusion of humans; data from Stephan *et al.* (1981). See also Passingham (1975) and Striedter (2005), Figure 5.4-A. Given that primates are more encephalized than artiodactyls, it is surprising to see that the neocortex-brain allometry is steeper in artiodactyls. One explanation for this could be that the area-volume transformation is positively biased; the neocortex is not a sphere, and it is possible that the sulci or folds in the cortex become more prominent as size increases. Unfortunately, I do not have observations of both surface area and volume of the neocortex to test this more explicitly.

3.4 Social-brain hypothesis

For brain size adaptation, the social categorization of *gregarious* and *solitary* from Pérez-Barbería & Gordon (2005) is the best fitting model, and our results confirm their findings despite differences in phylogenetic tree, set of species, brain data and choice of model. Gregariousness seems to have a large effect on the optimal absolute brain size, as the primary optimum for *gregarious* species is $e^{5.66-1.03} = 102$ times larger than for the optimum for *solitary* species. A discrepancy this large is likely because the *gregarious* species have larger bodies than the *solitary* species (Table 4, "Gregariousness" model), and that the estimate for the *solitary* optimum is outside the natural range in brain size. This may happen when the $t_{1/2}$-estimate is quite large (here 41 myr) compared to the phylogenetic tree depth. When accounting for body size, the optimal brain size for *gregarious* species is $e^{5.08-4.90} = 1.20$ times larger than the optimal brain size for *solitary* species, a 20% difference (Table 4, model "Gregariousness+Body").

Table 4: Models of log brain (g) on log body (g) and gregariousness. $n_{species} = 75$. Root depth of the tree is 44.8 myr, see Figure S1.[a]

Model	$t_{1/2}$ (myr) (Support region)		$\sigma_y^2/2\alpha$ ((log brain (g))^2) (Support region)		Optima			R^2 (%)	logL	AICc
					Intercept		log body (g)			
Allometry	4.99	(0, 30)	0.04	(0.03, 0.09)	5.01 ±0.03		0.61 ±0.02	91.72	7.47	-6.37
					Gregarious	Solitary				
Gregariousness	41.26	(12.38, ∞)	1.02	(0.43, ∞)	5.66 ±0.50	1.03 ±0.84		25.61	-61.8	132.23
Gregariousness+Body	4.48	(0, 32.4)	0.04	(0.02, 0.09)	5.08 ±0.04	4.90 ±0.06	0.58 ±0.02	92.42	9.90	-8.92

[a] See note in Table 2.

Neocortex size was also fitted on the social categorizations of *gregarious* and *solitary*. Again there is a large discrepancy in the primary optima of *gregarious* and *solitary* species in terms of absolute brain size, which is likely caused by discrepancy in body size. When we account for body size, the optimal neocortex size for *gregarious* species is $e^{9.74-9.48} = 1.30$ times larger than for *solitary* species (Table 5, model "Gregariousness+Brain"). While there is considerable phylogenetic effect in the allometry model, the phylogenetic effect drops considerably when gregariousness is included, as $t_{1/2} = 5.7$ myr, which is 21 % of the total tree depth (Table 5).

Table 5: Models of log neocortex (mm^2) on log body (g) and gregariousness. $n_{species} = 42$. Root depth of the tree is 27.19 myr, see Figure S7.[a]

Model	$t_{1/2}$ (myr)		$\sigma^2_y/2\alpha$ ([b,c])		Optima			R^2 (%)	logL	AICc
	(Support region)		(Support region)		Intercept		log brain (g)			
Allometry	∞	(2.14, ∞)	∞^c	(0.02, ∞)	9.69 ±0.10		0.86 ±0.04	90.88	15.5	-21.97
					Gregarious	Solitary				
Gregariousness	∞	(8.10, ∞)	0.67	(0.20, ∞)	10.17 ±0.27	4.95 ±1.03		35.25	-23.7	56.44
Gregariousness+Brain	5.73	(0, ∞)	0.02	(0.01, ∞)	9.74 ±0.04	9.48 ±0.07	0.78 ±0.04	93.86	18.1	-24.49

[a] See note in Table 2.

[b] The equilibrium variances are in units (log neocortex(mm^2))^2

[c] $\sigma^2_y = 0.002$ for the "Allometry" model, in units (log neocortex(mm^2))$^2 myr^{-1}$.

Next, I fitted optimal brain size on a different social category system, where *solitary* species are found primarily alone or in pairs, *intermediate-sized* groups are aggregations of 3-50 individuals, and *large* represents species with a group size larger than fifty (Caro *et al.*, 2004). For these models, two species (*Bison bonasus* and *Elaphurus davidianus*) were excluded due to lack of precise data on typical group sizes. There are large discrepancies between the primary optima on absolute brain size; however this is likely mostly because brain size correlates with body size. While the model fit favours the Allometry model (Table 6), there are some differences between the primary optima when accounting for body size. Notably *solitary* species have the smallest optimum, and e.g. the *intermediate* group has a $e^{5.10-4.85} = 1.28$ times larger optimal brain size than *solitary* species (Table 6, model "Groups+Body").

Table 6: Models of log brain (g) on social categories (Caro *et al.*, 2004). $n_{species} = 73$. Root depth of the tree is 44.8 myr, see Figure S2.[a]

Model	$t_{1/2}$ (myr)		$\sigma^2_y/2\alpha$ ([b])		Optima						R^2 (%)	logL	AICc
	(Support region)		(Support region)		Intercept					log brain (g)			
Allometry	5.20	(0, 32.92)	0.04	(0.03, 0.10)	5.00 ±0.04					0.61 ±0.02	91.5	6.89	-5.20
					S	S+I	I	I+L	S+I+L				
Groups	16.16	(7.62, 144.76)	0.39	(0.26, 2.47)	2.98 ±0.38	2.20 ±0.67	5.92 ±0.49	5.60 ±0.28	2.96 ±0.80		47.5	-50.21	116.14
Groups+Body	5.56	(1.5, 39.5)	0.04	(0.03, 0.11)	4.85 ±0.08	5.00 ±0.15	5.10 ±0.10	5.06 ±0.06	4.93 ±0.16	0.58 ±0.03	91.9	9.15	-0.05

[a] See note in Table 2. The group-size categories are Solitary (S), Intermediate (I) and Large (L), plus combinations of the three.

[b] The equilibrium variances are in units (log brain (g))^2

I initally fitted the neocortex as an OU model on group-size categories, however the estimated optima for the different group categories were far outside the observed range of biological variation. The models of neocortex on group-size categories have long phylogenetic half-lives, several times longer than the total tree length (27 myr, Table 7). When the trait model is approximately a Brownian motion, the optima can be reparameterized and the model interpreted as a Brownian motion with one or more trends. Since the species in the analyses are all extant, we can not predict the absolute direction of any single trend. For example, the trend for the *solitary* group size is $\tau_S = 7.92 \log \text{brain(g)} \cdot (100\text{myr})^{-1}$, (Table 7, model "Groups+Body") is the expected change in neocortex size per hundred million years. Since all of the species

included in the model are extant, and we don't have a true time series and the single trend is not in itself meaningful (Hansen, 1997). We can compare the contrast in trends between the groups, however, and e.g. the *solitary* species are expected to increase neocortex size by $e^{\frac{7.92-6.24}{100}} = 1.017\text{myr}^{-1}$ times, or 1.7% myr^{-1} relative to species of *intermediate* group sizes. While this is the opposite direction compared with the brain-size models (Table 6), the model fit of the neocortex model is quite poor. Interestingly, while the group-size categories account for 47.5 % of variation in absolute brain size (Table 6, model "Groups"), the categories only account for 11.8 % of variation in neocortex size (Table 7, model "Groups"). This is in contrast to the gregariousness models, where gregariousness seemed to better explain absolute neocortex size than absolute brain size (Tables 4 and 5, model "Gregariousness").

Table 7: Models of log neocortex (mm^2) on social categories (Caro *et al.*, 2004). $n_{species} = 42$. Root depth of the tree is 27.19 myr, see Figure S8.[a]

Model	$t_{1/2}$ (myr)		$\sigma_y^2/2\alpha$ [b,c]		Optima						R^2 (%)	logL	AICc
	(Support region)		(Support region)		Intercept					log brain (g)			
Allometry	∞	(2.14, ∞)	∞	(0.02, ∞)	9.69 ±0.10					0.86 ±0.04	90.88	15.5	-21.97
					Trend $\tau = 100 \cdot \alpha\theta$ (100 myr^{-1})								
					τ_S	τ_{S+I}	τ_I	τ_{I+L}	τ_{S+I+L}				
Groups	∞	(14.32, ∞)	∞	(0.35, ∞)	5.14 ±3.03	-1.22 ±6.88	1.53 ±2.35	0.00 ±7.75	11.45 ±6.82		11.77	-29.6	76.53
Groups+Body	109.53	(1.37, ∞)	0.29	(0.01, ∞)	7.92 ±1.00	6.29 ±2.05	6.24 ±0.73	6.11 ±0.06	9.30 ±2.10	0.84 ±0.04	92.01	17.84	-15.32

[a] See note in Table 2. The group-size categories are Solitary (S), Intermediate (I) and Large (L), plus combinations of the three.
[b] The equilibrium variances are in units (log neocortex (mm^2))^2.
[c] $\sigma_y^2 = 0.002$ for the "Allometry" model, $\sigma_y^2 = 0.002$ for the "Groups" model, in units (log neocortex(mm^2))$^2\text{myr}^{-1}$.
[d] The trend (τ) is the expected change in neocortex size per hundred million years.

Finally, I fitted models of brain size and neocortex size on the mean group size during the breeding season. For these models, data on mean group size were not available for all species, so the evolutionary allometry had to be estimated again in order to compare likelihoods. The mean group size during the breeding season seems to predict both absolute brain size and absolute neocortex size. This is likely only because it positively correlates with body size. The group size does not seem to influence either relative brain size or relative neocortex size, as the effect sizes are in both cases near, and within, one standard error of zero (Table 8 and 9, model "Group size+Body" and "Group size+Brain").

Table 8: Models of log brain (g) on log body (g) and log mean group size during the breeding season. $n_{species} = 42$. Root depth of the tree is 23.9 myr, see Figure S3.[a]

Model	$t_{1/2}$ (myr)		$\sigma_y^2/2\alpha$ ((log brain(g))^2)[b]		Optima			R^2 (%)	logL	AICc
	(Support region)		(Support region)		Intercept	log body (g)	log group size			
Allometry	9.53	(0, ∞)	0.02	(0.01, ∞)	5.03 ±0.04	0.59 ±0.02		95.1	15.4	-21.73
Group size	∞	(25.57, ∞)	∞	(0.54, ∞)	5.14 ±0.31		0.31 ±0.08	27.9	-32.51	74.11
Group size+Body	14.04	(0, ∞)	0.03	(0.01, ∞)	5.02 ±0.05	0.60 ±0.03	-0.02 ±0.03	94.8	15.6	-19.62

[a] See note in Table 2.
[b] $\sigma_y^2 = 0.003$ for the "Group size" model, in units (log brain(g))$^2\text{myr}^{-1}$.

Table 9: Models of log neocortex (mm^2) on body mass (g) and log mean group size during the breeding season. $n_{species} = 35$. Root depth of the tree is 23.9 myr, see Figure S9.[a]

Model	$t_{1/2}$ (myr)		$\sigma^2_y/2\alpha$ ([b,c])		Optima			R^2 (%)	logL	AICc
	(Support region)		(Support region)		Intercept	log brain (g)	log group size			
Allometry	8.60	(0, ∞)	0.02	(0.01, ∞)	9.64 ±0.04	0.89 ±0.04		94.59	15.9	-22.45
Group size	∞	(13.07, ∞)	∞	(0.33, ∞)	9.83 ±0.33		0.26 ±0.08	24.22	-24.3	58.02
Group size+Brain	7.96	(0, ∞)	0.02	(0.01, ∞)	9.64 ±0.04	0.89 ±0.04	0.003 ±0.03	94.65	15.9	-19.72

[a] See note in Table 2.

[b] The equilibrium variances are in units (log neocortex (mm^2))^2.

[c] $\sigma^2_y = 0.020$ for the "Group size" model, in units (log neocortex(mm^2))^{2}myr^{-1}.

3.5 Diet

I modeled optimal brain size as a function of dietary regimes. Taking into account body size, grazers have the largest optimal brain size, $e^{5.12-4.98} = 1.15$ times or 15% larger than mixed feeders (Table 10, model "Diet+Body"). If we take the standard errors into account, however, the optima all overlap, and the model fit is very poor, both in terms of absolute and relative brain size. It seems that diet does not influence optimal brain size.

Table 10: Models of log brain (g) on log body (g) and dietary regimes. $n_{species} = 75$. Root depth of the tree is 44.8 myr, see Figure S4.[a,b]

Model	$t_{1/2}$ (myr)		$\sigma^2_y/2\alpha$ ((log brain(g))^2)[c]		Optima				R^2 (%)	logL	AICc
	(Support region)		(Support region)		Intercept			log body (g)			
Allometry	4.99	(0, 30)	0.04	(0.03, 0.09)	5.01 ±0.03			0.61 ±0.02	91.72	7.47	-6.37
					Browsers	Grazers	Mixed feeders				
Diet+Body	0	(0, 18.75)	0.04	(0.02, 0.07)	5.05 ±0.05	5.12 ±0.07	4.98 ±0.03	0.60	93.21	8.11	-2.98
					Trend $\tau = 100 \cdot \alpha\theta$ (100 myr^{-1})						
					τ_{Br}	τ_{Gr}	τ_{Mf}				
Diet	∞	(20.4, ∞)	∞	(0.78, ∞)	-0.17 ±1.87	3.47 ±3.26	0.001 ±0.0003		1.59	-71.40	153.67

[a] See note in Table 2.

[b] The trend (τ) is the expected change in brain size per hundred million years.

[c] $\sigma^2_y = 0.037$ for the "Diet" model, in units (log brain(g))^{2}myr^{-1}.

The models of optimal neocortex size conflict with the previous model, in that the optimal neocortex is larger for mixed feeders than grazers, by a factor of $e^{9.76-9.38} = 1.46$ (Table 11, model "Diet+Body"). While the models of neocortex on dietary behaviour have bad model fit, and again the optima are similar with overlapping standard errors, indicating that relative neocortex size is likely not influenced by diet (Table 11).

Table 11: Models of log neocortex (mm^2) on log brain (g) and dietary regimes. $n_{species} = 42$. Root depth of the tree is 27.19 myr, see Figure S10.[a]

Model	$t_{1/2}$ (myr)	(Support region)	$\sigma_y^2/2\alpha$ ([b,c])	(Support region)	Optima				R^2 (%)	logL	AICc
					Intercept			log brain (g)			
Allometry	∞	(2.14, ∞)	∞	(0.02, ∞)	9.69 ±0.10			0.86 ±0.04	90.88	15.5	-21.97
					Browsers	Grazers	Mixed feeders				
Diet+Body	39.11	(0, ∞)	0.06	(0.01, ∞)	9.36 ±0.31	9.38 ±0.46	9.76 ±0.11	0.87 ±0.04	91.47	16.1	-17.81
					Trend $\tau = 100 \cdot \alpha\theta$ ($100\ myr^{-1}$)						
					τ_{Br}	τ_{Gr}	τ_{Mf}				
Diet	∞	(15.71, ∞)	∞	(0.4, ∞)	-0.68 ±1.81	3.91 ±2.60	0.0007 ±0.0000		7.43	-30.62	72.91

[a] See note in Table 2.
[b] The equilibrium variances are in units (log neocortex (mm^2))^2. The trend (τ) is the expected change in neocortex size per hundred million years.
[c] $\sigma_y^2 = 0.021$ for the "Diet" model, in units (log neocortex(mm^2))$^2 myr^{-1}$.

3.6 Habitat

I fitted models of brain size evolution in relation to habitat types. While it seems at first glance that the optimal brain size for open habitats is $e^{5.01-4.89} = 1.13$ times or 13% larger than for closed habitats, habitat explains for very little variation in brain size and there is not sufficient evidence for the that habitat has an impact on brain size.

Table 12: Models of log brain (g) on log body (g) and habitat types. $n_{species} = 75$. Root depth of the tree is 44.8 myr, see Figure S5.[a,b]

Model	$t_{1/2}$ (myr)	(Support region)	$\sigma_y^2/2\alpha$ (log brain(g))^2	(Support region)	Optima				R^2 (%)	logL	AICc
					Intercept			log body (g)			
Allometry	4.99	(0, 30)	0.04	(0.03, 0.09)	5.01 ±0.03			0.61 ±0.02	91.72	7.47	-6.37
					CH	OH	MH				
Habitat+Body	5.20	(0, 25.36)	0.04	(0.03, 0.08)	4.89 ±0.09	5.01 ±0.05	5.06 ±0.07	0.61 ±0.05	91.88	8.51	-3.79
					Trend $\tau = 100 \cdot \alpha\theta$ ($100\ myr^{-1}$)						
					τ_{CH}	τ_{OH}	τ_{MH}				
Habitat	∞	(17.92, ∞)	∞^c	(0.7, ∞)	-0.91 ±2.10	0.003 ±0.0005	2.80 ±2.26		3.34	-70.73	152.34

[a] See note in Table 2.
[b] The abbreviated optima are closed habitat (CH), open habitat (OH) and mixed habitat (MH). The trend (τ) is the expected change in brain size per hundred million years.
[c] $\sigma_y^2 = 0.036$ for the "Habitat" model, in units (log brain(g))$^2 myr^{-1}$.

The models of neocortex size on habitat show that the optimal relative neocortex size is largest for the open habitats (Table 13, model "Habitat+Body") at $e^{9.78} = 17677$ mm^2 given a brain size of about 160 g. The optimal relative neocortex sizes for closed and mixed habitats are estimated with high error, and they are slightly outside the natural variation of neocortex size. For this reason, and that there is no attraction toward the optimum ($t_{1/2} = \infty$), I reparameterized the optima as trends, but the optima estimates are not very far outside the natural variation in

brain size. Overall, habitat does not seem to adequately explain variation in relative neocortex size.

Table 13: Models of log neocortex (mm^2) on log brain (g) and habitat types. $n_{species} = 42$. Root depth of the tree is 27.19 myr, see Figure S11.[a]

Model	$t_{1/2}$ (my)		$\sigma_y^2/2\alpha$ [b,c]		Optima				R^2 (%)	logL	AICc
	(Support region)		(Support region)		Intercept			log brain (g)			
Allometry	∞	(2.14, ∞)	∞	(0.02, ∞)	9.69 ±0.10			0.86 ±0.04	90.88	15.5	-21.97
					Trend $\tau = 100 \cdot \alpha\theta$ (100 myr^{-1})						
					τ_{CH}	τ_{OH}	τ_{MH}				
Habitat+Body	∞	(0, ∞)	∞	(0.02, ∞)	1.96 ±0.68	2.64 ±0.03	1.70 ±0.65	0.87 ±0.04	91.50	16.7	-19.05
Habitat	∞	(16.37, ∞)	∞	(0.44, ∞)	1.15 ±2.32	0.002 ±0.0000	-0.20 ±2.25		0.69	-32.1	75.85

[a] See note in Table 2. The abbreviated optima are closed habitat (CH), open habitat (OH) and mixed habitat (MH). The trend (τ) is the expected change in neocortex size per hundred million years.
[b] The equilibrium variances are in units (log neocortex (mm^2))^2.
[c] $\sigma_y^2 = 0.002$ for the "Allometry" model, $\sigma_y^2 = 0.002$ for the "Habitat+Brain" model, $\sigma_y^2 = 0.023$ for the "Habitat" model, in units (log neocortex(mm^2))$^2 myr^{-1}$.

3.7 Dimorphism

The sexual dimorphism variable was estimated with large error for nearly all species. Because of this, the optima of the models that included sexual dimorphism were very sensitive to the inclusion of observational error, and the bias-correction gave a much steeper slope on dimorphism. According to this model, ungulates that exhibit a more positive (i.e. males are larger than female) sexual dimorphism have a larger optimal brain size.

Table 14: Models of log brain (g) on log body (g) and sexual dimorphism. $n_{species} = 68$. Root depth of the tree is 44.8 myr, see Figure S6.[a]

Model	$t_{1/2}$ (myr)		$\sigma_y^2/2\alpha$ ((log brain(g))^2)		Optima			R^2 (%)	logL	AICc
	(Support region)		(Support region)		Intercept	log body (g)	dimorphism (z^b)			
Allometry	3.71	(0, 17.25)	0.04	(0.03, 0.07)	5.01 ±0.03	0.62 ±0.02		91.66	4.78	-0.93
Dimorphism	46.39	(7.14, ∞)	1.4	(0.45, ∞)	3.94 ±0.53		3.94 ±0.09	8.01	-66.59	141.82
Dimorphism[c]	-	-	-	-	4.51 ±0.53		0.93 ±0.38	-	-	-
Dimorphism+Body	3.62	(0, 15.88)	0.04	(0.03, 0.07)	4.94 ±0.03	0.60 ±0.02	0.47 ±0.04	91.77	5.13	0.70
Dimorphism+Body[c]	-	-	-	-	4.99 ±0.04	0.60 ±0.02	0.13 ±0.15	-	-	-

[a] See note in Table 2.
[b] The sexual dimorphism variable is the log ratio of the body mass between the sexes, $z = \bar{m} - \bar{f}$, where $\bar{m}$ and $\bar{f}$ are the within-species means in body mass for males and females, respectively, after natural-log transformation.
[c] These models show the optima that have not been corrected for bias using the attenuation factor $\mathbf{K}$.

The models of neocortex on dimorphism are consistent with those of brain size; the bias-correction gives very different regression coefficients, but the model fit is poor. Relative neocortex size is likely not influenced by sexual dimorphism (Table 15).

Table 15: Models of log neocortex (mm^2) on log brain (g) and sexual dimorphism. $n_{species} = 37$. Root depth of the tree is 27.19 myr, see Figure S12.[a]

Model	$t_{1/2}$ (myr)		$\sigma^2_y/2\alpha$ [b,d]		Optima			R^2 (%)	logL	AICc
	(Support region)		(Support region)		Intercept	log brain (g)	dimorphism (z^b)			
Allometry	27.5	(0, ∞)	0.05	(0.02, ∞)	9.68 ±0.08	0.86 ±0.04		91.21	10.82	-12.39
Dimorphism	∞	(7.86, ∞)	∞	(0.33, ∞)	9.59 ±0.38		1.23 ±0.15	1.33	-31.99	73.22
Dimorphism[c]	-	-	-	-	9.70 ±0.39		0.36 ±0.51	-	-	-
Dimorphism+Brain	30.77	(0, ∞)	0.05	(0.02, ∞)	9.58 ±0.08	0.83 ±0.04	0.73 ±0.06	91.69	11.87	-11.81
Dimorphism+Brain[c]	-	-	-	-	9.64 ±0.08	0.85 ±0.04	0.25 ±0.17	-	-	-

[a] See note in Table 2.

[b] The equilibrium variances are in units (log neocortex (mm^2))^2. The sexual dimorphism variable is the log ratio of the body mass between the sexes, $z = \bar{m} - \bar{f}$, where $\bar{m}$ and $\bar{f}$ are the within-species means in body mass for males and females, respectively, after natural-log transformation.

[c] These models show the optima that have not been corrected for bias using the attenuation factor $\mathbf{K}$.

[d] $\sigma^2_y = 0.024$ for the "Dimorphism" model, in units (log neocortex(mm^2))$^2 myr^{-1}$.

3.8 Gestation time

The model of brain size on gestation time showed a slight negative slope when body size was accounted for. However, the model fit is poor and relative brain size is likely not influenced by gestation time.

Table 16: Models of log brain (g) on log body (g) and gestation time (days). $n_{species} = 74$. Root depth of the tree is 44.8 myr. The tree used is equivalent to Figure S1, minus *Cephalophus nigrifrons*.[a]

Model	$t_{1/2}$ (myr)		$\sigma^2_y/2\alpha$ ((log brain(g))^2)		Optima			R^2 (%)	logL	AICc
	(Support region)		(Support region)		Intercept	log body (g)	log gestation (days)			
Allometry	4.22	(0, 21.43)	0.04	(0.03, 0.08)	5.01 ±0.03	0.62 ±0.02		92.12	7.37	-6.15
Gestation	19.02	(6.25, ∞)	0.50	(0.27, ∞)	4.65 ±0.29		2.43 ±0.35	38.89	-56.44	121.46
Gestation+Body	3.90	(0, 19.35)	0.04	(0.02, 0.07)	5.01 ±0.03	0.63 ±0.03	-0.11 ±0.18	92.29	7.56	-4.23

[a] See note in Table 2.

The models of neocortex on gestation time also indicate that a longer gestation time predicts a smaller relative brain size. Although the model fit for this model is good, it is likely very sensitive to a few outliers that have small relative neocortex size and long gestation time (*Giraffa camelopardalis*, *Okapia johnstoni*, *Syncerus caffer*), see Figure 5. If these three species are removed from the model, the effect size of the gestation variable is much smaller, although still negative, and the allometry model is favoured by AICc.

Table 17: Models of log neocortex (mm^2) on log brain (g) and gestation time (days). $n_{species} = 41$. Root depth of the tree is 27.19 myr. The tree used is equivalent to Figure S7, minus *Cephalophus nigrifrons*.[a]

Model	$t_{1/2}$ (myr)		$\sigma^2_y/2\alpha$ [b]		Optima			R^2 (%)	logL	AICc
	(Support region)		(Support region)		Intercept	log brain (g)	log gestation (days)			
Allometry	∞	(0, ∞)	∞[c]	(0.02, ∞)	9.69 ±0.10	0.86 ±0.04		91.00	14.53	-19.95
Gestation	37.32	(5.24, ∞)	0.53	(0.18, ∞)	9.58 ±0.25		1.58 ±0.33	35.82	-24.20	57.51
Gestation+Body	3.61	(0, ∞)	0.02	(0.01, ∞)	9.67 ±0.03	0.97 ±0.05	-0.43 ±0.17	94.28	16.61	-21.50

[a] See note in Table 2.

[b] The equilibrium variances are in units (log neocortex (mm^2))^2.

[c] $\sigma^2_y = 0.002$ for the "Allometry" model, in units (log neocortex(mm^2))^2myr^{-1}.

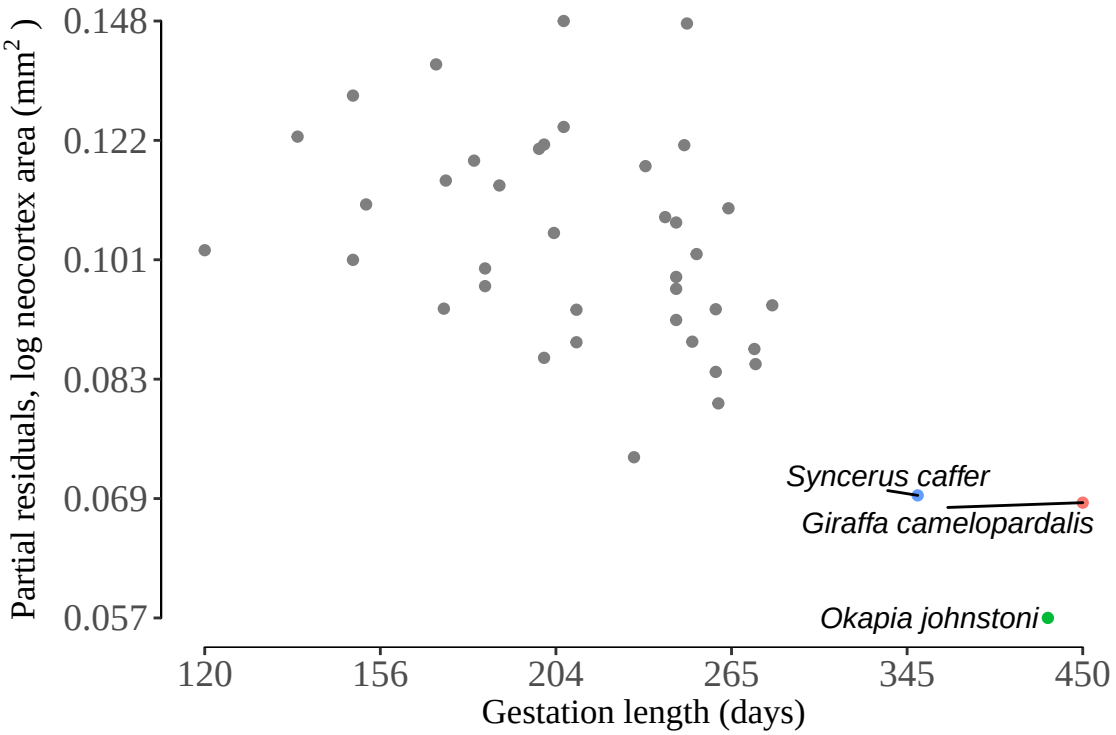

Figure 5: Scatter plot of partial residuals of neocortex size on brain size and gestation length, with highlighted outliers. The partial residuals are defined as $\mathbf{Y} - \mathbf{X}\hat{\theta} + \mathbf{X}_{\text{gestation}}\hat{\theta}_{\text{gestation}}$, see model "Gestation+Body", Table 17. Each point is a species, n = 41.

3.9 Metabolic rate

I fitted brain size as a function of body size and metabolic rate. This model included few species ($n = 16$) even when incorporating domesticated species (*Sus scrofa*, *Bos taurus*) and *Pecari tajacu*, that were excluded in prior analyses. The body size and metabolic rate variables were centered on their means prior to model fit, which means that the intercept is the optimal brain size for a species with 82.5 kg body mass and/or 81.5 watts basal metabolic rate. Metabolic rate is a very good predictor of brain size, almost as good as body size. While the joint model of

brain size on metabolic rate and body size accounts for more variation than the allometry model (Table 18), and the partial effect size of BMR is not zero, the AICc still favours the allometry model. Does relative brain size correlate with metabolic rate? Possibly, but the sample size is too low to make an informed judgement.

Table 18: Models of log brain (g) on log body (g) and mean log basal metabolic rate (watt). $n_{species} = 16$. Root depth of the tree is 67.23 myr, see Figure S13.[a]

Model	$t_{1/2}$ (myr)		$\sigma_y^2/2\alpha$ ((log brain(g))^2)		Optima			R^2 (%)	logL	AICc
	(Support region)		(Support region)		Intercept	log body (g)	log BMR (watt)			
Allometry	7.90	(0, ∞)	0.02	(0.01, ∞)	5.24 ±0.05	0.57 ±0.03		96.67	5.81	0.02
BMR	0	(0, 26.19)	0.05	(0.03, 0.12)	5.24 ±0.06		0.81 ±0.05	93.36	0.63	10.39
BMR+Body	0	(0, 76.90)	0.02	(0.01, 0.06)	5.25 ±0.04	0.40 ±0.09	0.25 ±0.13	97.30	7.55	0.90

[a] See note in Table 2.

4 Discussion

Using Ornstein-Uhlenbeck models of evolution in brain size and neocortex size, I have investigated the empirical basis for various adaptive hypotheses in artiodactyls, as well as the effects of evolutionary constraints due to shared ancestry. Examining relative brain size in 75 species and relative neocortex size in 42 species, I find that there is evidence, albeit weak, for the social-brain hypothesis. I did not find evidence that relative brain size or relative neocortex size is influenced by group size during the breeding season, diet, habitat, sexual dimorphism, gestation length or basal metabolic rate. Within species, I found that females on average have a larger relative brain size than that of males. While both absolute brain size and absolute neocortex size exhibit phylogenetic signal, this is likely only due to phylogenetic signal in body size and phylogenetically-structured adaptive regimes such as *gregariousness*.

4.0.1 What does brain size mean?

One important subject when studying brain size is assessing the biological function of brain size. The brain is the center of the nervous system and wields control of the other organs of the body, behaviour and thoughts (Striedter, 2005). While there are many definitions of intelligence (Legg & Hutter, 2007), the general criteria for intelligence are functions for which the brain is responsible. In humans, brain size is positively (but weakly) correlated with general mental ability (Galton, 1889) and general intelligence (g) (Ritchie *et al.*, 2015). Unfortunately, there is no universal test for general intelligence in non-human mammals, but absolute and relative brain size has been shown to predict problem-solving ability in carnivores (Benson-Amram *et al.*, 2016).

4.0.2 Evolutionary allometry

As demonstrated with the use of constraint models in an Ornstein-Uhlenbeck framework, the allometric slope of brain size on body size in Artiodactyla is about $b = 0.61 \pm 0.02$ (Table 2, model "Allometry"). This result is indistinguishable from a non-phylogenetic least-squares regression model. Since the phylogenetic half-life for the allometry model is short (5 Myr, Table 2, model "Allometry"), we can conclude that relative brain size in artiodactyls evolves rapidly on evolutionary timescales and is not constrained by phylogenetic relatedness. I also observed that the Ornstein-Uhlenbeck parameter estimates for the allometry models, including the optima, were in general robust to the incorporation of observational error in the model. This is likely due to the large variation in body size in artiodactyls, meaning that the within-species observational errors are small relative to the among-species variation. Oboussier & Schliemann (1966) used the ordinary least-squares method and found that the evolutionary allometric slope is $b = 0.56$ in bovids ($n = 35, \mathrm{R}^2 = 96\%$), while my estimate for bovids is $b = 0.59 \pm 0.02$ ($n = 46, \mathrm{R}^2 = 96\%$) using an Ornstein-Uhlenbeck model. Both are slightly shallower than the allometric slope in Artiodactyla, and this is expected at lower taxonomic levels (Martin & Harvey, 1985). Primates are in general more encephalized, as Isler *et al.* (2008) found the allometric slope of ECV

(endocranial volume) on body mass is $b = 0.77$ using the ordinary least-squares method, and $b = 0.57$ using the independent contrasts method (Felsenstein, 1985). Curiously, recent analysis of endocranial volume on body mass in primates using Ornstein-Uhlenbeck constraint models presents an allometric slope of $b = 0.60 \pm 0.02$, where $t_{1/2} = \infty$ (Grabowski *et al.*, 2016), almost identical to the evolutionary allometric slope in artiodactyls. The evolutionary allometric slope is slightly shallower in cichlid fishes, with $b = 0.50 \pm 0.03$ (Tsuboi *et al.*, 2016) estimated using phylogenetic generalized least squares (Grafen, 1989) with a model based on the Brownian motion.

4.0.3 Adaptation

I found that *gregarious* species had 20 % larger relative brain size than *solitary* species, in agreement with the reported 22 % from Pérez-Barbería & Gordon (2005). This effect also manifested itself in relative neocortex size, and while this resembles results from Shultz & Dunbar (2006), they used measurements of both the area and the mass of the neocortex. In this study the measurements of neocortex were in surface area (mm^2) exclusively. While the *gregariousness* models are the best-fitting models, there is a problem in terms of interpreting the biological significance of the distinction between *gregarious* and *solitary* species. The species were categorized as *solitary* if, year-round, they have a mean group size of fewer than six individuals, and *gregarious* if the mean group size is six or more individuals. This can seem like an arbitrary divide, however, since it does not seem to be based on any biological hypothesis. Clutton-Brock *et al.* (1980) used a similar description in their study of antlers in cervids, where species were categorized according to group sizes $\leqslant 2$, $3-5$ or $\geqslant 6$ in the breeding season. I did find some evidence, if weak, that brain size is smaller in species that are solitary or living in pairs (Table 6, model "Groups+Body"). Considering these results, it was peculiar that group size showed no influence on relative brain size or relative neocortex size, however the group sizes were explicitly reported during the breeding season, and as such they may be confounded with mating systems. I argue that, based on the evidence in artidoactyls, having a larger relative size of brain and neocortex is an adaptive response to living in a more social environment. The social-brain hypothesis has been tested extensively in primates (Dunbar & Shultz, 2007), but recent analysis has found that the relative brain size in primates is better explained by diet, and not sociality (DeCasien *et al.*, 2017). In squirrels, sociality is a good predictor of absolute brain size, but not relative brain size (Matějů *et al.*, 2016).

A positive correlation between relative brain size and gestation time has previously been demonstrated in ungulates (Pérez-Barbería & Gordon, 2005), however this study included elephants and perissodactyls (*Tapirus indicus*, *Tapirus bairdii*, *Rhinoceros bicornis*, *Equus burchelli*). Elephants are larger than all ungulates in terms of body mass, their brain size deviates positively from the allometric relationship in respect to ungulates (Pérez-Barbería & Gordon, 2005), and they have a long gestation time with at around 640 days (Lueders *et al.*, 2012). I found that gestation time is not a good predictor of relative brain size; one possible reason for this incongruent result is that I did not include the aforementioned species,

particularly the elephant which is an outlier. Initially, I found that there was a negative relationship between relative neocortex size and gestation time (Table 17). However, this model is likely sensitive to a few species that have small relative neocortex size and long gestation time (*Giraffa camelopardalis*, *Okapia johnstoni*, *Syncerus caffer*). I suspect that the influence of gestation time on relative brain size and relative neocortex size is sensitive to these extreme outliers, and that it is difficult to justify the maternal investment hypothesis in artiodactyls.

Sexual dimorphism did not show any influence on relative brain size or relative neocortex size, and it does not seem as if the brain is a sexually selected trait. Still, it would be adviseable to further investigate relationships with other measures of sexual selection, e.g. horns in bovids, antlers in cervids, mating displays or hormonal differences between the sexes.

Relative brain size and relative neocortex size was not influenced by habitat or diet. It does not seem like brain size is larger in species that live in open habitats, even if they need to potentially process more visual information. As diet has been found to predict relative brain size in primates (DeCasien *et al.*, 2017), more specifically the amount of fruit intake, this negative result was surprising. One explanation could be that primates also eat more diverse food groups that are high in nutrients such as fruits and meat. As far as the macronutritional content is concerned, it is likely that grazers and browsers are not sufficiently differentiated as is the case with frugivory in primates. Pérez-Barbería & Gordon (2005) tested if frugivorous ungulates are more encephalized relative to body size, but found no correlation.

4.0.4 Historical constraints

While brain size in ungulates have been studied using phylogenetic models before, there have been used different frameworks and statistical implementations (Pérez-Barbería & Gordon, 2005; Shultz & Dunbar, 2006, 2010; Pérez-Barbería *et al.*, 2007). Since the application of Ornstein-Uhlenbeck models in studying ungulate brain evolution is novel, there are challenges when comparing the different trait models. One commonly used metric for assessing phylogenetic effect is the phylogenetic heritability (λ) (Lynch, 1991; see also Pagel, 1999), which is a modification of the phylogenetic variance-covariance matrix. If $\lambda = 1$ then the phylogenetic variance-covariance matrix is unaltered from the original model of evolution, usually a Brownian motion, and if $\lambda = 0$ then there are no correlated residuals and the expression of the trait is not associated with the phylogeny. Shultz & Dunbar (2006) found that brain size exhibits a strong phylogenetic signal for various models ($0.69 \geqslant \lambda \geqslant 0.86$). On the contrary, I find that for all models of brain size that include body size as a covariate, the phylogenetic half-lives are quite short and the regression coefficients are in most cases nearly indistinguishable from non-phylogenetic models. While Shultz & Dunbar (2006) found that there was no evident phylogenetic signal in relative neocortex size ($\lambda = 0$), it is unclear whether they meant relative neocortex in terms of scaling with body size, or in terms of scaling with brain size. I find that the neocortex evolves according to a Brownian motion if modeled as a function of brain size, but not if modeled as a function of body size (Table 3). One possible explanation for this may be that, in my dataset, the neocortex size was measured with better precision than both brain and body size, and that brain size

was measured with better precision than body size. If the observational error is much larger than the correlated errors expected due to historical constraints, the model estimates may be biased in favour of phylogenetically independent evolution. One problem is that there are too few observations to estimate the phylogenetic half-life in neocortex models with good precision, and in some cases the marginal support regions span the entire positive number line (Table 3). Another reason for incongruent results could be that previous studies have used phylogenetic cladograms based on both molecular and morphological markers, while I used a phylogenetic tree with fossil time calibration of branch lengths (Toljagić *et al.*, 2017).

4.1 Further work

The biggest improvement studies of brain size would most likely be to measure additional brains, particularly in species where sampling is bad or non-existent. While targeting wild, healthy adults to kill and study the brain (as in Oboussier & Schliemann, 1966) can be prohibitively expensive or even unethical, it is also possible to measure the endocranial volume in museum specimens as a proxy for brain size (Pérez-Barbería & Gordon, 2005). The lack of original measurements and too much reliance on literature data is a typical problem in comparative studies of brain size (Smith & Jungers, 1997; Healy & Rowe, 2007). There is more available literature data on brain size and neocortex size in artiodactyls, particularly in gazelles, and a relatively easy improvement would be to expand or create a larger phylogenetic tree using DNA sequences from a database (e.g. NCBI Resource Coordinators, 2017) to incorporate these species in the phylogenetic analyses. The mixed-effect models used to determine the influence of sex on brain size are potentially not suited for this kind of analysis, since the species are not modeled with a phylogenetic covariance structure, and are assumed to be independent. Since relative brain size seems to have evolved rather independently of phylogenetic relationships in artiodactyls (Table 2), this may not be a problem, but a more correct approach would be to fit a mixed-effect model with an Ornstein-Uhlenbeck covariance structure among the species groups to test whether the assumption holds. Unfortunately, there is no software that can fit this kind of model at present time.

5 References

Anderson, A.E., Medin, D.E. & Bowden, D.C. 1974. Growth and morphometry of the carcass, selected bones, organs, and glands of mule deer. *Wildlife Monographs* **39**: 3–122.

Bartoszek, K., Pienaar, J., Mostad, P., Andersson, S. & Hansen, T.F. 2012. A phylogenetic comparative method for studying multivariate adaptation. *Journal of Theoretical Biology* **314**: 204–215. https://doi.org/10.1016/j.jtbi.2012.08.005.

Bates, D., Maechler, M., Bolker, B. & Walker, S. 2015. Package lme4. *Journal of Statistical Software* **67**: 1–91. https://doi.org/http://lme4.r-forge.r-project.org.

Benson-Amram, S., Dantzer, B., Stricker, G., Swanson, E.M. & Holekamp, K.E. 2016. Brain size predicts problem-solving ability in mammalian carnivores. *Proceedings of the National Academy of Sciences* **113**: 2532–2537. https://doi.org/10.1073/pnas.1505913113.

Bercovitch, F.B. & Berry, P.S.M. 2010. Ecological determinants of herd size in the Thornicroft's giraffe of Zambia. *African Journal of Ecology* **48**: 962–971. https://doi.org/10.1111/j.1365-2028.2009.01198.x.

Bro-Jørgensen, J. 2007. The intensity of sexual selection predicts weapon size in male bovids. *Evolution* **61**: 1316–1326. https://doi.org/10.1111/j.1558-5646.2007.00111.x.

Butler, M.A. & King, A.A. 2004. Phylogenetic comparative analysis: a modeling approach for adaptive evolution. *American Naturalist* **164**: 683–695. https://doi.org/10.1086/426002.

Byrd, R.H., Lu, P., Nocedal, J. & Zhu, C. 1995. A limited memory algorithm for bound constrained optimization. *SIAM Journal on Scientific Computing* **16**: 1190–1208. https://doi.org/10.1137/0916069.

Caro, T.M., Graham, C.M., Stoner, C.J. & Vargas, J.K. 2004. Adaptive significance of antipredator behaviour in artiodactyls. *Animal Behaviour* **67**: 205–228. https://doi.org/10.1016/j.anbehav.2002.12.007.

Clutton-Brock, T.H. & Harvey, P.H. 1977. Primate ecology and social organization. *Journal of Zoology* **183**: 1–39. https://doi.org/10.1111/j.1469-7998.1977.tb04171.x.

Clutton-Brock, T.H., Albon, S.D. & Harvey, P.H. 1980. Antlers, body size and breeding group size in the Cervidae. *Nature* **285**: 565–567. https://doi.org/10.1038/285565a0.

Crile, G. & Quiring, D.P. 1940. A record of the body weight and certain organ and gland weight of 3734 animals. *Ohio Journal of Science* **40**: 219–59. Retrieved from http://hdl.handle.net/1811/3110.

DeCasien, A.R., Williams, S.A. & Higham, J.P. 2017. Primate brain size is predicted by diet but

not sociality. *Nature Ecology & Evolution* **1**: 0112. https://doi.org/10.1038/s41559-017-0112.

Dubois, E. 1898. Ueber die Abhängigkeit des Hirngewichtes von der Körpergrösse bei den Säugethieren. *Archiv für Anthropologie* **25**: 1–28.

Duiker. n.d. Retrieved from http://www.krugerpark.co.za/africa_duiker.html.

Dunbar, R.I.M. 1998. The social brain hypothesis. *Evolutionary Anthropology* **9**: 178–190. https://doi.org/10.1002/(SICI)1520-6505(1998)6:5<178::AID-EVAN5>3.3.CO;2-P.

Dunbar, R.I.M. & Shultz, S. 2007. Understanding primate brain evolution. *Proceedings of the Royal Society B* **362**: 649–658. https://doi.org/10.1098/rstb.2006.2001.

Ebinger, P. 1974. A cytoarchitectonic volumetric comparison of brains in wild and domestic sheep. *Zeitschrift für Anatomie und Entwicklungsgeschichte* **144**: 267–302. https://doi.org/10.1007/BF00522811.

Escudero, M., Hipp, A.L., Hansen, T.F., Voje, K.L. & Luceño, M. 2012. Selection and inertia in the evolution of holocentric chromosomes in sedges (*Carex*, Cyperaceae). *New Phytologist* **195**: 237–247. https://doi.org/10.1111/j.1469-8137.2012.04137.x.

Estes, R., Gregersen, E., Pallardy, R., Chauhan, Y., Tikkanen, A. & Sampaolo, M. 1998. Dik-dik. Retrieved from https://www.britannica.com/animal/dik-dik.

Felsenstein, J. 1985. Phylogenies and the comparative method. *American Naturalist* **125**: 3–147. https://doi.org/10.1086/284325.

Galton, F. 1889. On head growth in students at the university of Cambridge. *The Journal of the Anthropological Institute of Great Britain and Ireland* **18**: 155–156.

Goldberg, D. 1991. What every computer scientist should know about floating-point arithmetic. *ACM Computing Surveys* **23**: 5–48. https://doi.org/10.1145/103162.103163.

Gould, S.J. 1975. Allometry in primates, with emphasis on scaling and the evolution of the brain. *Contributions to primatology* **5**: 244–292.

Grabowski, M., Voje, K.L. & Hansen, T.F. 2016. Evolutionary modeling and correcting for observation error support a 3/5 brain-body allometry for primates. *Journal of Human Evolution* **94**: 106–116. https://doi.org/10.1016/j.jhevol.2016.03.001.

Grafen, A. 1989. The phylogenetic regression. *Proceedings of the Royal Society B* **326**: 119–157. https://doi.org/10.1098/rstb.1989.0106.

Grubb, P. 1993. The Afrotropical Hippopotamuses *Hippopotamus* and *Hexaprotodon*. In: *Pigs, peccaries and hippos* (W. L. Oliver, ed), p. 41. IUCN, Gland, Switzerland.

Haarmann, K. & Oboussier, H. 1972. Morphologishce und quantitative Neocortexuntersuchungen bei Boviden, ein Beitrag zur Phylogenie dieser Familie. II. Formen geringen Körpergewichts (3kg - 25kg) aus den Subfamilien Cephalophinae und Antilopinae. *Mitteilungen aus dem*

Hamburgischen Zoologischen Museum und Institut **68**: 231–269.

Hadfield, J.D. 2010. MCMC methods for multi-response generalized linear mixed models: The MCMCglmm R package. *Journal of Statistical Software* **33**: 1–22. https://doi.org/10.1002/ana.22635.

Halley, A.C. 2016. Prenatal brain-body allometry in mammals. *Brain, Behavior and Evolution* **88**: 14–24. https://doi.org/10.1159/000447254.

Hansen, T.F. 1997. Stabilizing selection and the comparative analysis of adaptation. *Evolution* **51**: 1341–1351. https://doi.org/10.2307/2411186.

Hansen, T.F. 2014. Use and misuse of comparative methods in the study of adaptation. In: *Modern phylogenetic comparative methods and their application in evolutionary biology* (Z. L. Garamszegi, ed), pp. 351–379. Springer, Berlin, Heidelberg. https://doi.org/10.1007/978-3-662-43550-2_14.

Hansen, T.F. & Bartoszek, K. 2012. Interpreting the evolutionary regression: The interplay between observational and biological errors in phylogenetic comparative studies. *Systematic Biology* **61**: 413–425. https://doi.org/10.1093/sysbio/syr122.

Hansen, T.F., Pienaar, J. & Orzack, S.H. 2008. A comparative method for studying adaptation to a randomly evolving environment. *Evolution* **62**: 1965–1977. https://doi.org/10.1111/j.1558-5646.2008.00412.x.

Harvey, P.H. & Pagel, M. 1988. The allometric approach to species differences in brain size. *Human Evolution* **3**: 461–472. https://doi.org/10.1007/BF02436332.

Harvey, P.H., Clutton-Brock, T.H. & Mace, G.M. 1980. Brain size and ecology in small mammals and primates. *Proceedings of the National Academy of Sciences* **77**: 4387–4389. https://doi.org/10.1073/pnas.77.7.4387.

Healy, S.D. & Rowe, C. 2007. A critique of comparative studies of brain size. *Proceedings of the Royal Society B* **274**: 453–464. https://doi.org/10.1098/rspb.2006.3748.

Hernández Fernández, M. & Vrba, E.S. 2005. A complete estimate of the phylogenetic relationships in Ruminantia: a dated species-level supertree of the extant ruminants. *Biological reviews of the Cambridge Philosophical Society* **80**: 269–302. https://doi.org/10.1017/s1464793104006670.

Hrdlička, A. 1905. Brain weight in vertebrates. *Smithsonian Institution* **3**.

Hurvich, C.M. & Tsai, C.-L. 1989. Regression and time series model selection in small samples. *Biometrika* **76**: 297–307. https://doi.org/10.1093/biomet/76.2.297.

Huxley, J.S. & Teissier, G. 1936. Terminology of relative growth. *Nature* **137**: 780–781.

https://doi.org/10.1038/148225a0.

Isler, K., Kirk, E.C., Miller, J.M.A., Albrecht, G.A., Gelvin, B.R. & Martin, R.D. 2008. Endocranial volumes of primate species: scaling analyses using a comprehensive and reliable data set. *Journal of Human Evolution* **55**: 967–978. https://doi.org/10.1016/j.jhevol.2008.08.004.

Kotrschal, A., Rogell, B., Bundsen, A., Svensson, B., Zajitschek, S. & Brännström, I. *et al.* 2013. Artificial selection on relative brain size in the guppy reveals costs and benefits of evolving a larger brain. *Current Biology* **23**: 168–171. https://doi.org/10.1016/j.cub.2012.11.058.

Kruska, D. 1987. How fast can total brain size change in mammals? *Journal für Hirnforschung* **28**: 59–70. Retrieved from http://www.ncbi.nlm.nih.gov/pubmed/3598176.

Labra, A., Pienaar, J. & Hansen, T.F. 2009. Evolution of thermal physiology in liolaemus lizards: adaptation, phylogenetic inertia, and niche tracking. *The American Naturalist* **174**: 204–220. https://doi.org/10.1086/600088.

Lapicque, L. 1898. Sur la relation du poids de l'encéphale aux poids du corps. *Comptes rendus séances Soc. Biol. Fil.* **5**: 62.

Legg, S. & Hutter, M. 2007. A collection of definitions of intelligence. *Frontiers in Artificial Intelligence and applications* **157**: 17–24. https://doi.org/10.1207/s15327051hci0301_2.

Lueders, I., Niemuller, C., Rich, P., Gray, C., Hermes, R. & Goeritz, F. *et al.* 2012. Gestating for 22 months: luteal development and pregnancy maintenance in elephants. *Proceedings of the Royal Society B* **279**: 3687–3696. https://doi.org/10.1098/rspb.2012.1038.

Lynch, M. 1991. Methods for the analysis of comparative data in evolutionary biology. *Evolution* **45**: 1065–1080. https://doi.org/10.2307/2409716.

Martin, R. & Harvey, P.H. 1985. Brain size allometry ontogeny and phylogeny. In: *Size and scaling in primate biology* (W. L. Jungers, ed), pp. 147–173. Springer, US.

Matějů, J., Kratochvíl, L., Pavelková, Z., Pavelková Řičánková, V., Vohralík, V. & Němec, P. 2016. Absolute, not relative brain size correlates with sociality in ground squirrels. *Proceedings of the Royal Society B* **283**. https://doi.org/10.1098/rspb.2015.2725.

McNab, B.K. 1997. On the utility of uniformity in the definition of basal rate of metabolism. *Physiological and biochemical zoology* **70**: 718–720. https://doi.org/10.1086/515881.

Mendoza, M. & Palmqvist, P. 2008. Hypsodonty in ungulates: An adaptation for grass consumption or for foraging in open habitat? *Journal of Zoology* **274**: 134–142. https://doi.org/10.1111/j.1469-7998.2007.00365.x.

Mendoza, M., Janis, C.M. & Palmqvist, P. 2002. Characterizing complex craniodental patterns related to feeding behaviour in ungulates: a multivariate approach. *Journal of Zoology* **258**.

https://doi.org/10.1017/S0952836902001346.

Mendoza, M., Janis, C.M. & Palmqvist, P. 2005. Ecological patterns in the trophic-size structure of large mammal communities: a 'taxon-free' characterization. *Evolutionary Ecology Research* **7**: 505–530. Retrieved from http://webpersonal.uma.es/de/ppb/EvolEcolRes.pdf.

Mink, J.W., Blumenschine, R.J. & Adams, D.B. 1981. Ratio of central nervous system to body metabolism in vertebrates: its constancy and functional basis. *The American journal of physiology* **241**: R203–R212.

Myers, P., Espinosa, R., Parr, C., Jones, T., Hammond, G. & Dewey, T. 2017. Animal diversity. Retrieved from http://animaldiversity.org/.

Nakagawa, S. & Schielzeth, H. 2013. A general and simple method for obtaining R2 from generalized linear mixed-effects models. *Methods in Ecology and Evolution* **4**: 133–142. https://doi.org/10.1111/j.2041-210x.2012.00261.x.

NCBI Resource Coordinators. 2017. Database resources of the national center for biotechnology information. *Nucleic Acids Research* **45**: D12–D17. https://doi.org/10.1093/nar/gkw1071.

Nchanji, A.C. & Amubode, F.O. 2002. The physical and morphological characteristics of the red-fronted gazelle (*Gazella rufifrons kanuri* Gray 1846) in Waza National Park, Cameroon. *Journal of Zoology* **256**: 505–509. https://doi.org/10.1017/S0952836902000559.

Oboussier, H. 1963a. Die Pferdeantilope (*Hippotragus equinus cottoni*, Dollman und Burlace 1928) Ergebnisse der Forschungsreisen dach Süd-Angola. *Zeitschrift für Morphologie und Ökologie der Tiere* **52**: 688–713.

Oboussier, H. 1963b. Hirn und Hypophyse des Kaffernbüffels (*Syncerus caffer* Sparrman 1779) Ergebnisse einer Forschungsreise nach Südangola. *Aeta anat.* **54**: 205–219.

Oboussier, H. 1972. Morphologische und quantitative Neocortexuntersuchungen bei Boviden, ein Beitrag zur Phylogenie dieser Familie III. Formen über 75 kg Körpergewicht. *Mitteilungen aus dem Hamburgischen Zoologischen Museum und Institut* **68**: 271–292.

Oboussier, H. 1974. Beiträge zur Kenntnis afrikanischer Gazellen unter besonderer Berücksichtigung des Körperbaus, der Hypophyse und der Hirngrösse. *Mitteilungen aus dem Hamburgischen Zoologischen Museum und Institut* **71**: 235–257.

Oboussier, H. 1978. Zur Kenntnis des Bergnyalas (*Tragelaphus buxtoni*) und des Bongos (*Taurotragus euryceros*). Untersuchungen über den Körperbau und das Gehirn. *Zeitschrift für Säugetierkunde* **43**: 114–125.

Oboussier, H. 1979. Evolution of the brain and phylogenetic development of african Bovidae. *South African Journal of Zoology* **14**: 119–124. https://doi.org/10.1080/02541858.1979.11447660.

Oboussier, H. & Möller, G. 1971. Zur Kenntnis des Gehirns der Giraffidae (Pecora, Artiodactyla,

Mammalia) - ein Vergleich der Neocortex-Oberflächengrösse). *Zeitschrift für Säugetierkunde* **36**: 291–296.

Oboussier, H. & Schliemann, H. 1966. Hirn-körpergewichtsbeziehungen bei boviden. *Zeitschrift für Säugetierkunde* **31**: 464–471.

Oboussier, H. & Von Tyszka, H. 1964. Beiträge zur Kenntnis der Reduncini (Hippotraginae-bovidae) Süd-angolas Hirnfurchenbild und Hypophyse: Ergebnisse der Forschungsreisen von Prof. Dr. H. Oboussier nach Angola 1959 und 1961. *Zeitschrift für Morphologie und Ökologie der Tiere* **53**: 362–386.

O'Meara, B.C. & Beaulieu, J.M. 2014. Modelling stabilizing selection: The attraction of Ornstein-Uhlenbeck models. In: *Modern phylogenetic comparative methods and their application in evolutionary biology* (Z. L. Garamszegi, ed), pp. 381–393. Springer, Berlin, Heidelberg. https://doi.org/10.1007/978-3-662-43550-2_15.

Pagel, M. 1994. Detecting correlated evolution on phylogenies: a general method for the comparative analysis of discrete characters. *Proceedings of the Royal Society B* **255**: 37–45. https://doi.org/10.1098/rspb.1994.0006.

Pagel, M. 1999. Inferring the historical patterns of biological evolution. *Nature* **401**: 877–884. https://doi.org/10.1038/44766.

Paradis, E., Claude, J. & Strimmer, K. 2004. APE: Analyses of phylogenetics and evolution in R language. *Bioinformatics* **20**: 289–290. https://doi.org/10.1093/bioinformatics/btg412.

Passingham, R.E. 1975. Changes in the size and organisation of the brain in man and his ancestors. *Brain, Behavior and Evolution* **11**: 73–90. https://doi.org/10.1159/000123626.

Pérez-Barbería, F.J. & Gordon, I.J. 2005. Gregariousness increases brain size in ungulates. *Oecologia* **145**: 41–52. https://doi.org/10.1007/s00442-005-0067-7.

Pérez-Barbería, F.J., Gordon, I.J. & Pagel, M. 2002. The origins of sexual dimorphism in body size in ungulates. *Evolution; international journal of organic evolution* **56**: 1276–1285. https://doi.org/10.1554/0014-3820(2002)056.

Pérez-Barbería, F.J., Shultz, S. & Dunbar, R.I.M. 2007. Evidence for coevolution of sociality and relative brain size in three orders of mammals. *Evolution* **61**: 2811–2821. https://doi.org/10.1111/j.1558-5646.2007.00229.x.

Price, S.A., Bininda-Emonds, O.R.P. & Gittleman, J.L. 2005. A complete phylogeny of the whales, dolphins and even-toed hoofed mammals (Cetartiodactyla). *Biological Reviews* **80**. https://doi.org/10.1017/S1464793105006743.

R Core Team. 2017. R: A language and environment for statistical computing. Vienna, Austria. Retrieved from https://www.r-project.org/.

Ritchie, S.J., Booth, T., Hernández, M., Corley, J., Muñoz Maniega, S. & Gow, A.J. *et al.* 2015.

Beyond a bigger brain: Multivariable structural brain imaging and intelligence. *Intelligence* **51**. https://doi.org/10.1016/j.intell.2015.05.001.

Ronnefeld, U. 1970. Morphologische und quantitative Neocortexuntersuchungen bei Boviden, ein Beitrag zur Phylogenie dieser Familie. I. Formen mittlerer Körpergrösse (25 kg bis 75 kg). *Gegenbaurs Morphologische Jahrbuch* **115**: 161–230.

Savage, V., Gillooly, J., Woodruff, W., West, G., Allen, A. & Enquist, B.J. *et al.* 2004. The predominance of quarter-power scaling in biology. *Functional Ecology* **18**: 257–282. Retrieved from http://onlinelibrary.wiley.com/doi/10.1111/j.0269-8463.2004.00856.x/full.

Shultz, S. & Dunbar, R.I.M. 2006. Both social and ecological factors predict ungulate brain size. *Proceedings of the Royal Society B* **273**: 207–215. https://doi.org/10.1098/rspb.2005.3283.

Shultz, S. & Dunbar, R.I.M. 2010. Encephalization is not a universal macroevolutionary phenomenon in mammals but is associated with sociality. *Proceedings of the National Academy of Sciences* **107**: 21582–21586. https://doi.org/10.1073/pnas.1005246107.

Silva, M. & Downing, J.A. 1995. *CRC handbook of mammalian body masses.* CRC Press, Boca Raton, FL.

Smith, R.J. & Jungers, W.L. 1997. Body mass in comparative primatology. *Academic Press Limited Journal of Human Evolution* **32**: 523–559.

Snell, O. 1892. Die Abhängigkeit des Hirngewichtes von dem Körpergewicht und den geistigen Fähigkeiten. *Archiv für Psychiatrie und Nervenkrankheiten* **23**: 436–446. https://doi.org/10.1007/BF01843462.

Stephan, H. 1960. Methodische Studien über den quantitativen Vergleich architektonischer Struktureinheiten des Gehirns. *Zeitschrift für wissenschaftliche Zoologie* **164**: 143–172.

Stephan, H., Frahm, H. & Baron, G. 1981. New and revised data on volumes of brain structures in insectivores and primates. *Folia Primatologica* **35**: 1–29. https://doi.org/10.1159/000155963.

Striedter, G.F. 2005. *Principles of brain evolution.* Sinauer Associates, Sunderland, Massachusetts, USA.

Toljagić, O., Voje, K.L., Matschiner, M., Liow, L.H. & Hansen, T.F. 2017. Millions of years behind: Slow adaptation of ruminants to grasslands. *Systematic Biology*, doi: 10.1093/sysbio/syx059. https://doi.org/10.1093/sysbio/syx059.

Tragelaphus imberbis, lesser kudu. n.d. Retrieved from http://www.ultimateungulate.com/Artiodactyla/Tragelaphus_imberbis.html.

Tsuboi, M., Kotrschal, A., Hayward, A., Buechel, S.D., Zidar, J. & Kolm, N. 2016. Evolution of brain–body allometry in Lake Tanganyika cichlids. *Evolution* **70**: 1559–1568. https:

//doi.org/10.1111/evo.12965.

Tyszka, H. von. 1966. Das Großhirnfurchenbild als Merkmal der Evolution: Untersuchungen an Boviden I. *Mitteilungen aus dem Hamburgischen Zoologischen Museum und Institut* **63**: 121–158.

Weber, M. 1896. Vorstudien über das Hirngewicht der Säugethiere. In: *Festschrift zum siebenzigsten geburtstage von carl gegenbaur am 21. august 1896.* Verlag von Wilhelm Engelman, Leipzig.

Wemmer, C. & Wilson, D. 1987. Cervid brain size and natural history. In: *Biology and management of the cervidae* (W. CM, ed). Smithsonian Institution Press, Washington DC; London.

Wilson, D.E. & Mittermeier, R.A. 2011. *Handbook of the mammals of the world. Volume 2: Hoofed mammals* (D. E. Wilson & R. A. Mittermeier, eds). Lynx Edicions, Barcelona.

Yu, G., Smith, D.K., Zhu, H., Guan, Y. & Lam, T.T.Y. 2017. ggtree: an R package for visualization and annotation of phylogenetic trees with their covariates and other associated data. *Methods in Ecology and Evolution* **8**: 28–36. https://doi.org/10.1111/2041-210X.12628.

Zuur, A.F., Ieno, E.N., Walker, N., Saveliev, A.A. & Smith, G.M. 2009. *Mixed effects models and extensions in ecology with R* (M. Gail, K. Krickeberg, J. Samet, A. Tsiatis, & W. Wong, eds). Springer, New York, NY, USA. https://doi.org/10.1007/978-0-387-87458-6.

6 Appendix A: SLOUCH

I used the software SLOUCH (Stochastic Linear Ornstein-Uhlenbeck Comparative Hypotheses) implemented in R (R Core Team, 2017) to fit all of the Ornstein-Uhlenbeck models in this thesis. It was first published in Hansen *et al.* (2008), and has later been modified and improved with new features as necessary by various authors (Labra *et al.*, 2009; Hansen & Bartoszek, 2012; Bartoszek *et al.*, 2012; Escudero *et al.*, 2012; Grabowski *et al.*, 2016; Toljagić *et al.*, 2017). While more features are in principle a good thing, a larger code base may also present challenges when maintaining the software. As part of this thesis I refactored large parts of the code architecture with the aim of creating a more maintaineable, concise and higher quality code base. The total R code has been reduced from about 4300 to about 1000 lines of code, excluding documentation and automated test suites. While the models of trait evolution are functionally unchanged, changes have been made to improve performance, numerical stability, diagnostic error messages and convenience in general, such as the implementation of a hill climber optimization routine (see Materials & Methods). In order to facilitate this development I used the Git version control system to track all changes, and the repository is hosted on the authors' github profile (https://www.github.com/kopperud/slouch).

The original version of SLOUCH was an addition to OUCH (Ornstein-Uhlenbeck Comparative Hypotheses) (Butler & King, 2004) and used its implementation of displaying and manipulating phylogenetic trees. Since then, the R package community has mostly favoured the package APE (Analysis of Phylogenetics and Evolution) (Paradis *et al.*, 2004) when dealing with phylogenetic trees. I have changed the input format of phylogenetic trees in SLOUCH to use the APE format, reimplementing functionality as necessary. While there is no conceptual difference or advantage with this approach, the tree format is now more compatible with other R packages that use APE, of which there are at least 189 on CRAN (Comprehensive R Archive Network) alone. Common operations such as importing trees from various formats, manipulating topology or branch lengths, estimating ancestral characters and visual display of trees are now much more accessible and convenient.

The computational performance has also been improved. The performance of estimating parameters in OU models with continuous Brownian-motion covariates has been improved by possibly several orders of magnitude, thanks to better memory management. One such model improved from 15 minutes run-time to about 4 seconds, at $n = 86$ with a 35×35 parameter grid search. R is a high-level interpreted language primarily designed for easy interactive use, but native R can be slow, and for this reason most of R itself is written in low-level compiled languages such as Fortran or C. I decided to rewrite some of the most performance-critical inner functions in C++, improving the performance of models with categorical covariates. One of the remaining bottlenecks in parameter estimation is the GLS (generalized least squares) regression coefficient estimator. To alleviate this, I used the Cholesky factorization of the residual variance-covariance matrix to reparameterize the model when computing the coefficients. Suppose we have a linear model (see Materials & Methods)

$$\mathbf{y} = \mathbf{X}\boldsymbol{\theta} + \boldsymbol{r}, \boldsymbol{r} \sim N(\mathbf{0}, \mathbf{V}) \tag{9}$$

The GLS estimator for this model is

$$\hat{\boldsymbol{\theta}}_{GLS} = (\mathbf{X}^T\mathbf{V}^{-1}\mathbf{X})^{-1}\mathbf{X}^T\mathbf{V}^{-1}\mathbf{y} \tag{10}$$

Since $\mathbf{V}$ is a variance-covariance matrix, we know that it is symmetric and positive semidefinite. If $\mathbf{V}$ is symmetric positive definite, we can compute the Cholesky decomposition $\mathbf{V} = \mathbf{L}\mathbf{L}^T$, where $\mathbf{L}$ is a lower triangular matrix. Let's say we transform our linear model by $\mathbf{L}^{-1}$,

$$\mathbf{L}^{-1}\mathbf{y} = \mathbf{L}^{-1}\mathbf{X}\boldsymbol{\theta} + \mathbf{L}^{-1}\boldsymbol{r} \tag{11}$$

The OLS (ordinary least squares) solution to this model is

$$\begin{aligned}
\hat{\boldsymbol{\theta}}_{OLS-transformed} &= ((\mathbf{L}^{-1}\mathbf{X})^T\mathbf{L}^{-1}\mathbf{X})^{-1}(\mathbf{L}^{-1}\mathbf{X})^T\mathbf{L}^{-1}\mathbf{y} \\
&= (\mathbf{X}^T(\mathbf{L}^{-1})^T\mathbf{L}^{-1}\mathbf{X})^{-1}\mathbf{X}^T(\mathbf{L}^{-1})^T\mathbf{L}^{-1}\mathbf{y} \\
&= (\mathbf{X}^T(\mathbf{L}\mathbf{L}^T)^{-1}\mathbf{X})^{-1}\mathbf{X}^T(\mathbf{L}\mathbf{L}^T)^{-1}\mathbf{y} \\
&= (\mathbf{X}^T\mathbf{V}^{-1}\mathbf{X})^{-1}\mathbf{X}^T\mathbf{V}^{-1}\mathbf{y} \\
\hat{\boldsymbol{\theta}}_{OLS-transformed} &= \hat{\boldsymbol{\theta}}_{GLS}
\end{aligned} \tag{12}$$

This shows that the OLS solution to a model transformed by $\mathbf{L}^{-1}$ is algebraically equivalent to applying the GLS solution directly. Using the optimized R "lm" library for solving OLS models using QR decomposition, standard routines for Cholesky decomposition and solving triangular systems, I observed an approximate four times increase in computational efficiency. I also used to the Cholesky decomposition to compute the log determinant used in the log likelihood function,

$$\begin{aligned}
\log|\mathbf{V}| &= \log\left|\mathbf{L}\mathbf{L}^T\right| \\
&= \log|\mathbf{L}|^2 \\
&= 2\log|\mathbf{L}| \\
&= 2\log\prod_{i=1}^{n}\mathrm{L}_{ii} \\
&= 2\sum_{i=1}^{n}\log(\mathrm{L}_{ii})
\end{aligned} \tag{13}$$

where n is the number of species, and L_{ii} are the diagonal elements of $\mathbf{L}$. While this approach is faster when discounting the time used to decompose $\mathbf{V}$, the main advantage comes from transforming a product to a sum when compared with calculating the entire determinant first. R primarily uses double precision floating point numbers (Goldberg, 1991) to represent decimal numbers. If n is large the product of eigenvalues may exceed the dynamic range of the data structure used to store the numbers and return either a positive infinite or "NA", but with a sum this is unlikely to happen.

The grid search for best parameter estimates can now be run in parallel, which may be useful if the software is run on a system with multiple CPU cores. If n is large, however, it may be best

to instead compile R against a multithreaded BLAS (Basic Linear Algebra Subprograms), since the computational bottlenecks have been reduced to common matrix operations. Previously, the model outputs were only printed in the console, but now they are returned as composite object of class 'slouch', with associated methods for printing and plotting. This way it is easier to manipulate the outputs programmatically. Finally, I provide a short introduction with syntax examples to illustrate how SLOUCH can be used.

6.1 User guide

SLOUCH is an implementation of a particular phylogenetic comparative method. It can fit univariate among-species Ornstein-Uhlenbeck models of phenotypic trait evolution, where the trait evolves towards a primary optimum. Optima can be fitted either as discrete regimes as niches on the phylogenetic tree, and/or with continuous covariates. This document is not meant to be exhaustive nor cover the biological interpretations in any depth; it is merely a short introduction on software syntax and a few technical issues. For more information about the theoretical background, how the method is derived, and how to interpret the models, see the associated literature (Hansen, 1997, 2014; Butler & King, 2004; Hansen *et al.*, 2008; Bartoszek *et al.*, 2012; Hansen & Bartoszek, 2012; Escudero *et al.*, 2012; O'Meara & Beaulieu, 2014).

6.1.1 Prerequisites

In order to fit Ornstein-Uhlenbeck models in SLOUCH, we will need to have a rooted phylogenetic tree of interest in the `phylo` format, from package `ape`. Polytomies and non-branching edges are allowed. Both ultrametric and non-ultrametric trees can be used, but this will have implications for reliable estimation of certain parameters. For the purposes of illustrating syntax, we will use a dataset of artiodactyl neocortices bundled with the package (see `?neocortex`), and a corresponding phylogenetic tree (Toljagić *et al.*, 2017). First, we will organize the neocortex data and associated annotation data.

```
## Package "treeio" can be installed from bioconductor by entering:
## source("https://bioconductor.org/biocLite.R")
## biocLite("treeio")

library(ape)
library(slouch)
library(treeio)
library(dplyr)

tree <- treeio::read.beast(paste0("http://datadryad.org/bitstream/",
                                  "handle/10255/dryad.139618/",
                                  "cetartiodactyla_gtr.tre?sequence=1"))

## Save and organize the annotation data included in the tree
phy <- tree@phylo
n <- length(phy$tip.label)
nodes_internal <- n:nrow(phy$edge)
nodes_tip <- 1:n
diet <- data.frame(species = phy$tip.label,
                   diet = tree@stats$diet[nodes_tip])
```

```
phy$node.label <- tree@stats$diet[nodes_internal]

## Load the neocortex dataset, add diet information for the terminal edges
data(neocortex)
neocortex <- neocortex %>%
  left_join(diet, by = "species")

## Prune the phylogenetic tree for species without neocortex data
ineligible <- !phy$tip.label %in% neocortex$species
phy <- drop.tip(phy, tip = phy$tip.label[ineligible])

## Plot the tree
oldmar <- par("mar");
par(mar = c(0,0,0,0))
plot(ladderize(phy), cex = 0.6)
```

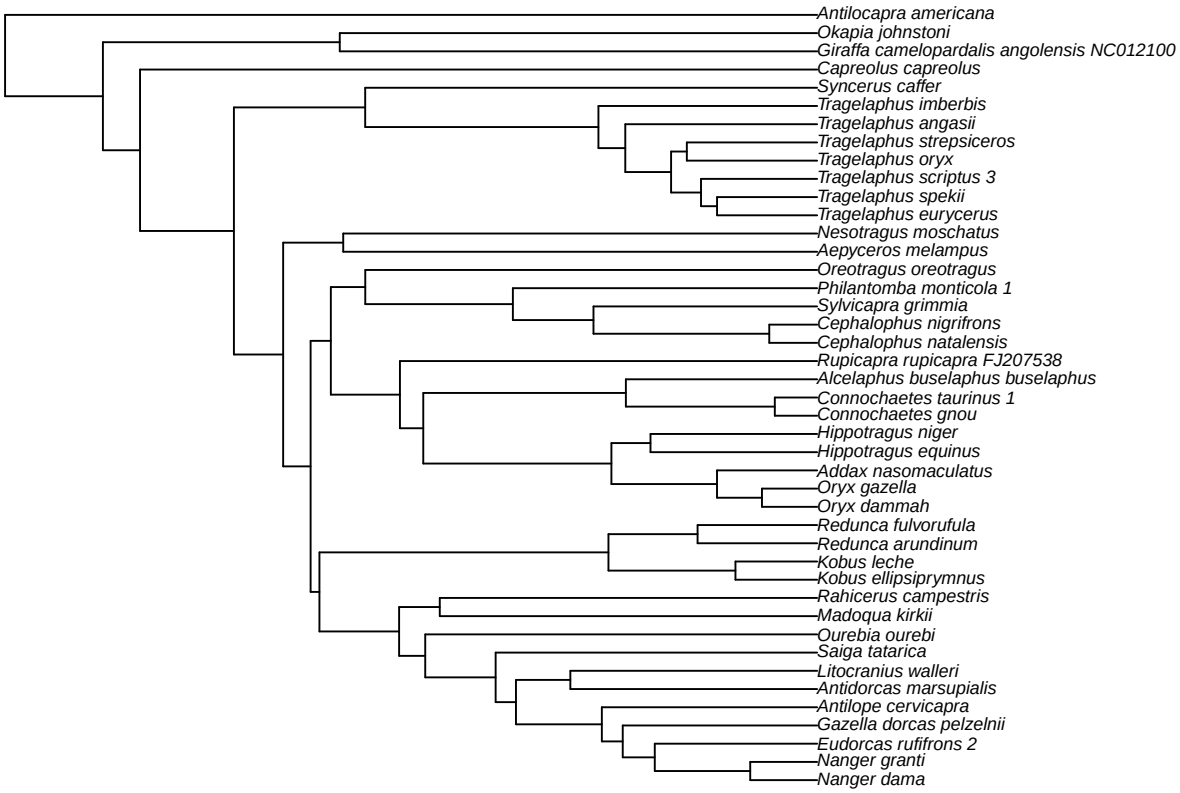


```
par(mar = oldmar)
```

Now, we have a phylogenetic tree with corresponding morphological data for all of the extant species. If you use your own data to fit models, it is recommended to store the data for the terminal branches in a data frame or in a similar data structure. In order to line up the data frame with the tree, SLOUCH requires the species in the data frame need to be in a particular order.

```
## Check whether they are lined up correctly
neocortex$species == phy$tip.label
```

```
##  [1] FALSE FALSE FALSE FALSE FALSE  TRUE FALSE FALSE FALSE  TRUE  TRUE
## [12]  TRUE  TRUE FALSE FALSE FALSE FALSE FALSE FALSE FALSE FALSE FALSE
## [23] FALSE FALSE FALSE FALSE FALSE FALSE FALSE FALSE FALSE FALSE FALSE
## [34] FALSE FALSE FALSE FALSE FALSE FALSE FALSE FALSE FALSE FALSE
```

Unsurprisingly, not all of the species are in their correct places; we will have to reorder the data frame. Here is one way to do it.

```
neocortex <- neocortex[match(phy$tip.label, neocortex$species), ]

## Check if they line up again
neocortex$species == phy$tip.label
```

```
##  [1] TRUE TRUE TRUE TRUE TRUE TRUE TRUE TRUE TRUE TRUE TRUE TRUE TRUE TRUE
## [15] TRUE TRUE TRUE TRUE TRUE TRUE TRUE TRUE TRUE TRUE TRUE TRUE TRUE TRUE
## [29] TRUE TRUE TRUE TRUE TRUE TRUE TRUE TRUE TRUE TRUE TRUE TRUE TRUE TRUE
## [43] TRUE
```

6.1.2 Single-optimum model

Now we are ready to fit the first models, for which we will use the function `slouch.fit`. The following is an intercept-only model, or a single-optimum model. In `slouch`, there are two main techniques for estimating the most likely α and σ_y^2 parameters. In this particular implementation the σ_y^2 is reparameterized as $\sigma_y^2/2\alpha$, which is the variance of the residuals of the response variable when it is stationary around the optimum. The α is reparameterized as $t_{1/2} = \log(2)/\alpha$, which is the phylogenetic half-life. The first way is to use a grid-search of likely parameters from user input, which may take some trial and error.

```
library(slouch)
model0 <- slouch.fit(phy = phy,
                     hl_values = seq(0, 12, length.out = 10),
                     vy_values = seq(0.1, 1, length.out = 10),
                     species = neocortex$species,
                     response = neocortex$neocortex_area_mm2_log_mean)


model1 <- slouch.fit(phy = phy,
                     hl_values = seq(0, 150, length.out = 25),
                     vy_values = seq(0.1, 2.5, length.out = 25),
```

```
                    species = neocortex$species,
                    response = neocortex$neocortex_area_mm2_log_mean)
par(mfrow=c(1,2), mar = c(0,4,2,3))
plot(model0, use.par = FALSE)
plot(model1, use.par = FALSE)
par(mfrow = c(1,1), mar = oldmar)
```

Grid search **Grid search**

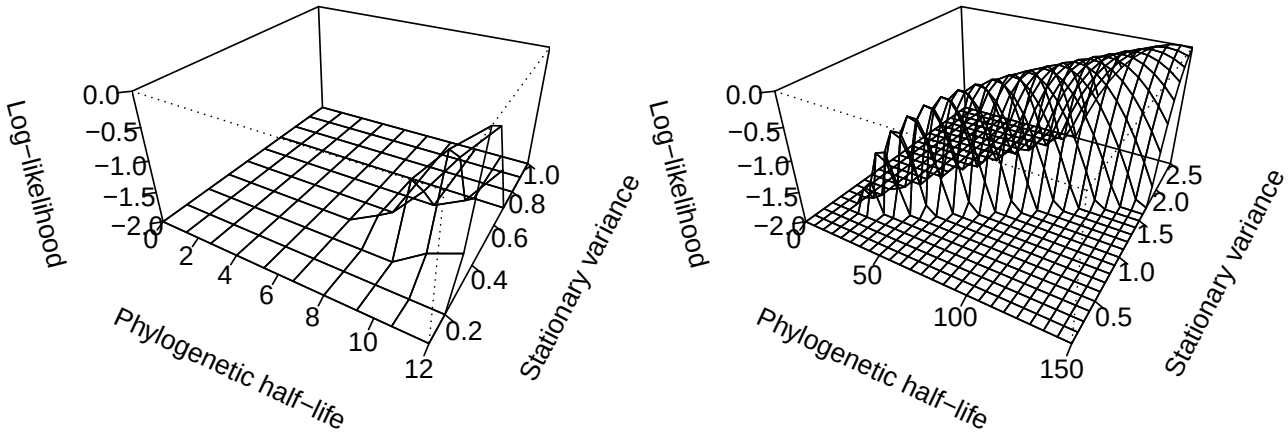

These plots of the likelihood surfaces are both based on the same data, but with different grid location and resolution. The optima and model fit statistics that are reported in the output are conditional on the combination of these $t_{1/2}$ and $\sigma_y^2/2\alpha$ that give the highest log-likelihood; in this case the peak of the surface in the likelihood plot. If the grid-search does not contain the true maximum likelihood, the model outputs will reflect this. It is also possible to use other packages to plot the grid-search likelihood surface, for a more aesthetic look (not run).

```
library(plotly)
p <- plot_ly(x = model0$supportplot$hl,
             y = model0$supportplot$vy,
             z = model0$supportplot$z) %>%
```

```
  add_surface() %>%
  layout(title = "Grid-search",
         scene = list(xaxis = list(title = "Phylogenetic half-life"),
                      yaxis = list(title = "Stationary variance"),
                      zaxis = list(title = "Log-likelihood")))

p
```

Another, perhaps more convenient way of estimating parameters is to use the hillclimber function. On default it will start on a random combination of $t_{1/2}$ and $\sigma_y^2/2\alpha$, but this may also be specified. While the hillclimber might seem both faster and more accurate at first glance, there are some drawbacks. If the likelihood search space has one or more local maxima, the hillclimber may converge at a sub-optimal location and give parameter estimates that are not truly maximum-likelihood estimates. Additionally, even though the hillclimber may converge at some local or global maximum, it will not indicate whether the support region of the parameters is narrow or wide. One problem when using the hillclimber is that, depending on the specified model, the residual variance-covariance matrix $\mathbf{V}$ may collapse if $\sigma_y^2/2\alpha$ reaches zero. The immediate consequence is that matrix is non-invertible, and the program will crash. If within-species observational error is non-zero and added to the model, this does not happen. In order to use the hillclimber in this scenario, it may be necessary to constrain its search space such that $\sigma_y^2/2\alpha$ does not enter zero or close to zero. The exact feasible boundary for this may depend on the scale of the response trait.

```
model2 <- slouch.fit(phy = phy,
                     species = neocortex$species,
                     response = neocortex$neocortex_area_mm2_log_mean,
                     hillclimb = TRUE,
                     lower = c(0, 0.01))
model2$oupar
```

```
##                                    Estimate
## Rate of adaptation              1.249193e-06
## Phylogenetic half-life          5.548762e+05
## Stationary variance             9.107522e+03
## Phylogenetic correction factor 1.698253e-05
```

```
plot(model2)
```

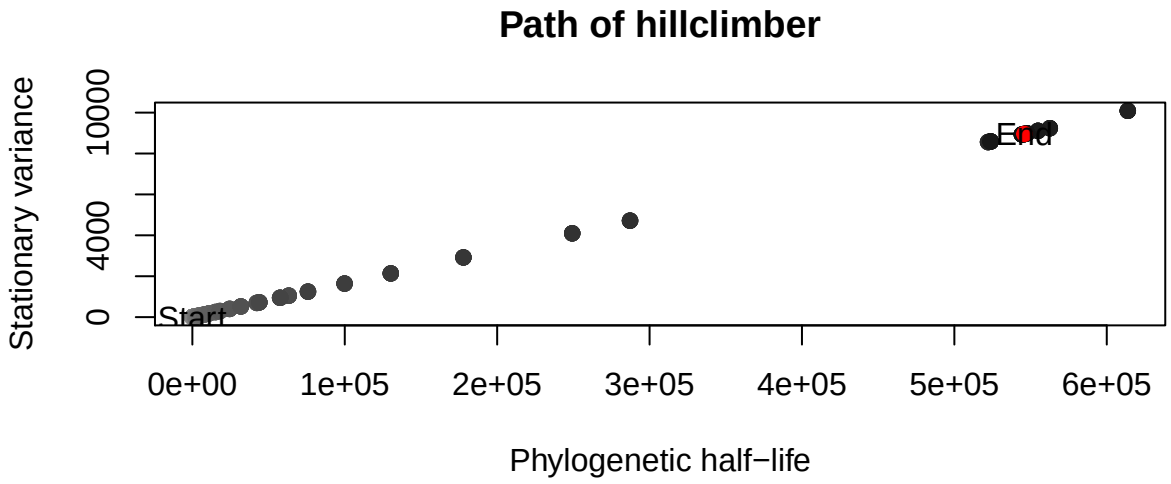

The maximum-likelihood estimate of the phylogenetic half-life ($t_{1/2} = \log(2)/\alpha$) was very large for this model, and the rate of adaptation (α) was practically zero. The units of the phylogenetic half-life are the same units as the branch lengths in the phylogenetic tree, `phy$edge.length`. The total depth, or distance from the root, can for all nodes be calculated with `node.depth.edgelength(phy)`. For this phylogenetic tree the maximum depth is about 27 million years. Given that the estimated half-life $t_{1/2}$ was many times larger than the total length of the phylogeny, and that α is very close to zero, we can conclude that there is next to no strength of attraction towards the optimum. If there is no such pull, the model collapses to a Brownian motion.

6.1.3 Optima as a linear regression

SLOUCH can also fit the optimum as a linear regression with one or more continuous covariates. The covariates may either be fitted as direct effects without a phylogenetic covariance structure, or as univariate Brownian-motion variables. We will first fit log brain mass as a direct effect covariate.

```
model3 <- slouch.fit(phy = phy,
                     species = neocortex$species,
                     response = neocortex$neocortex_area_mm2_log_mean,
                     fixed.cov = neocortex$brain_mass_g_log_mean,
                     lower = c(0, 0.01),
                     hillclimb = TRUE)
par(mfrow = c(1,2))
plot(model3)
```

```r
plot(x = neocortex$brain_mass_g_log_mean,
     y = neocortex$neocortex_area_mm2_log_mean,
     xlab = "Mean log brain mass (g)",
     ylab = "Mean log neocortex area (mm2)",
     main = "Trait plot")
abline(lm(neocortex_area_mm2_log_mean ~ brain_mass_g_log_mean,
          data = neocortex),
       col = "black", lwd = 2)
abline(model3$opt.reg$coefficients[,1],
       col = "orange", lwd = 2)
model3$opt.reg$coefficients
```

```
##                                  Estimates Std. error
## Intercept                        5.4488683 0.23769229
## neocortex$brain_mass_g_log_mean 0.8339189 0.04414703
```

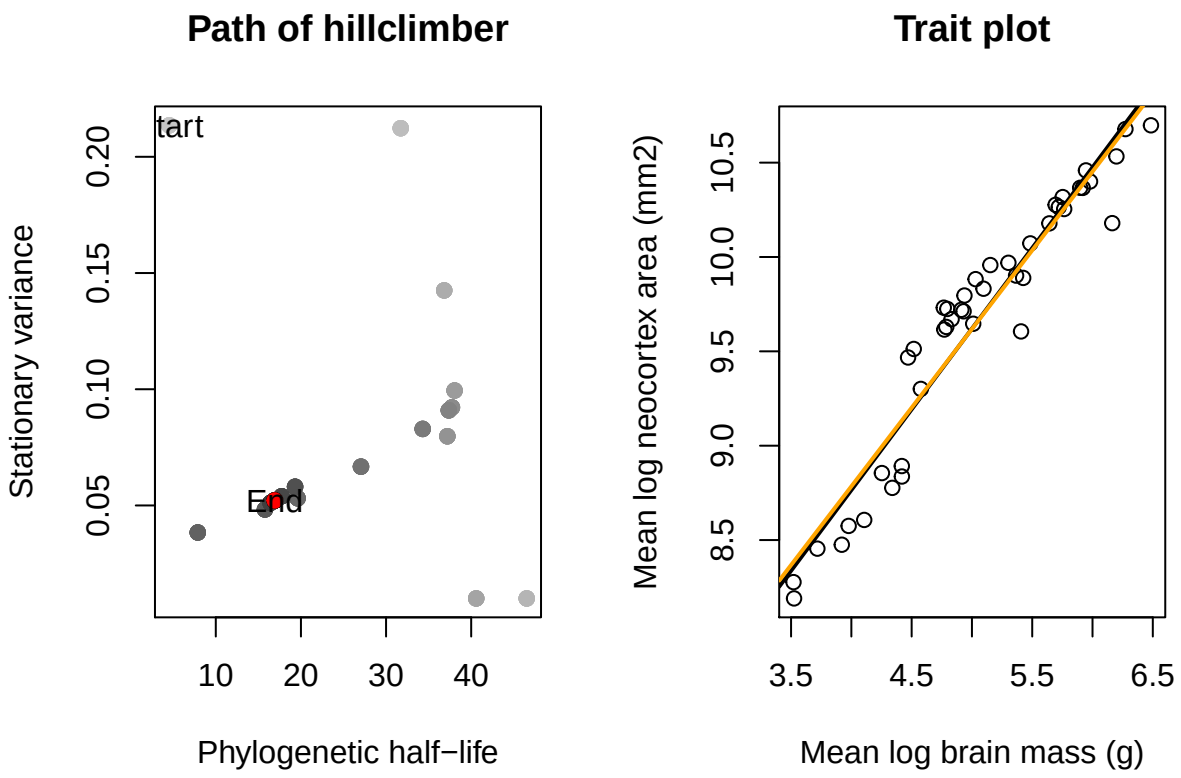

While the single-optimum model showed a very strong phylogenetic inertia, in this model it is somewhat lower with a phylogenetic half-life ($t_{1/2}$) of 16.9 myr. In this case, the regression line estimated using ordinary least squares is almost indistinguishable from the Ornstein-Uhlenbeck optimal regression. It is also possible to fit a model with multiple continuous covariates, however the input to `fixed.cov` must be a matrix or data frame that has column names.

```
model4 <-
  slouch.fit(phy = phy,
             species = neocortex$species,
             response = neocortex$neocortex_area_mm2_log_mean,
             fixed.cov = cbind(brain = neocortex$brain_mass_g_log_mean,
                               body = neocortex$body_mass_g_log_mean),
             lower = c(0, 0.01),
             hillclimb = TRUE)
par(mfrow = c(1,1))
plot(model4)
```

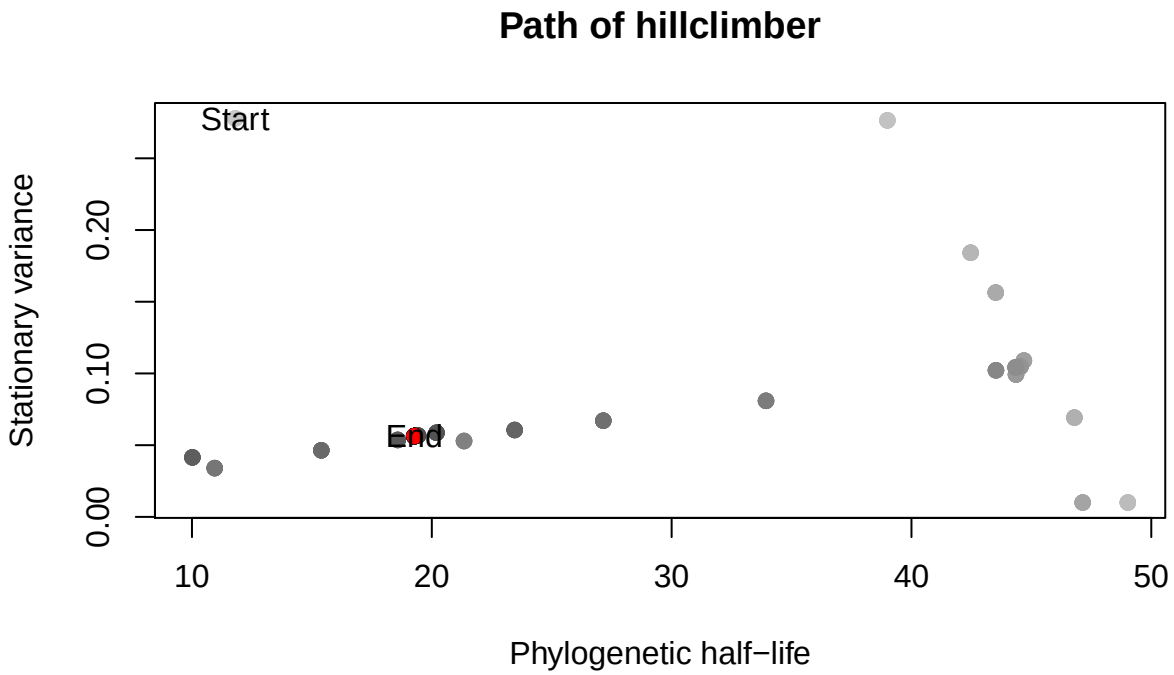

6.1.4 Multiple optima & phylo-format

SLOUCH can fit models with multiple adaptive regimes or niches over the branches of the phylogenetic tree. We will fit neocortex size as a function of diet in artiodactyls. Trees in the `phylo` format are represented by the edges found in `phy$edge`, where each edge connects two vertices or nodes. All of the tip nodes have indices starting from 1, 2, 3 ... until n_{tips}, in this case 43. The root node has index n_{tips}+1, here 44, and the rest of the internal nodes have indices (n_{tips}+2, n_{tips}+3, ..., n_{nodes}). When running this type of model, we will need to specify the internal adaptive regimes in the order of node indices (n_{tips}+1, n_{tips}+2, n_{tips}+3, ..., n_{nodes}). In order to plot and visually verify that the ancestral state configuration is sensible, we need to have all the regimes in the order of the **edges**, not the nodes.

```
## Inspect the internal node regimes
## These have order n+1, n+2, n+3 ...
internal_regimes <- factor(phy$node.label)

## Concatenate tip and internal regimes. These will have order 1,2,3 ...
regimes <- c(neocortex$diet, internal_regimes)

## Pick out the regimes of the edges, in the order of phy$edge
edge_regimes <- factor(regimes[phy$edge[,2]])

oldmar <- par("mar"); par(mfrow = c(1,1), mar = c(0,0,0,0))
plot(phy,
     edge.color = c("Black", "Orange", "blue")[edge_regimes],
     edge.width = 3, cex = 0.6)
```

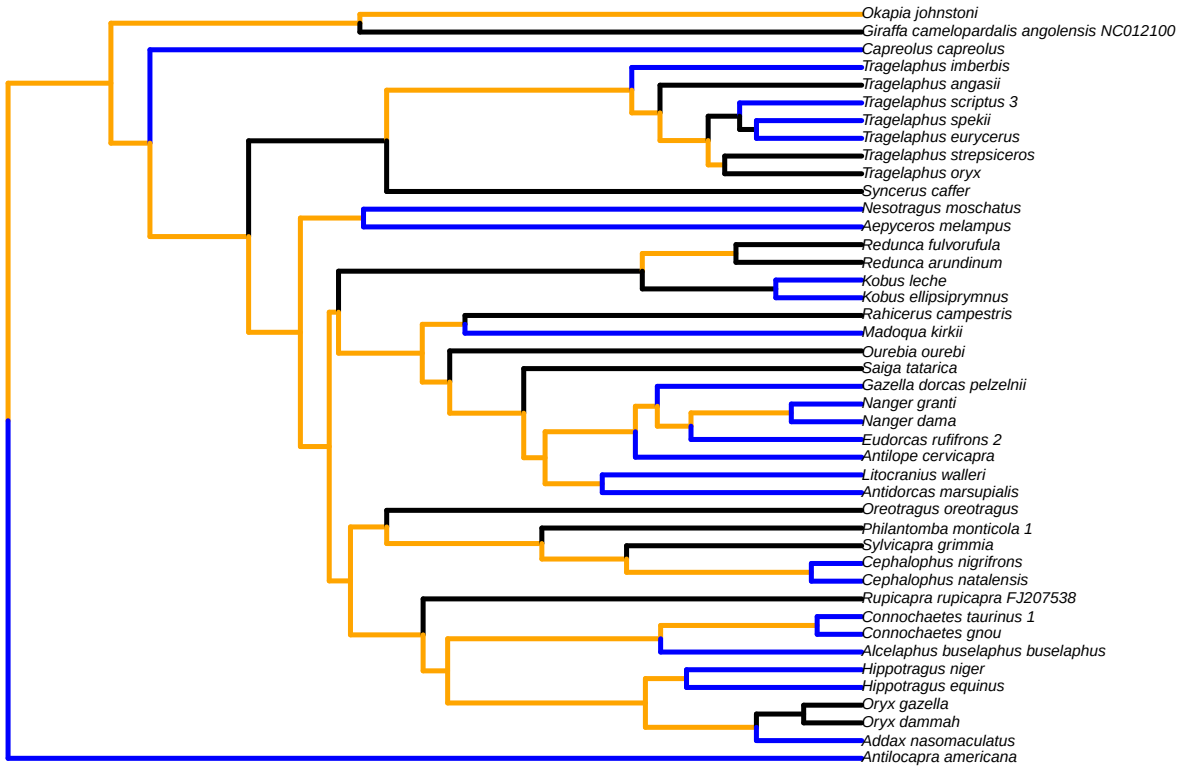


```
par <- par(mar = oldmar, mfrow = c(1,2))
```

If it looks like there are no visible mistakes, we can go ahead and fit the model in SLOUCH.

```
model5 <- slouch.fit(phy = phy,
                     species = neocortex$species,
                     response = neocortex$neocortex_area_mm2_log_mean,
                     fixed.cov = neocortex$brain_mass_g_log_mean,
```

```
                      fixed.fact = neocortex$diet,
                      hillclimb = TRUE,
                      lower = c(0, 0.01))

model5$opt.reg$coefficients
```

```
##                                  Estimates Std. error
## Br                               5.1894858 0.20391429
## Gr                               4.7276433 0.32026376
## MF                               5.3439055 0.19314835
## neocortex$brain_mass_g_log_mean 0.8677243 0.03810015
```

6.1.5 Adaptation model

SLOUCH can also fit models with continuous covariates that themselves have a phylogenetic covariance structure. Currently the only option is to model them as univariate Brownian motions. If $\alpha > 0$, the optimal regression and the evolutionary regression will differ. Here, both the grid-search and the hillclimber routine are used to find the maximum-likelihood estimates for $t_{1/2}$ and $\sigma_y^2/2\alpha$.

```
model6 <- slouch.fit(phy = phy,
                      hl_values = seq(0, 5, length.out = 25),
                      vy_values = seq(0.001, 0.05, length.out = 25),
                      species = neocortex$species,
                      response = neocortex$neocortex_area_mm2_log_mean,
                      random.cov = neocortex$brain_mass_g_log_mean,
                      hillclimb = TRUE,
                      lower = c(0, 0.0005))

model6$opt.reg$coefficients
```

```
##                                  Estimates Std. error
## Intercept                        5.3406859 0.21881752
## neocortex$brain_mass_g_log_mean 0.9864637 0.04678965
```

```
par(mar = c(4,4,2,3))
plot(model6)
```

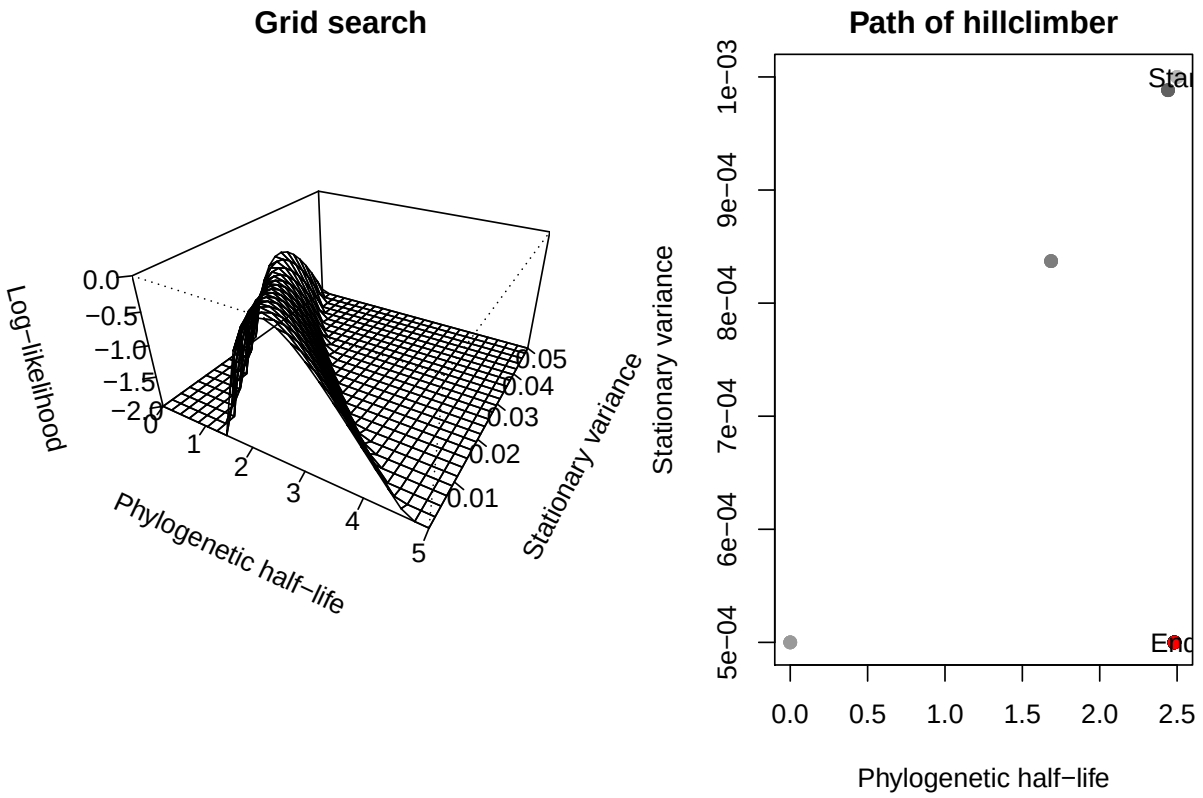

6.1.6 Observational error

Slouch can incorporate estimates of observational error by specifying the within-species estimation variances. For example, if X is the mean log brain mass for each species, the statistic for the measurement error argument would be the variance of the mean log brain mass for each species.

```
model7 <- slouch.fit(phy = phy,
                     hl_values = seq(0, 4, length.out = 25),
                     vy_values = seq(0.001, 0.05, length.out = 25),
                     species = neocortex$species,
                     response = neocortex$neocortex_area_mm2_log_mean,
                     me.response = neocortex$neocortex_se_squared,
                     random.cov = neocortex$brain_mass_g_log_mean,
                     me.random.cov = neocortex$brain_se_squared,
                     hillclimb = TRUE,
                     lower = c(0, 0.001))

plot(model7)
```

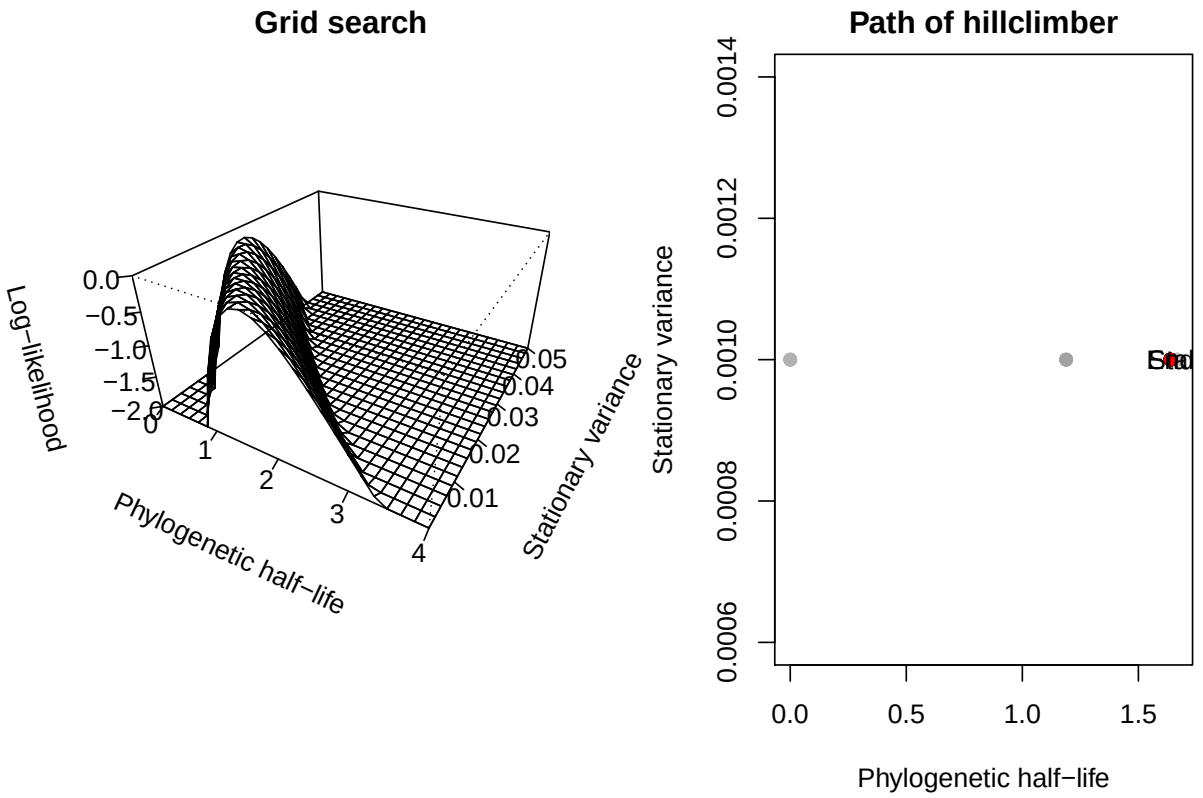

The generalized least squares estimator may be biased when measurement error is incorporated. A bias correction for these regression coefficients is implemented according to Hansen & Bartoszek (2012), but the parameter search and the reported model-fit statistics are conditional on the *naive* optimal regression.

7 Appendix B: Brain data

This appendix includes summary statistics for brain size and body size in 75 species, neocortex size for 42 species and gestation time for 74 species. The information comes from the following references: 1. (Crile & Quiring, 1940); 2. (Oboussier, 1972); 3. (Haarmann & Oboussier, 1972); 4. (Oboussier, 1974); 5. (Ronnefeld, 1970); 6. (Oboussier, 1978); 7. (Oboussier & Möller, 1971); 8. (Oboussier, 1963b); 9. (Oboussier, 1963a); 10. (Oboussier & Von Tyszka, 1964); 10. (Oboussier & Von Tyszka, 1964); 11. (Anderson *et al.*, 1974); 12. (Hrdlička, 1905); 13. (Pérez-Barbería & Gordon, 2005); 14. (Tyszka, 1966); 15. (Wemmer & Wilson, 1987); 16 (Wilson & Mittermeier, 2011); 17 (Estes *et al.*, 1998); 18 (Duiker, n.d.); 19 (*Tragelaphus imberbis*, lesser kudu, n.d.).

Table S1: Log means, standard deviations, sample sizes and references for body size and brain size in each species.

Species	Mean log body (g)	n_{body}	Mean log brain (g)	n_{brain}	Ref
Addax nasomaculatus	11.64 ± 0.08	2	5.30 ± 0.12	2	4
Aepyceros melampus	10.92 ± 0.18	9	5.18 ± 0.11	10	13, 5, 2
Alcelaphus buselaphus	11.81 ± 0.20	11	5.63 ± 0.12	11	13, 3
Alces alces	12.97 ± 0.12	3	6.08 ± 0.17	4	13, 15
Antidorcas marsupialis	10.49 ± 0.21	15	4.91 ± 0.06	15	5, 1
Antilocapra americana	10.88 ± 0.06	3	4.74 ± 0.12	22	13
Antilope cervicapra	10.53	1	4.93 ± 0.07	2	13
Axis axis	11.12 ± 0.29	2	4.90 ± 0.01	2	15
Axis porcinus	10.69	1	5.05	1	13
Bison bison	13.40 ± 0.23	3	6.54 ± 0.06	4	13
Bison bonasus	13.25	1	6.50	1	13
Blastocerus dichotomus	11.77 ± 0.11	2	5.08 ± 0.16	2	15
Boselaphus tragocamelus	12.18	1	5.81	1	13
Capreolus capreolus	9.88 ± 0.25	7	4.59 ± 0.10	11	12, 13, 15
Capricornis crispus	10.52 ± 0.00	2	4.91 ± 0.11	2	13
Cephalophus natalensis	9.35 ± 0.12	2	4.30 ± 0.16	2	3
Cephalophus nigrifrons	9.43 ± 0.17	2	4.43 ± 0.01	3	2
Cervus elaphus	12.41 ± 0.39	3	5.91 ± 0.06	3	13, 15
Cervus nippon	11.20 ± 0.29	2	4.69 ± 0.03	2	15
Connochaetes gnou	11.92	1	5.72	1	2
Connochaetes taurinus	12.05 ± 0.15	10	5.93 ± 0.05	10	13, 14, 3
Dama dama	10.91 ± 0.35	3	5.27 ± 0.21	5	13, 15
Damaliscus pygargus	11.16	1	5.72 ± 0.32	2	13
Elaphodus cephalophus	9.80	1	4.30 ± 0.12	2	15
Elaphurus davidianus	12.04 ± 0.18	2	5.82 ± 0.22	4	13, 15
Eudorcas rufifrons	10.16 ± 0.08	3	4.57 ± 0.08	3	4
Gazella dorcas	9.69 ± 0.11	8	4.25 ± 0.13	12	13, 3, 4
Giraffa camelopardalis	13.65 ± 0.29	4	6.54 ± 0.14	4	13, 7
Hippotragus equinus	12.40 ± 0.09	12	5.96 ± 0.06	12	13, 2, 9, 4
Hippotragus niger	12.20 ± 0.18	5	5.84 ± 0.17	6	13, 2, 4
Hydropotes inermis	9.45 ± 0.08	3	3.89 ± 0.22	3	13, 15

Species	Mean log body (g)	n_{body}	Mean log brain (g)	n_{brain}	Ref
Hyemoschus aquaticus	9.29	1	3.25 ± 0.39	2	13
Kobus ellipsiprymnus	12.31 ± 0.03	7	5.78 ± 0.06	7	13, 2, 10
Kobus leche	11.56 ± 0.24	5	5.34 ± 0.09	5	13, 2, 10
Litocranius walleri	10.45	1	4.90 ± 0.12	2	13
Madoqua kirkii	8.47 ± 0.14	10	3.51 ± 0.08	10	13, 3
Madoqua saltiana	7.80	1	3.14 ± 0.09	2	13
Mazama americana	10.32 ± 0.28	3	4.59 ± 0.27	3	13, 15
Mazama gouazoubira	9.47 ± 0.38	2	4.01 ± 0.11	2	15
Moschus moschiferus	9.48 ± 0.05	3	3.67 ± 0.23	4	13, 15
Muntiacus muntjak	9.59 ± 0.22	7	4.57 ± 0.12	9	13, 15
Muntiacus reevesi	9.47 ± 0.11	3	3.93 ± 0.10	3	13, 15
Nanger dama	10.99 ± 0.19	2	5.01 ± 0.01	2	4
Nanger granti	10.82 ± 0.21	6	5.02 ± 0.09	6	13, 4
Neotragus moschatus	8.23 ± 0.21	3	3.39 ± 0.24	3	13, 3
Odocoileus hemionus	11.13 ± 0.19	53	5.25 ± 0.11	55	11, 13
Odocoileus virginianus	11.11 ± 0.31	3	5.11 ± 0.29	4	13, 15
Okapia johnstoni	12.29 ± 0.13	2	6.19 ± 0.05	2	13, 7
Oreotragus oreotragus	9.45 ± 0.16	6	3.98 ± 0.09	8	13, 3
Oryx dammah	11.77 ± 0.06	2	5.48 ± 0.05	2	4
Oryx gazella	12.02 ± 0.24	5	5.68 ± 0.08	5	2, 4
Ourebia ourebi	9.61 ± 0.09	9	4.08 ± 0.09	15	13, 3
Ovibos moschatus	12.61	1	6.02 ± 0.04	2	13
Ozotoceros bezoarcticus	10.55 ± 0.08	3	4.52 ± 0.25	3	13, 15
Philantomba monticola	8.48 ± 0.08	3	3.74 ± 0.07	3	13, 3
Pudu mephistophiles	9.51	1	3.45 ± 0.07	2	15
Raphicerus campestris	9.23 ± 0.19	11	3.93 ± 0.07	14	13, 3
Rangifer tarandus	11.47 ± 0.41	2	5.67 ± 0.07	2	1
Redunca arundinum	10.97 ± 0.15	11	4.96 ± 0.08	14	13, 5, 10
Rucervus duvauceli	12.13 ± 0.23	3	5.35 ± 0.10	3	13, 15
Rucervus eldi	11.38 ± 0.18	3	5.29 ± 0.09	4	13
Rupicapra pyrenaica	10.43	1	4.74	1	13
Rupicapra rupicapra	10.53 ± 0.10	3	4.81 ± 0.09	4	13
Rusa timorensis	11.03 ± 0.23	2	5.13 ± 0.14	2	15
Rusa unicolor	12.18 ± 0.26	3	5.50 ± 0.32	3	13, 15
Saiga tatarica	10.56 ± 0.14	3	4.71 ± 0.09	5	13
Sylvicapra grimmia	9.49 ± 0.33	12	4.32 ± 0.13	17	13, 3
Syncerus caffer	13.32 ± 0.35	8	6.35 ± 0.18	8	13, 2, 9, 1
Tragelaphus angasii	11.71 ± 0.14	2	5.49 ± 0.09	2	13, 2
Tragelaphus eurycerus	12.25	1	5.97 ± 0.06	2	6
Tragelaphus imberbis	11.84	1	5.36	1	2
Tragelaphus oryx	13.08 ± 0.26	11	6.19 ± 0.11	11	13, 14, 2
Tragelaphus scriptus	10.65 ± 0.21	3	5.12 ± 0.13	4	13, 1
Tragelaphus spekii	10.78 ± 0.19	2	5.05 ± 0.11	2	14
Tragelaphus strepsiceros	12.43 ± 0.18	6	5.96 ± 0.19	8	13, 2, 6

Table S2: Log means, standard deviations, sample sizes and references for neocortex, and gestation time in each species.

Species	Mean log neocortex (mm^2)*	n_{neo}	Ref	Mean gestation time (days)	Ref
Addax nasomaculatus	9.67 ± 0.15	3	4	264	16
Aepyceros melampus	9.96 ± 0.09	22	5	200	16
Alcelaphus buselaphus	10.28 ± 0.16	10	2	240	16
Alces alces				234	16
Antidorcas marsupialis	9.72 ± 0.12	13	5	206	16
Antilocapra americana	9.72 ± 0.01	2	5	248	16
Antilope cervicapra	9.62 ± 0.03	2	5	153	16
Axis axis				233	16
Axis porcinus				230	16
Bison bison				285	16
Bison bonasus				267	16
Blastocerus dichotomus				271	16
Boselaphus tragocamelus				245	16
Capreolus capreolus	9.47 ± 0.05	2	5	150	16
Capricornis crispus				215	16
Cephalophus natalensis	8.84 ± 0.01	2	3	210	18
Cephalophus nigrifrons	8.89 ± 0.03	6	3		
Cervus elaphus				235	16
Cervus nippon				230	16
Connochaetes gnou	10.26 ± 0.05	2	2	244	16
Connochaetes taurinus	10.37 ± 0.12	6	2	250	16
Dama dama				232	16
Damaliscus pygargus				240	16
Elaphodus cephalophus				180	16
Elaphurus davidianus				285	16
Eudorcas rufifrons	9.30 ± 0.13	5	4	187	16
Gazella dorcas	8.85 ± 0.15	11	3, 4	183	16
Giraffa camelopardalis	10.70	1	7	450	16
Hippotragus equinus	10.46 ± 0.02	12	2, 4	282	16
Hippotragus niger	10.18 ± 0.03	4	2, 4	260	16
Hydropotes inermis				168	16
Hyemoschus aquaticus				199	16
Kobus ellipsiprymnus	10.25 ± 0.05	6	2	244	16
Kobus leche	9.61 ± 0.16	2	2	229	16
Litocranius walleri	9.88 ± 0.16	4	5	206	16
Madoqua kirkii	8.28 ± 0.08	16	3	193	16
Madoqua saltiana				168	17
Mazama americana				240	16
Mazama gouazoubira				209	16
Moschus moschiferus				187	16
Muntiacus muntjak				210	16
Muntiacus reevesi				210	16
Nanger dama	9.65 ± 0.06	3	4	203	16

Species	Mean log neocortex (mm^2)*	n_{neo}	Ref	Mean gestation time (days)	Ref
Nanger granti	9.80 ± 0.06	8	4, 5	198	16
Neotragus moschatus	8.19 ± 0.07	4	3	427	16
Odocoileus hemionus				203	16
Odocoileus virginianus				198	16
Okapia johnstoni	10.18	1	7	427	16
Oreotragus oreotragus	8.61 ± 0.03	4	3	150	16
Oryx dammah	10.07 ± 0.13	3	4	252	16
Oryx gazella	10.32 ± 0.02	4	2, 4	244	16
Ourebia ourebi	8.57 ± 0.01	4	3	210	16
Ovibos moschatus				240	16
Ozotoceros bezoarcticus				220	16
Philantomba monticola	8.39 ± 0.11	6	3	120	13
Pudu mephistophiles				214	16
Raphicerus campestris	8.48 ± 0.14	18	3	172	16
Rangifer tarandus				229	16
Redunca arundinum	9.71 ± 0.07	9	5	233	16
Rucervus duvauceli				250	16
Rucervus eldi				240	16
Rupicapra pyrenaica				170	16
Rupicapra rupicapra	9.73 ± 0.02	4	5	170	16
Rusa timorensis				251	16
Rusa unicolor				254	16
Saiga tatarica	9.51 ± 0.08	2	5	138	16
Sylvicapra grimmia	8.78 ± 0.12	16	3	200	16
Syncerus caffer	10.53 ± 0.11	4	2	351	16
Tragelaphus angasii	9.89 ± 0.03	2	2	259	16
Tragelaphus eurycerus	10.40 ± 0.11	4	6	275	16
Tragelaphus imberbis	9.90 ± 0.01	2	2	244	19
Tragelaphus oryx	10.68 ± 0.02	2	5	259	16
Tragelaphus scriptus	9.67 ± 0.12	6	5	183	13
Tragelaphus spekii	9.83 ± 0.13	8	5	247	13
Tragelaphus strepsiceros	10.37 ± 0.12	12	2, 6	275	16

* Single hemisphere

8 Appendix C: Phylogenetic trees

All trees and ancestral reconstructions of diet and habitat are based on Toljagić *et al.* (2017), and the trees were plotted using the R-package "ggtree" (Yu *et al.*, 2017).

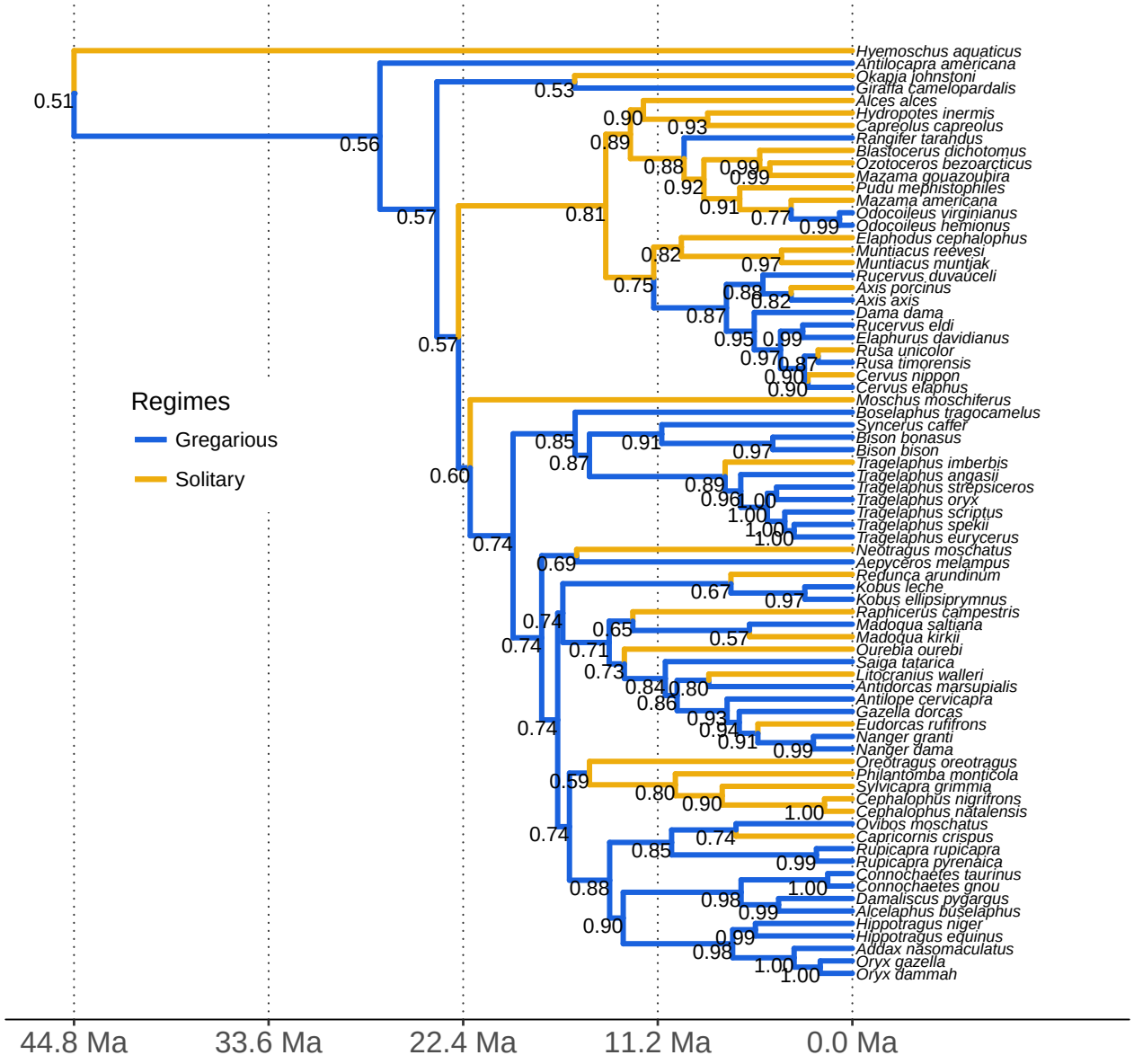

Figure S1: Ancestral state reconstructions of gregariousness, *sensu* Pérez-Barbería & Gordon (2005). The values at the internal nodes are log likelihoods for the respective reconstructed regime at the node, scaled from 0 to 1. $n = 75$.

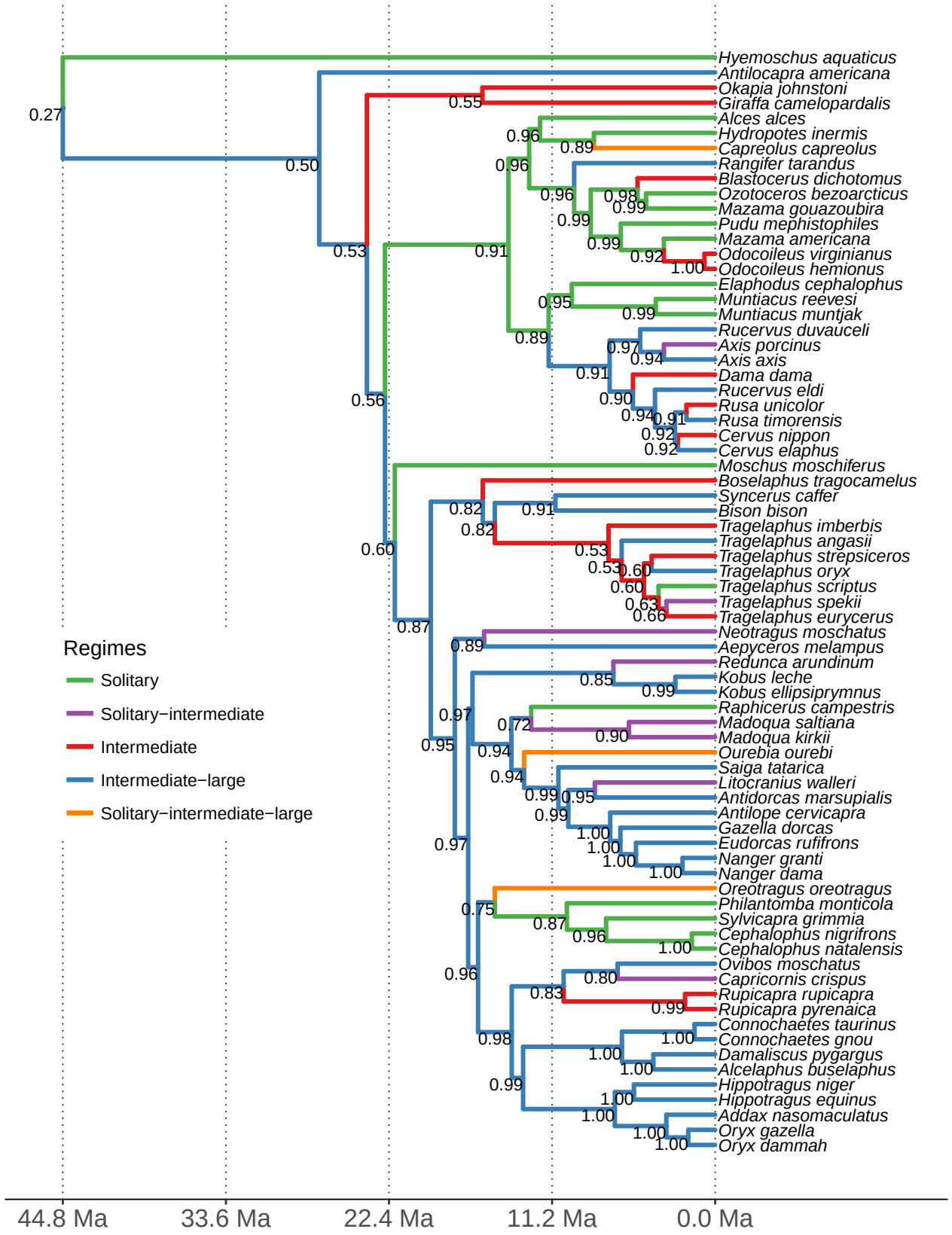

Figure S2: Ancestral state reconstructions of sociality, *sensu* Caro *et al.*, (2004). The values at the internal nodes are log likelihoods for the respective reconstructed regime at the node, scaled from 0 to 1. $n = 73$.

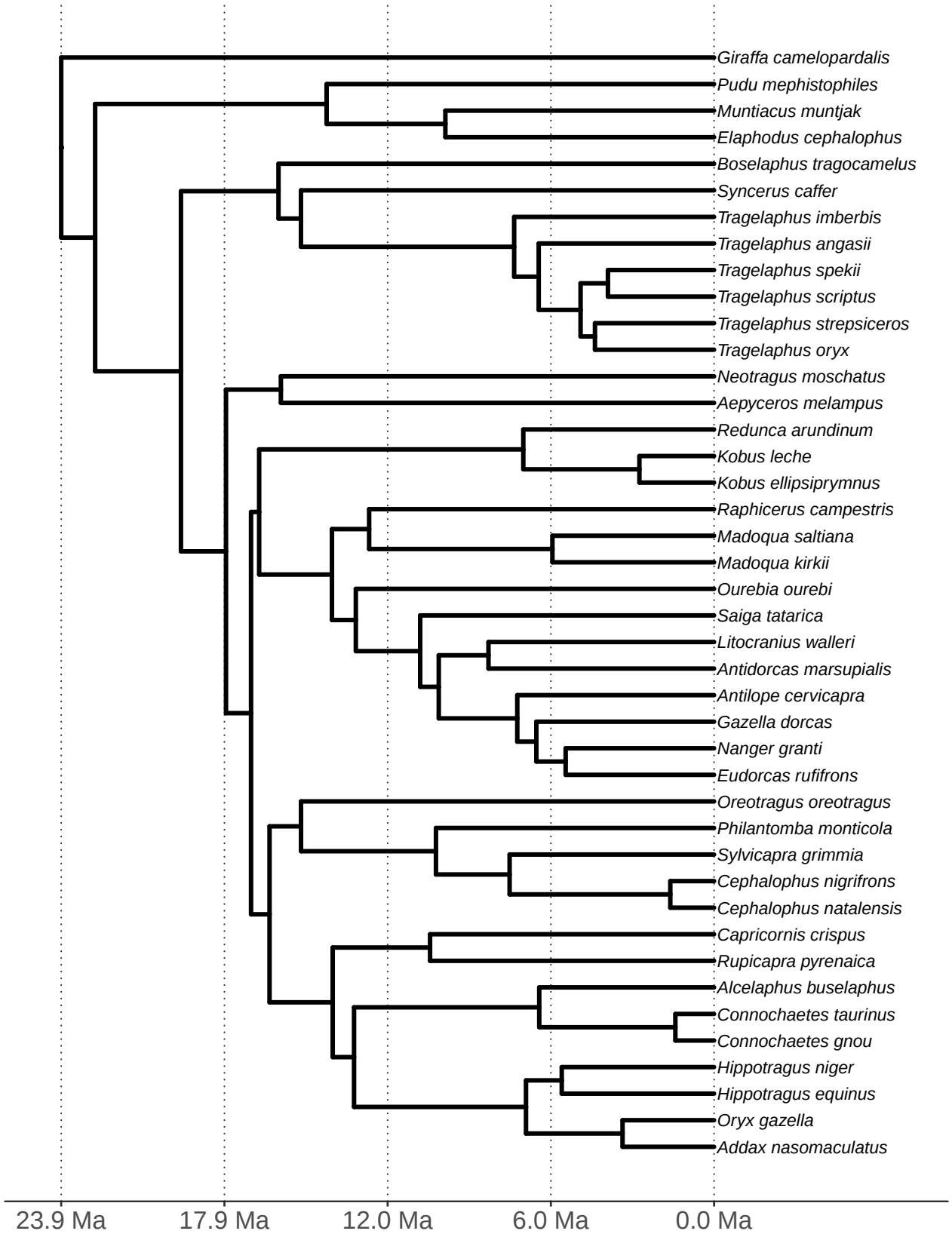

Figure S3: This tree was used to model log brain size on log mean group size during breeding season, see Table 8. $n = 42$.

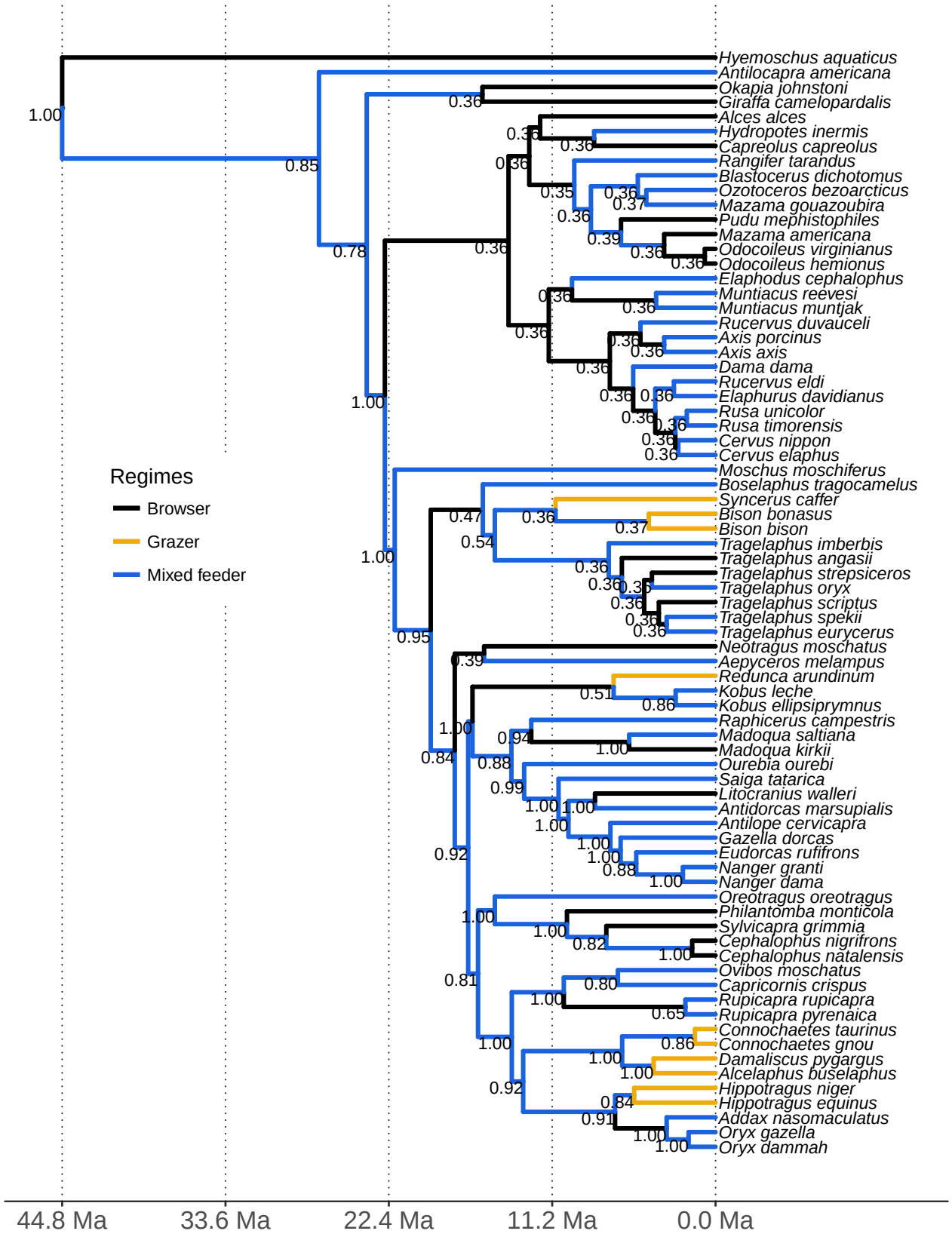

Figure S4: Ancestral state reconstructions of diet, based on Toljagíc *et al.*, (2017). The values at the internal nodes are posterior probabilities for the respective reconstructed regime at the node, scaled from 0 to 1. $n = 75$.

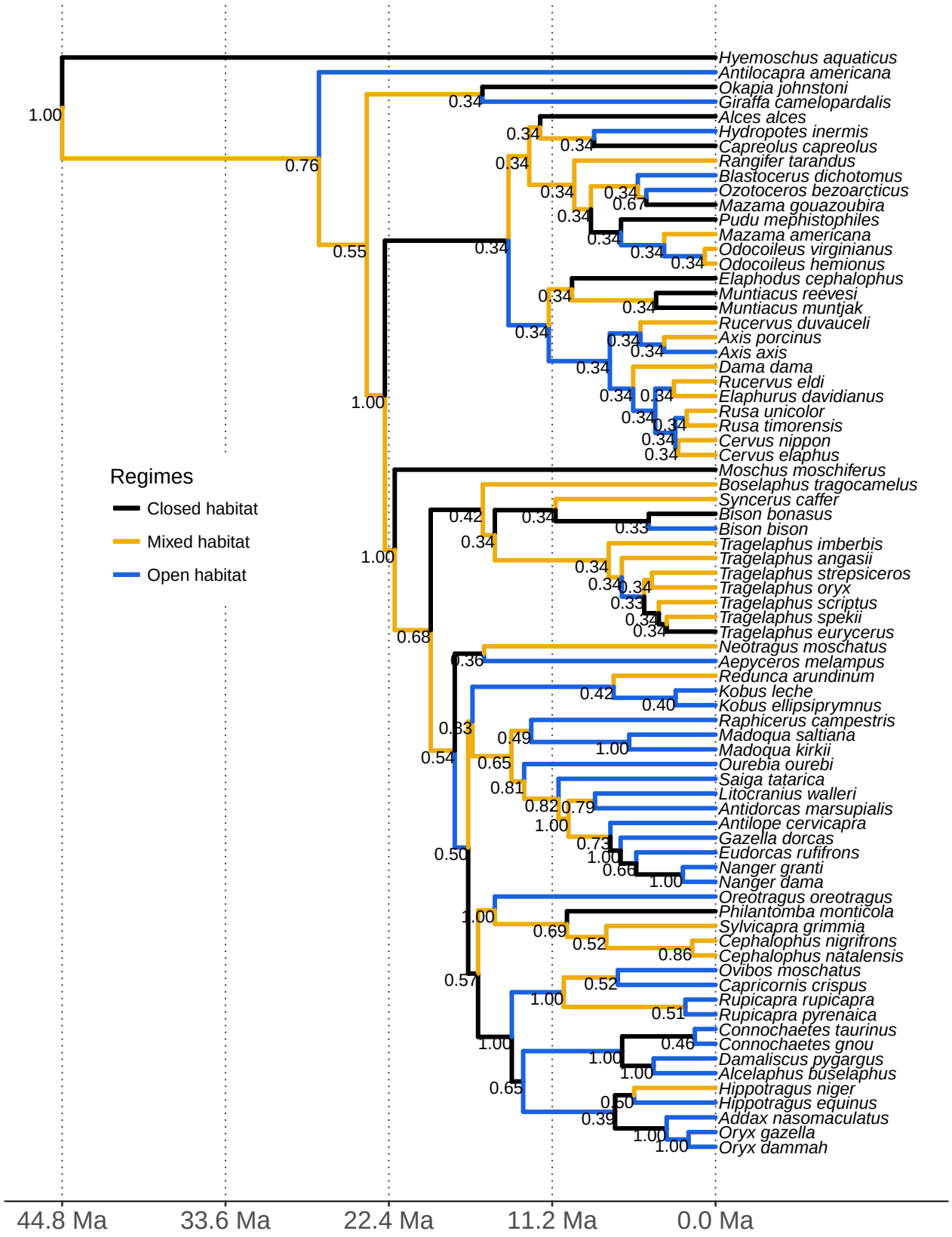

Figure S5: Ancestral state reconstructions of habitat, based on Toljagíc *et al.*, (2017). The values at the internal nodes are posterior probabilities for the respective reconstructed regime at the node, scaled from 0 to 1. $n = 75$.

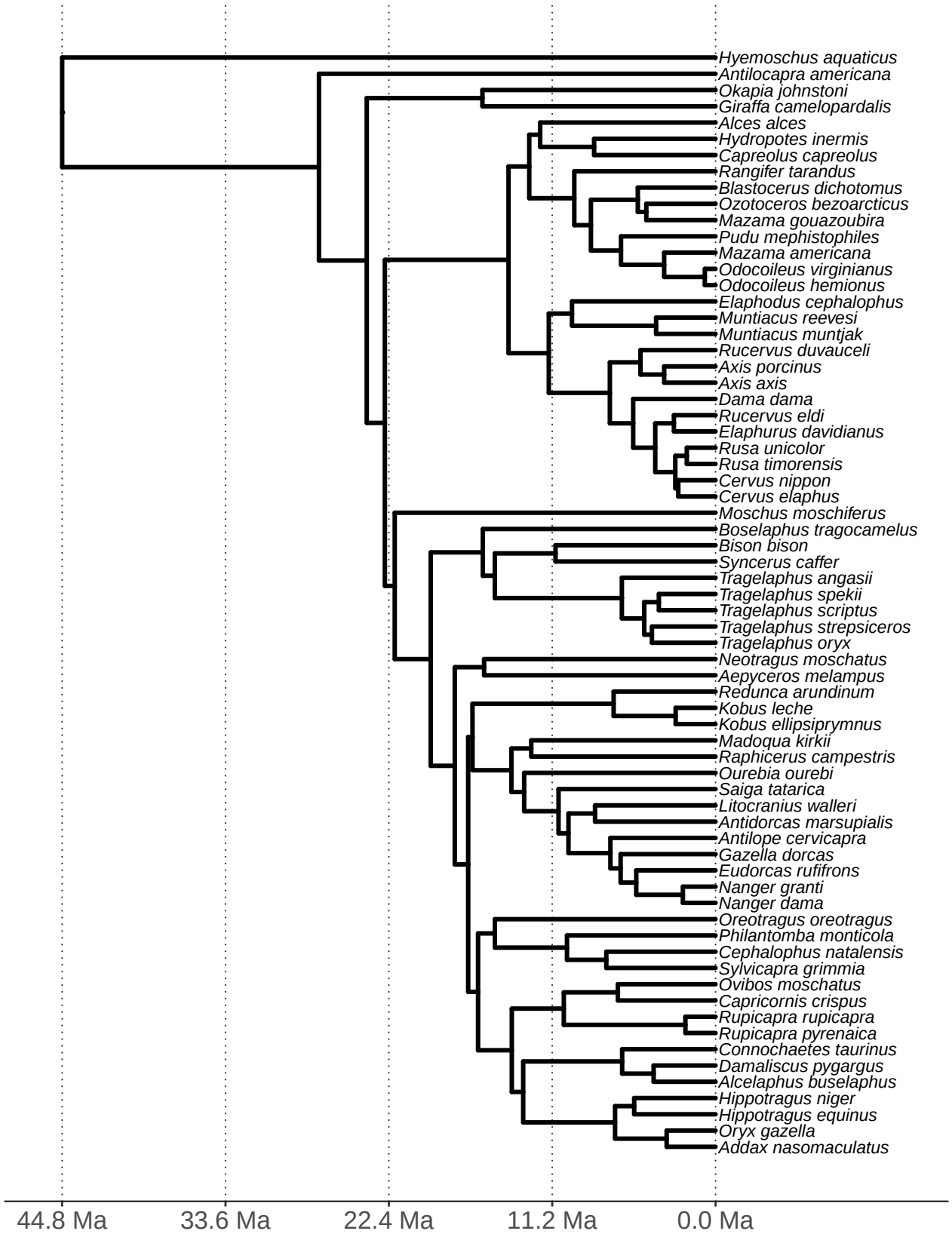

Figure S6: This tree was used to model log brain mass on sexual dimorphism, see Table 14. $n = 68$.

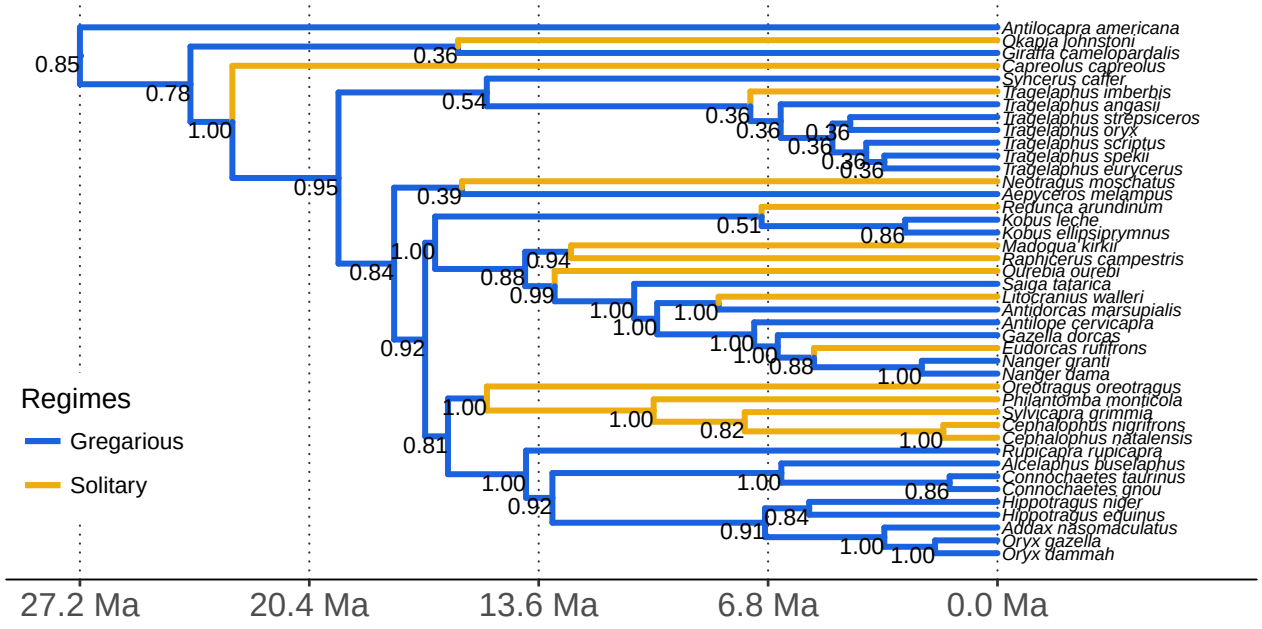

Figure S7: Ancestral state reconstructions of gregariousness, *sensu* Pérez-Barbería & Gordon (2005). The values at the internal nodes are log likelihoods for the respective reconstructed regime at the node, scaled from 0 to 1. $n = 42$.

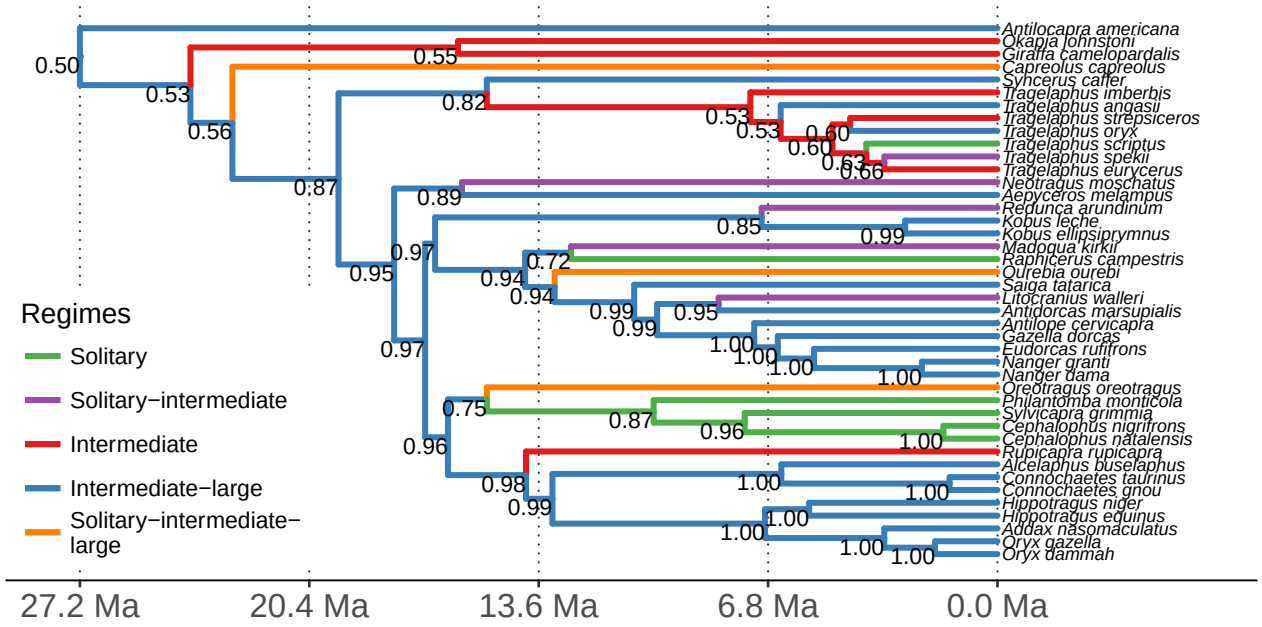

Figure S8: Ancestral state reconstructions of sociality, *sensu* Caro *et al.*, (2004). The values at the internal nodes are log likelihoods for the respective reconstructed regime at the node, scaled from 0 to 1. $n = 42$.

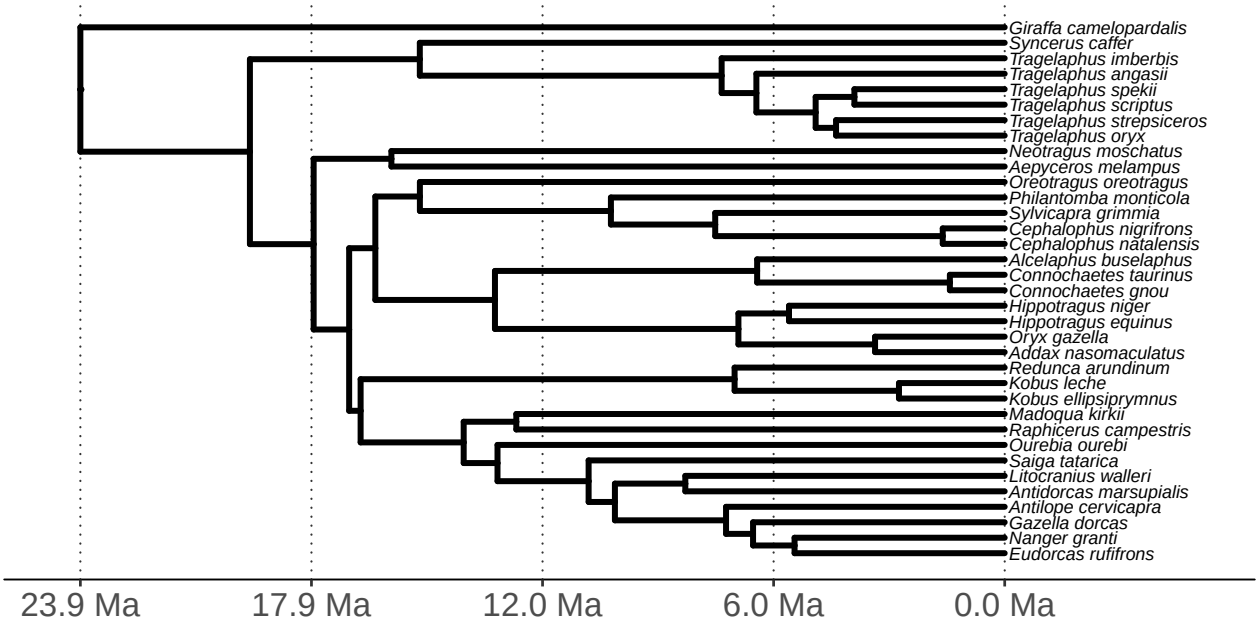

Figure S9: This tree was used to model log neocortex area on log mean group size during the breeding season, see Table 9. $n = 35$.

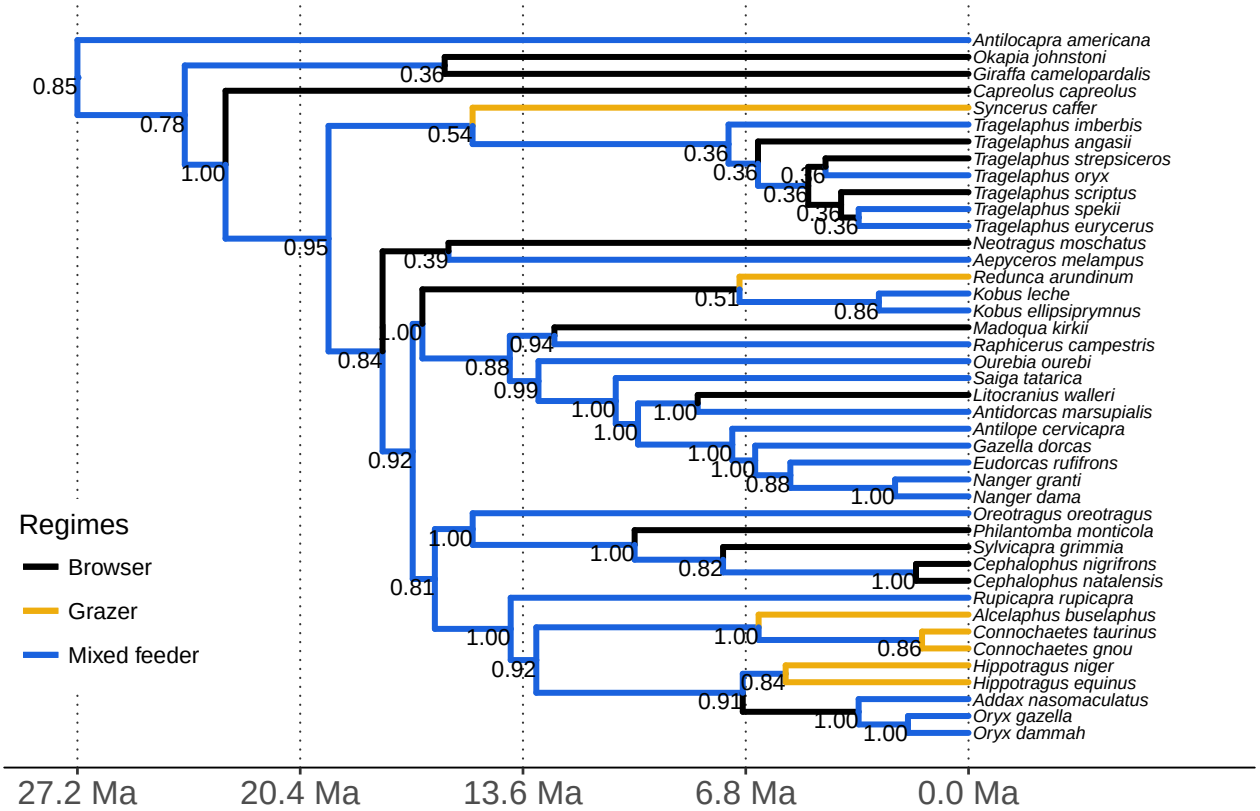

Figure S10: Ancestral state reconstructions of diet, based on Toljagíc *et al.*, (2017). The values at the internal nodes are posterior probabilities for the respective reconstructed regime at the node, scaled from 0 to 1. $n = 42$.

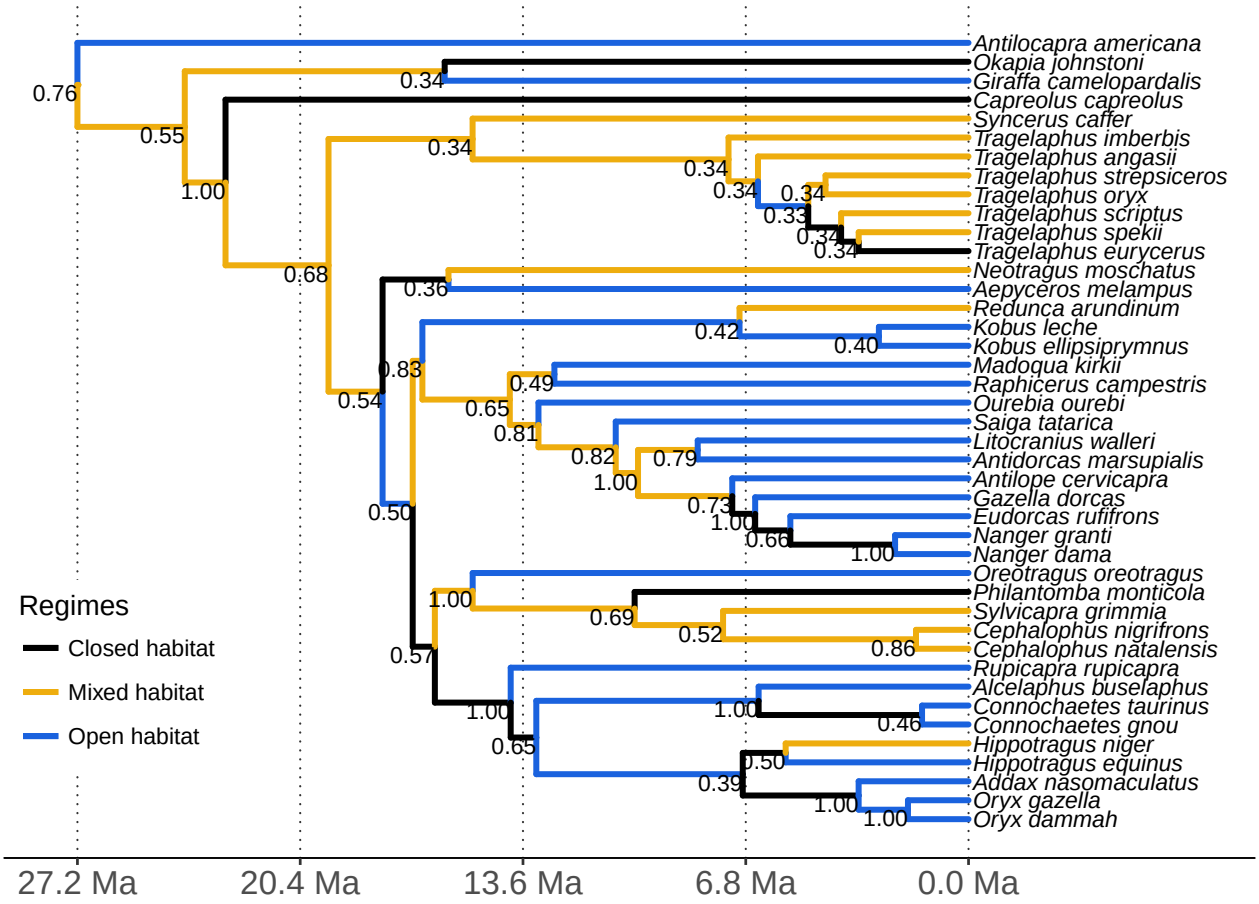

Figure S11: Ancestral state reconstructions of habitat, based on Toljagíc *et al.*, (2017). The values at the internal nodes are posterior probabilities for the respective reconstructed regime at the node, scaled from 0 to 1. $n = 42$.

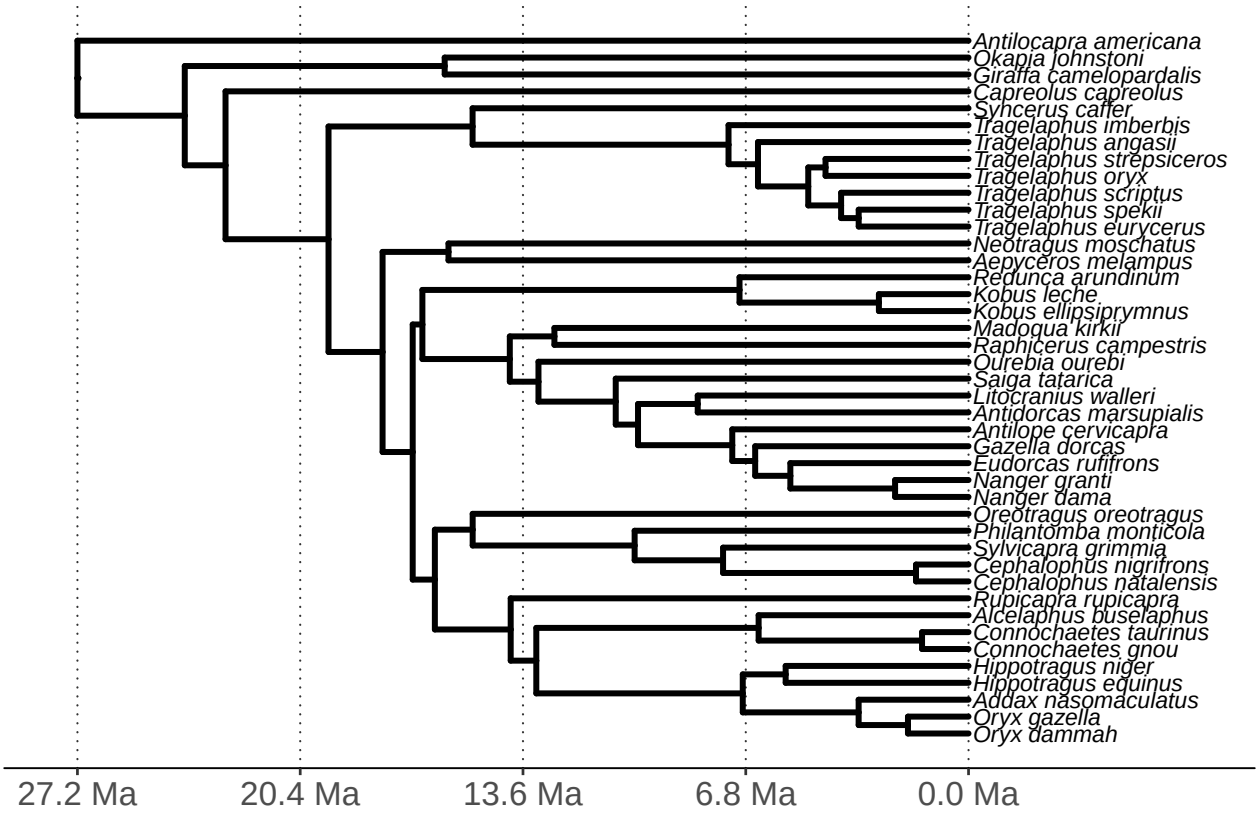

Figure S12: This tree was used to model log neocortex area on sexual dimorphism, see Table 15. $n = 37$.

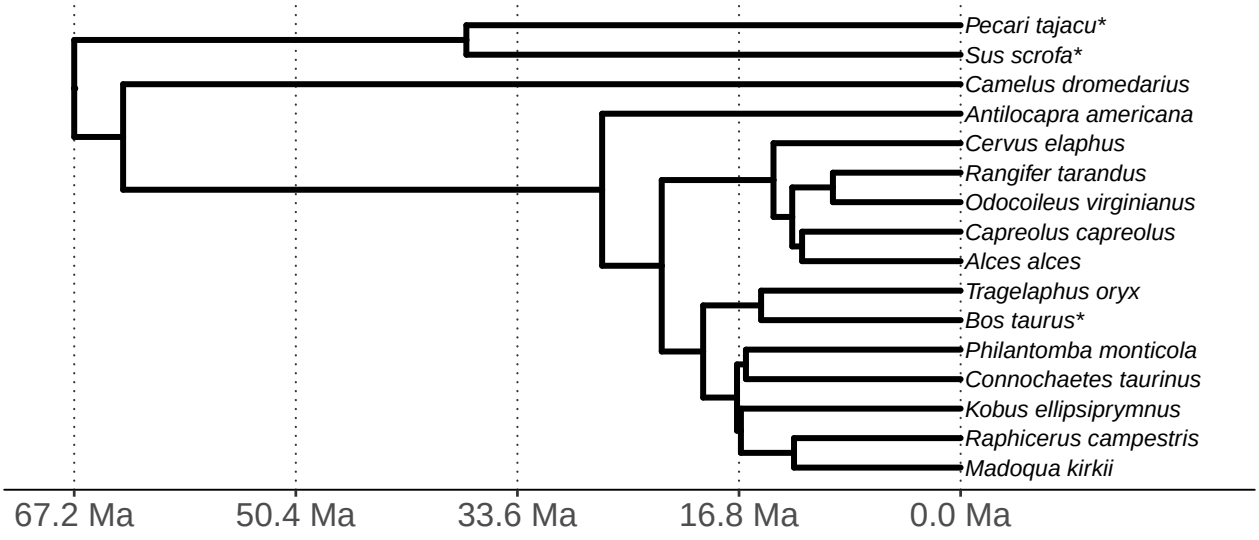

Figure S13: This tree was used to model log brain mass on log basal metabolic rate, see Table 18. $n = 16$. *These species were used exclusively for the models with basal metabolic rate, and are not included in any of the other models or trees.